National Library of Canada
Acquisitions and Bibliographic Services Branch
395 Wellington Street
Ottawa, Ontario
K1A 0N4

Bibliothèque nationale du Canada
Direction des acquisitions et des services bibliographiques
395, rue Wellington
Ottawa (Ontario)
K1A 0N4

Your file Votre référence

Our file Notre référence

NOTICE

The quality of this microform is heavily dependent upon the quality of the original thesis submitted for microfilming. Every effort has been made to ensure the highest quality of reproduction possible.

If pages are missing, contact the university which granted the degree.

Some pages may have indistinct print especially if the original pages were typed with a poor typewriter ribbon or if the university sent us an inferior photocopy.

AVIS

La qualité de cette microforme dépend grandement de la qualité de la thèse soumise au microfilmage. Nous avons tout fait pour assurer une qualité supérieure de reproduction.

S'il manque des pages, veuillez communiquer avec l'université qui a conféré le grade.

La qualité d'impression de certaines pages peut laisser à désirer, surtout si les pages originales ont été dactylographiées à l'aide d'un ruban usé ou si l'université nous a fait parvenir une photocopie de qualité inférieure.

Canada

UNIVERSITY OF ALBERTA

PARASITE-INDUCED ADENOSINE UPTAKE BY MALARIA-INFECTED HUMAN ERYTHROCYTES

BY

ROBERT ALEXANDRE DUPUIT

A thesis submitted to the Faculty of Graduate Studies and Research in partial fulfillment of the requirements for the degree of MASTER of SCIENCE.

DEPARTMENT OF PHARMACOLOGY

Edmonton, Alberta

Spring 1995

ISBN 0-612-01601-3

Canada

UNIVERSITY OF ALBERTA

RELEASE FORM

NAME OF AUTHOR: Robert Alexandre Dupuit

TITLE OF THESIS: Parasite-induced Adenosine Uptake by Malaria-infected Human Erythrocytes

DEGREE: Master of Science

YEAR THIS DEGREE GRANTED: 1995

Robert A Dupuit

Robert A. Dupuit

#307, 4203-107 Street

Edmonton, Alberta

Canada

T6J 2W8

Date: 5 JAN. 1995

UNIVERSITY OF ALBERTA

FACULTY OF GRADUATE STUDIES AND RESEARCH

The undersigned certify that they have read, and recommend to the Faculty of Graduate Studies and Research for acceptance, a thesis entitled PARASITE-INDUCED ADENOSINE UPTAKE BY MALARIA-INFECTED HUMAN ERYTHROCYTES submitted by ROBERT ALEXANDRE DUPUIT in partial fulfillment of the requirements for the degree of MASTER OF SCIENCE.

Dr. Wendy P. Gati

Dr. Alexander S. Clanachan

Dr. Alan R. P. Paterson

Dr. James D. Young

Date: 16 DEC. 1994

DEDICATION

This thesis is dedicated to my family. I thank my parents, Alex and Alice Dupuit, for their continuous guidance in everything I do, and have done. I also thank my wife Ruth, whose unconditional support helps keeps me striving towards greater achievements and gives more meaning to what I do achieve.

ABSTRACT

The human malarial parasite, *Plasmodium falciparum*, requires an exogenous source of purines for survival. This suggests the possibility of using parasite-toxic purine nucleosides as anti-malarials.

In human erythrocytes (RBCs), adenosine (Ado) influx occurs via a transporter-mediated process, which is stereoselective for D-Ado and is potently inhibited by nitrobenzylthioinosine (NBMPR). However, in *P. falciparum*-infected human erythrocytes (pRBCs), a component of Ado influx was NBMPR-insensitive and was not stereoselective. These cells remained impermeable to sucrose suggesting that the new route of Ado entry had solute selectivity characteristics beyond that of size alone.

Further examination of Ado entry into pRBCs indicated that, in contrast to the influx of other permeants that enter pRBCs, but not RBCs, pRBC-specific Ado influx was saturable (Km~14mM), suggesting the involvement of a mediated route of Ado entry. A lack of significant inhibition of L-Ado influx by the glucose transport inhibitor cytochalasin B indicated that L-Ado was not entering pRBCs via a glucose transport process. In contrast, both phloridzin and furosemide, compounds previously identified by others as inhibitors of pRBC-specific solute entry, inhibited the influx of L-Ado in pRBCs (IC_{50} phloridzin ~50μM, IC_{50} furosemide ~4μM). Furosemide was much more selective for the parasite-induced Ado entry process than was phloridzin, as unlike phloridzin, 50μM furosemide did not affect Ado influx via the erythrocytic nucleoside transporter. Furosemide was also a potent inhibitor of the pRBC-specific entry of D-Ado, L-glucose and D-sorbitol into pRBCs (IC_{50} <10μM), suggesting that these permeants shared a route of entry into pRBCs with L-Ado. Further evidence for a shared route of solute entry was provided by the reduction by 20mM L-Ado of

the entry of 2mM L-glucose or 2mM D-sorbitol into pRBCs to ~30% and ~60% of control values, respectively.

In order to be useful clinically, a purine nucleoside should be metabolically converted into a parasite-toxic intermediate. A comparison of Ado metabolism in pRBCs and RBCs indicated that the rates of conversion of D-Ado and L-Ado to nucleotides were increased in pRBCs, as was the rate of deamination of L-Ado. L-nucleosides may have potential as anti-malarial agents based on selectivity of transport and metabolism in pRBCs.

ACKNOWLEGEMENT

I would like to acknowledge the advice and support I have received from my supervisor, Dr. Wendy Gati, as well as the other members of my supervisory committee. I would also like to thank the Department of Pharmacology, Nordic Laboratories and the Alberta Heritage Foundation for Medical Research for their financial support during my studies.

TABLE OF CONTENTS

MATERIALS and METHODS

LIST OF TABLES

LIST OF FIGURES

ABBREVIATIONS

ADA	adenosine deaminase
Ado	adenosine (9-β-D- **and/or** 9-β-L-ribofuranosyladenine)
D-Ado	9-β-D-ribofuranosyladenine, D-adenosine
L-Ado	9-β-L-ribofuranosyladenine, L-adenosine
ADP	adenosine 5'-diphosphate
AK	adenosine kinase
AMP	adenosine 5'-monophosphate
AMPS	adenylosuccinate
APRTase	adenine phosphoribosyltransferase
ara-A	adenine arabinoside
ara-C	cytosine arabinoside
ATCase	aspartate transcarbamoylase
ATP	adenosine 5'-triphosphate
AZT	3'-azidothymidine
cAMP	adenosine 3',5'-cyclic monophosphate
CB	cytochalasin B
2-CdA	2-chloro-2'-deoxyadenosine
cDNA	complimentary DNA
cGMP	guanosine 3',5'-cyclic monophosphate
cpm	counts per minute
3'-dAdo	3'-deoxyadenosine
D-PBS	Dulbecco's phosphate buffered saline with 5mM glucose
ddC	2',3'-dideoxycytidine
ddI	2',3'-dideoxyinosine
deCof	2'-deoxycoformycin

DHO-DHase	dihydroorotate dehydrogenase
DNA	deoxyribonucleic acid
DPM	dipyridamole
DZP	dilazep
EHNA	*erythro*-9-(2-hydroxy-3-nonyl)adenine
expt	experiment(s)
FAD	flavin-adenine dinucleotide
Fara-A	fludarabine, 2-fluoroadenine arabinoside
FPIX	ferriprotoporphyrin IX
g	the force of gravity
GDP	guanosine 5'-diphosphate
L-Gluc	L-glucose
Glut1	human, erythrocytic glucose transporter
GMP	guanosine 5'-monophosphate
GTP	guanosine 5'-triphosphate
HEPES	4-(2-hydroxyethyl)-1-piperazineethanesulfonic acid
HGPRTase	hypoxanthine-guanine phosphoribosyltransferase
Hyp	hypoxanthine
IC_{50}	concentration causing a half maximal inhibition
IMP	inosine 5'-monophosphate
Ino	inosine (9-β-D- **and/or** 9-β-L-ribofuranosylhypoxanthine)
L-Ino	9-β-L-ribofuranosylhypoxanthine, L-inosine
INPLOT	InPlot® GraphPad version 4.04
6-MP riboside	6-mercaptopurine riboside
min	minute(s)
mRNA	messenger RNA
NAD	nicotinamide-adenine dinucleotide

NBMPR	nitrobenzylthioinosine, 6-[(4-nitrobenzyl)thio]-9-β-D-ribofuranosylpurine
ODCase	orotidylate decarboxylase
OPRTase	orotate phosphoribosyltransferase
PALA	*N*-phosphonoacetyl-L-aspartate
(%P)	parasitemia (percentage of erythrocytes containing malarial parasites)
PNP	purine nucleoside phosphorylase
RBCs	human erythrocytes
bRBCs	*Babesia bovis*-infected bovine erythrocytes
pRBCs	*Plasmodium falciparum*-infected human erythrocytes
RHGBS	culture medium (RPMI 1640 medium with HEPES, Gentamicin, sodium bicarbonate and human serum)
RNA	ribonucleic acid
RPMI^t	transport medium (RMPI 1640 medium with HEPES and NaCl)
S-D-PBS	Dulbecco's PBS with 300mM sorbitol
SDS-PAGE	Sodium dodecyl sulphate -polyacrylamide gel electrophoresis
sec	second(s)
D-Sorb	D-sorbitol
Thd	thymidine (β-D-ribofuranosylthymine)
TLC	thin-layer chromatography
Urd	uridine (β-D-ribofuranosyluracil)
Xne	xanthine
XMP	xanthosine 5'-monophosphate
XPRTase	xanthine phosphoribosyltransferase

INTRODUCTION

I. MALARIA: HISTORY AND PATHOLOGY

Knowledge of the disease we know as malaria dates to some of the earliest records of man's history. As early as three thousand years ago, the Chinese recorded the existence of "paroxysmal manifestations of chill and fever". By the fifth century B.C., the Greeks had noted the various periodicities of these fevers (1).

The fevers and chills we commonly associate with the disease were long attributed to bad air or "mal'aria" found near stagnant swamps. This was thought to suggest that the causative agent must be able to enter the human host and was even predicted to involve insects by Lancisi in 1717 (2). As early as 1716, Lancisi had described dark pigment in post-mortem examinations of the spleen and brain tissues of those afflicted with malaria, however, it was Virchow who linked the presence of pigment (hemozoin) to the malarial fever in 1848 (2). It was a French Army surgeon, Charles Louis Alphonse Laveran, who is credited with discovering the *Plasmodium* parasite itself while examining blood from a malaria sufferer (2).

Strong evidence that the *Plasmodium* parasite was, indeed, the causative agent of malaria was provided by Gerhardt in 1884 (2) as well as Marchiafava and Celli in 1885 (1). Those scientists described the transmission of the disease to subjects by inoculation with infected blood. *Plasmodium falciparum* was discovered simultaneously in 1890 by Canalis and also Marchiafava and Celli (2). Evidence for the natural mode of transmission of the parasite into humans was supplied by Sir Ronald Ross. In 1897 he discovered the parasite in the stomach of *Anopheles* mosquitoes that had fed on malaria-infected humans. In 1898 he also demonstrated that only those mosquitoes which had fed on birds

infected with the malarial parasite were able to transmit it to previously uninfected birds thus demonstrating the complete cycle of infection from bird to mosquito and back to birds (2).

It is now known that, in addition to the *Plasmodia* that infect birds or humans, *Plasmodium* species also infect reptiles, rodents or non-human primates. Those species have proven useful for malaria research as it has been possible not only to obtain a large amount of information about *Plasmodium* biology, but animal models have also provided an opportunity for drug testing. Of the many *Plasmodium* species known, there are four that can cause malaria in humans. These are *P. ovale, P. malariae, P. vivax,* and *P. falciparum*. The first two listed are fairly widespread but generally produce relatively mild symptoms and very little mortality. *P. vivax* is predominant in most parts of the world where malaria is found and is the only species found in temperate zones. *P. vivax* can cause severe infections and even death on occasion. It is *P. falciparum* that is the most devastating malarial parasite. This species is generally limited to the tropics and subtropics, but is responsible for the vast majority of the over one million deaths attributed to malaria each year (3).

The complete life-cycle of malaria is quite complex, (discussed in Section III.1.) but it is the asexual erythrocytic portion of the cycle that is responsible for the clinical symptoms of malaria. It is the lysis of malaria-infected erythrocytes that is responsible for the symptoms of fever and chills, but there are a number of other clinical symptoms, which vary with the severity of the infection. Infection with *P. falciparum* is the most serious and presents the highest degree of morbidity and mortality. The symptoms of malarial infections are due to hemolysis of *Plasmodium*-infected and normal erythrocytes (pRBCs and RBCs), release of parasite metabolites and the resulting immune response, as well as the formation of malarial pigment (hemozoin) by the parasite (4). The fever and

chills associated with infection are most severe in *P. falciparum* infections. It is not uncommon for fevers to reach 40°C (3). The rupture of erythrocytes, both uninfected and infected, causes increased phagocytic action by host macrophages that results in anaemia and an increase in liver and spleen sizes. Surface changes of pRBCs can lead to clogging of capillaries by these cells and result in tissue anoxia (4). These effects are tissue-dependent and can be very debilitating. In severe attacks of *P. falciparum* malaria it is possible to develop severe anaemia, renal failure, pulmonary edema, hypoglycemia, circulatory collapse and shock, spontaneous bleeding of the gastrointestinal tract, repeated generalized convulsions, aciaemia/acidosis, haemoglobinuria and even coma (3).

II. THERAPEUTICS OF MALARIA

The long established recognition of malaria as a disease entity has led to a wide variety of treatments for the infection. These have ranged from attempts at spiritual healing in early times, to bizarre natural remedies, to the synthetic drugs of today. A key to malaria therapy was the introduction of *Cinchona* bark into Europe and the Americas in the 1600's (2). Quinine, the active ingredient in the bark was isolated in 1820 by Caventou (2) and for a long time was the only effective anti-malarial agent available. This drug, known as a blood schizonticide because of its ability to impede the asexual development of the parasite (see Section III.1., Fig. 1), is thought to act by inhibition of DNA replication and RNA transcription by forming a complex with DNA (4). An alternative mechanism of action for quinine may involve its ability to inhibit the activity of the parasite heme polymerase as discussed below for chloroquine. This hypothesis is based on the ability of quinine to effectively inhibit heme polymerase *in vitro* (IC_{50}~18μM) (5).

Production of quinine by synthetic procedures, though possible, is not commercially viable (4). Interestingly, although a number of synthetic anti-malarials have been developed, the mode of actions for any are unknown (6). This is true even of the drug that has been the mainstay of anti-malarial therapy, chloroquine. The mechanism of action of this drug is still unknown although at least three possibilities have been described. The breakdown of hemoglobin by the parasite produces large amounts of a toxic by-product, ferriprotoporphyrin IX (FPIX). Although RBCs can degrade FPIX, the parasite cannot and instead sequesters FPIX in food vacuoles where it is complexed as malaria pigment (haemozoin). One postulated mode of action suggested that chloroquine bound to FPIX in the food vacuole prevents its incorporation into pigment (7). Alternatively, it has been postulated that the ability of chloroquine to act as a weak base in the acidic food vacuole prevents the breakdown of hemoglobin to amino acids by acidic proteases (8). A third hypothesis was put forward in 1992 by Slater and Cerami (9) who found that chloroquine inhibited a parasite enzyme that was responsible for the polymerization of the parasite-toxic FPIX into haemozoin. It was hypothesized that inhibition of this enzyme by chloroquine *in vitro* resulted in parasite death (9).

The limited effectiveness, and the widespread use of chloroquine has resulted in the appearance of many chloroquine-resistant strains of *P. falciparum*, as well as some resistance in *P. vivax* (10). By 1992, chloroquine resistance had been reported in all areas with *P. falciparum* except the Middle East, Egypt, parts of Central America, Mexico and Hispaniola (4). In chloroquine-resistant areas, quinine is now the drug of choice (3,4). A disturbing observation is the existence of populations with naturally occurring resistance to mefloquine (11), a modern antimalarial drug recommended for prophylaxis in areas of chloroquine resistance (12). Artemisinin, a natural antimalarial derived

from the Chinese medicinal plant qinghao, has shown great promise in a number of clinical trials and it is hoped that this drug may have wider applicability in the near future (13).

In addition to chemotherapy, a large effort has been directed towards lessening the severity of an infection by chemoprophylactic means. The World Health Organization recommends chemoprophylaxis regimens for travellers, consisting of chloroquine or mefloquine (12). Alternative steps are also being examined to prevent transmission of the disease including mosquito control as well as the search for an effective vaccine or vaccines. Very encouraging has been the development of a vaccine designated SPf66, which has shown protective effects in both animal studies and a phase-III clinical trial (see ref. 14 for a brief review).

In spite of the variety of drug treatments available, the incidence of and mortality due to malaria is on the increase. This has led to searches for new approaches to malaria therapy including new drugs and vaccine development. A key to the future success of these approaches may lie with a better understanding of parasite biology and its relationship to the host erythrocyte.

III. HOST-PARASITE RELATIONSHIPS

Since *Plasmodia* are dependent on the availability of both a vector for transmission (mosquito) as well as a host (human) there exists the possibility for therapeutic intervention in either. The general life cycle of *Plasmodia* is very similar for all species and hosts, so this section will be concerned only with the life cycle of *Plasmodium falciparum*. The life-cycle of *P. falciparum* is quite complex and consists of sexual reproduction in the mosquito vector, as well as asexual replication and production of gametes in the human host.

III.1. Life Cycle

III.1.A. Mosquito

Only the females belonging to approximately 60 of the 200 species of *Anopheles* mosquito are capable of malaria transmission (4). When one of these mosquitoes takes a blood meal from a *P. falciparum*-infected subject, microgametocytes (male) and macrogametocytes (female) are ingested with the blood. Macrogametocytes are fertilized, after flagellar loss by the microgametocytes, resulting in the formation of a zygote which subsequently matures into an oökinete and then an oöcyst in the mosquito's gut. Then follows the development of sporozoites, some of which migrate to the salivary gland.

III.1.B. Host

When the mosquito takes her next blood meal some of the sporozoites are transferred in the saliva to the next host. Approximately 40 min after injection the sporozoites enter liver parenchymal cells and undergo what is known as the exo-erythrocytic cycle during which the parasite undergoes asexual replication producing thousands of merozoites in each infected cell. Rupture of the liver cells results in the release of these merozoites into the circulation. *P. falciparum* merozoites are capable of invading erythrocytes of any age and begin to undergo asexual replication (schizogony).

During schizogony, after invasion of the erythrocyte (UI), the merozoite (M) develops into a ring stage (R) organism, which develops into trophozoite (T) and schizont (S) stages before the host cell bursts, releasing 8-24 merozoites into the circulation (Fig. 1). This asexual erythrocytic cycle continues as long as the infection is present. Alternatively. the parasite can enter into gametogony [illegible] the micro- and macrogametocytes are formed, thus allowing the parasite to be transferred to a new host by the feeding *anopheline* mosquito.

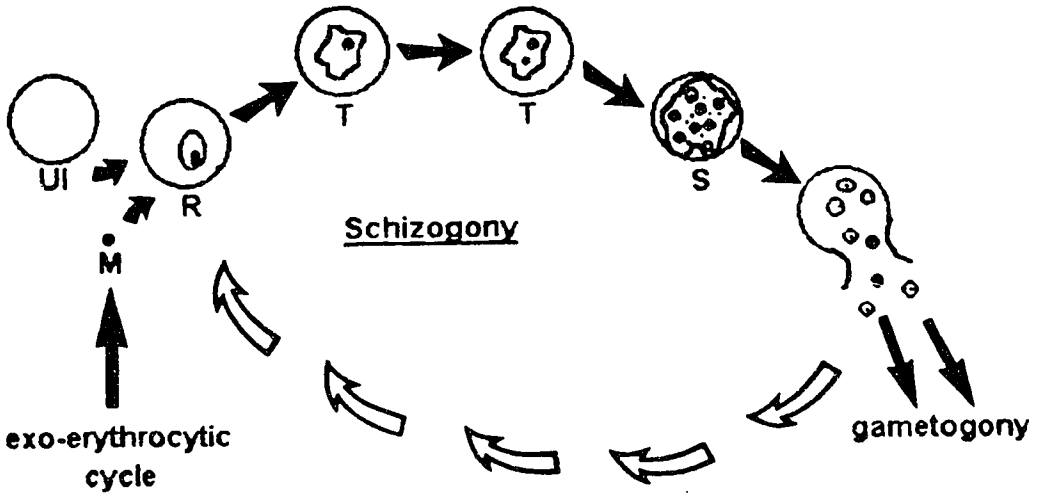

Fig. 1. The asexual erythrocytic cycle of *Plasmodium falciparum*.

III.2. Changes to the Host Erythrocyte during parasite development

III.2.A. General changes

The development of the parasite during the asexual erythrocytic cycle, first described by Golgi in 1885 (1), is related to the symptoms and pathology of the disease. The asexual erythrocytic cycle is also the target for the majority of the commonly used anti-malarials discussed above. The parasite's development in the erythrocyte results in a number of changes to both the structure and function of the host cell. These changes allow the parasite to exist in its own micro-environment inside the host cell. In addition to its own cell membrane, the parasite is also surrounded by a vacuolar (parasitophorous) membrane, possibly obtained in part from the host cell membrane during invasion (15), thus making the cytosol of the host cell the parasite's extracellular environment. The parasite is capable of altering this environment to suit its needs. These changes have a variety of effects on the erythrocyte, one of the most striking of which is the destruction of the sodium gradient seen in normal erythrocytes (16,17). This results in a parasite-infected cell cytosol with a high concentration of sodium compared to normal cells thus allowing a sodium gradient to be established

between the parasite, which is in the low-sodium parasitophorous vacuole, and the host cytoplasm (17). There are also a number of metabolic differences between uninfected and parasite-infected erythrocytes. The parasite has a substantially greater requirement for nutrients than does its erythrocyte host. The parasite must obtain these nutrients from the host cell cytosol. Unlike the host cell, the parasite has a requirement for protein synthesis and hence for a ready supply of amino acids. The parasite can obtain the amino acids necessary for its rapid growth from the breakdown of host cell hemoglobin or from free amino acids in the host cell cytosol (18). There is also a 40- to 100-fold increase in glucose consumption and lactate production in the erythrocyte when it is infected with the malarial parasite (6). This is apparently due to increased glycolysis by the parasite which has glycolytic enzymes with much higher (5- to 520- fold) specific activities than many of the erythrocytic counterparts (19). Mature mammalian erythrocytes lack a nucleus and are unable to synthesize DNA or RNA while the parasite needs rapid nucleic acid synthesis for its growth. The parasite is able to synthesize its own pyrimidines (20,21,22, see below; Section V.) while the primary source of purines appears to be hypoxanthine (Hyp) (23) which can be obtained either by salvage of the nucleobase or by the metabolism of adenosine (Ado) (6, see below).

Changes to the host erythrocyte are not solely intracellular. There are also numerous changes in the characteristics of the cell membrane. Infection with *P. falciparum* results in changes to the host cell membrane which include alterations in the membrane cholesterol, lipid and protein composition (6). These changes result in increased erythrocyte fragility, increased cyto-adherence and also increased susceptibility to phagocytosis. A further consequence of parasite infection is an altered permeability of the host cell membrane to a wide variety of small solutes.

III.2.B. Membrane permeation in malaria-infected erythrocytes

One of the most interesting changes induced in the host erythrocyte by infection with *Plasmodia*, is the altered host cell membrane permeability to a wide variety of small solutes. Studies using non-human models of malaria have considerably aided the research now underway with *P. falciparum*. In the late 60's it was recognized that there are permeability differences between *Plasmodium*-infected erythrocytes and uninfected cells. Dunn (16) showed that sodium transport was altered in *P. knowlesi*-infected erythrocytes from Rhesus monkeys. Sherman was able to demonstrate altered amino acid and glucose entry in duck pRBCs infected with *P. lophurae* (24,25). Rodent malarias have also provided useful models in studies of glucose (26,27) and nucleoside permeation (28,29,30,31).

A major breakthrough in malaria research was the development of techniques for the long-term culturing of *P. falciparum in vitro* (32). For instance, this development allowed for the examination of the permeability properties of human erythrocytes infected with malarial parasites. An early example of membrane permeability differences between RBCs and *P. falciparum*-infected erythrocytes was seen by Lambros and Vanderberg in 1979 (33). They were able, using sorbitol or mannitol, but not sucrose, to selectively lyse erythrocytes that contained mature parasites (trophozoites and schizonts) while uninfected cells remained intact. However, it was not until 1982 that this effect was attributed to altered erythrocyte permeability in *P. falciparum*-infected cells. Kutner *et al.* (34) found that infection with *P. falciparum* resulted in an increased erythrocyte permeability to a number of anionic probes to which RBCs were not permeable. They suggested that an altered erythrocyte membrane permeability may have been the cause of the selective lysis seen by Lambros and Vanderberg. Kutner *et al.* further demonstrated (34) that the observed

permeability changes were growth stage specific and dependent on protein synthesis.

In 1985, Ginsburg *et al.* (35) demonstrated an increased permeability in parasite-infected erythrocytes for a number of polyols and amino acids by utilizing the technique of osmotic lysis (see also ref. 36). It has since been demonstrated that *P. falciparum*-infected RBCs show enhanced permeability to a wide variety of metabolically important solutes including cations (17,37), anions (38,39), carbohydrates (35,39,40), amino acids (18,35,39,41), and nucleosides (39,42,43,44). It has been suggested (e.g., in refs. 35 and 41) that the parasite-altered host membrane permeability may have evolved due to the parasite's high demand for nutrients and/or its need to eliminate large levels of waste produced by the metabolism of these nutrients.

The pathway(s) responsible for the parasite-induced entry of these compounds into *P. falciparum*-infected erythrocytes has not been identified. However, the entry route has been reported to be unsaturable (39), and non-stereoselective (e.g., see refs. 35,39,45). Early studies suggested that a single, positively charged, weakly hydrophobic, pore-like pathway with a fixed radius was responsible for the parasite-induced solute entry (35,46). Phloretin and phloridzin were both shown to be effective inhibitors of solute entry by this route (47,48). However, as a more diverse range of solutes was examined, this theory, in part due to a wide variation in the effectiveness of inhibition by phloridzin, was modified to include three possible entry routes (49). These comprised a pore-like route for hydrophilic and anionic substances, a protein-lipid interface for the more hydrophobic substances, and also modified erythrocytic carriers.

Kirk *et al.* (39,45) have reported that the entry of a wide range of solutes is inhibited to a similar extent by a number of anion channel inhibitors including

furosemide and 5-nitro-2-(3-phenylpropylamino)-benzoic acid (NPPB). It has also been shown that hydrophobicity may be a major determinant of solute entry, especially among solutes of similar size (e.g. sucrose and Ado) (39,45). Kirk *et al.* have suggested that one pathway with characteristics similar to those of a chloride channel may be responsible for the malaria-induced entry of solutes into pRBCs (45).

IV. MEMBRANE PERMEATION OF NUCLEOSIDES

IV.1. General Characteristics of Nucleoside Permeation

The physiological nucleosides, though quite small (M.W. ~250), are relatively hydrophilic and are able to cross cell membranes by diffusion only very slowly. In mammalian cells, the rapid entry of nucleosides is attributable to a variety of nucleoside transport processes (see ref. 50 for a recent review). Two major classes of nucleoside transporters have been described: namely, concentrative and equilibrative. There are now four systems that have been described in which nucleoside influx is coupled to the movement of sodium ions down a concentration gradient. These concentrative nucleoside transporters differ in their substrate selectivity and their sensitivity to inhibition by nitrobenzylthio-inosine (NBMPR) and dipyridamole (DPM). Three systems have been described that are concentrative and also insensitive to NBMPR and DPM. They are distinguished by their solute selectivity and have been designated "*cif*" (concentrative, insensitive, formycin B), "*cit*" (concentrative, insensitive, thymidine) or "*cib*" (concentrative, insensitive, broad) by Belt and co-workers (51,52). Recently, a system has been reported in leukemia cells from patients with acute or chronic lymphocytic leukemia that is concentrative and is sensitive to inhibition by NBMPR and DPM and has been designated "*cs*" (53).

Two equilibrative, facilitated diffusion systems have been described, both of which have broad substrate selectivities. The first is sensitive to inhibition by NBMPR and is designated "*es*" for equilibrative, sensitive. A second system, designated "*ei* ", is also equilibrative, but is insensitive to 1μM NBMPR (50). This system is inhibited by DPM, however, the concentration necessary for inhibition varies somewhat among cell types (50).

IV.2. Membrane Permeation of Nucleosides in Uninfected Erythrocytes

Human and mouse erythrocytes both utilize *es* transporters for the movement of nucleosides across their plasma membranes. This transporter, which is present in the human erythrocyte membrane at an abundance of ~10,000 copies/cell (54) allows the facilitated diffusion of a wide variety of nucleosides and their analogs (55,56). The protein responsible for this transfer has been shown to be a glycoprotein with a molecular weight of about 55,000 daltons, which co-migrates with the erythrocytic glucose transport protein (Glut1) as "band 4.5" on SDS-PAGE (57). This nucleoside transporter protein has been purified to near homogeneity and reconstituted in vesicles (54).

The erythrocytic *es* nucleoside transporter allows the selective entry of pentofuranosides of purine and pyrimidine bases. A wide variety of substitutions can be made to the nucleobase moiety of the nucleoside while still allowing the compound to be a permeant for the transporter. Substitutions at the 2'-position of the sugar are also well tolerated. In contrast, the transporter is sensitive to substitution at the 3'-position of the sugar (58).

Nucleoside transport into human RBCs is potently inhibited by a variety of N^6- and S^6- nitrobenzyl-substituted 9-β-D-ribofuranosyl derivatives of adenine (Ade) or 6-thiopurine (59,60,61). NBMPR binds to the transporter polypeptide (K_D~1nM) and is a potent inhibitor of nucleoside transport in these and other

cells. As well, dilazep (DZP) (62), DPM (63), and mioflazine derivatives (64) are effective inhibitors of nucleoside transport in erythrocytes. The glucose transport inhibitor cytochalasin B (CB) (Ki~140nM (65)) can also inhibit nucleoside influx in human erythrocytes (IC_{50} of ~30μM for inhibition of uridine (Urd) influx) (66).

The *es* transporter is stereoselective for the D-enantiomers of several nucleosides (e.g. 57). Studies using mouse erythrocytes and mouse leukemia (L1210) cells have indicated that β-L-adenosine (L-Ado) is a poor substrate for the transporter and is able to enter these cells slowly via nucleoside transport processes in addition to diffusion (67).

IV.3. Membrane Permeation of Nucleosides in Parasite-infected Erythrocytes

As mentioned above, infection with, and growth of, *Plasmodia* in erythrocytes causes changes in the membrane permeability of the host cell to a variety of small solutes including nucleosides. Neame and Homewood (28) were among the first to examine nucleoside permeation in *Plasmodium*-infected erythrocytes. They examined the entry of pyrimidine nucleosides into *P. berghei*-infected mouse erythrocytes and found that, in contrast to earlier results (68), pyrimidine nucleosides were able to enter pRBCs. Hansen *et al.* saw an increased rate of entry of Ado, inosine (Ino), Ade and Hyp into *P. berghei* - infected erythrocytes relative to that in uninfected control cells (29).

Gati *et al.* (30) were able to show the existence of a parasite-induced Ado entry route in *P. yoelii*-infected mouse erythrocytes that was not inhibited by NBMPR. The exclusion of sucrose from those cells indicated that solute permeation was not determined solely by solute size. It was further demonstrated (31) that the entry of Ado into pRBCs occurred via three routes: the *es* system of RBCs, and two additional parasite-induced routes that were

insensitive to NBMPR. Kinetic characteristics of one of the latter routes were similar to those of the *es* nucleoside transporter while the other route was unsaturable. The unsaturable route was without enantiomeric selectivity and allowed the entry of the non-physiological L-enantiomer of Ado. L-Ado entry, like that of small solutes into *P. falciparum*-infected human erythrocytes (69), was sensitive to inhibition by furosemide (31).

In human erythrocytes infected with *P. falciparum*, the properties of Ado permeation may be similar to those reported in the studies with *P. yoelii* (31). Gero *et al.* (42,43) demonstrated that development of the parasite from the ring to schizont stage was coupled with changes in the Ado and the tubercidin permeability of the host cell. They saw (42) an increase in nucleoside transport inhibitor-insensitive Ado entry with growth stage development. They also reported a decrease in the number of erythrocytic nucleoside transporters as deduced from a decrease in the number of NBMPR binding sites (42).

It was recently suggested (44) that NBMPR-insensitive Ado influx in *P. falciparum*-infected RBCs comprised two components similar to those described in *P. yoelii* (31), in that one was saturable and the other was not; however, supporting data were not shown. Kirk *et al.* have reported the apparently unsaturable entry of thymidine (Thd) into *P. falciparum*-infected erythrocytes (39).

V. METABOLISM OF NUCLEOSIDES

V.1. General Characteristics of Nucleoside Metabolism

Those cells that are incapable of *de novo* synthesis of nucleotides must rely entirely on their ability to salvage free nucleosides and nucleobases by converting them into nucleotides. Purine and pyrimidine bases are released intracellularly as a result of nucleotide metabolism. While pyrimidines are not significantly salvaged by mammalian cells, purine bases can be returned to

nucleotides by the activities of phosphoribosyltransferases. As well, the transport processes discussed above (Section IV.) contribute to the salvage of extracellular nucleosides, which can then be metabolized intracellularly by the purine nucleoside salvage enzymes found in most cell types.

V.2. Nucleoside Metabolism in Human Erythrocytes

V.2.A. Pyrimidines

Mature human erythrocytes are unable to synthesize pyrimidine nucleotides *de novo* due to a lack of dihydroorotate dehydrogenase (DHO-DHase) activity (70). Urd and Thd are substrates for membrane transport processes in erythrocytes, but are not metabolized due to a lack of the appropriate salvage enzymes (71,72).

V.2.B. Purine nucleosides

Mature human erythrocytes are devoid of nucleic acid and protein synthesis, but do possess ATP. These cells are incapable of *de novo* purine nucleotide biosynthesis and must obtain purine nucleotides via the action of purine salvage enzymes (see Fig. 2). Ado, which is released into the circulation by a number of tissues including brain, kidney and skeletal muscle (6), can be taken up into erythrocytes by the erythrocytic nucleoside transporter (see above, Section IV.2.). Ado, at normal physiological concentrations (<1μM) can then be phosphorylated to AMP by adenosine kinase (AK). AMP can also be obtained by the phosphoribosylation of Ade by adenine phosphoribosyltransferase (APRTase) although the plasma levels of Ade are quite low (70). Alternatively, at high concentrations, such as occur during tissue breakdown (73), Ado can be deaminated to Ino by adenosine deaminase (ADA) and then further metabolized

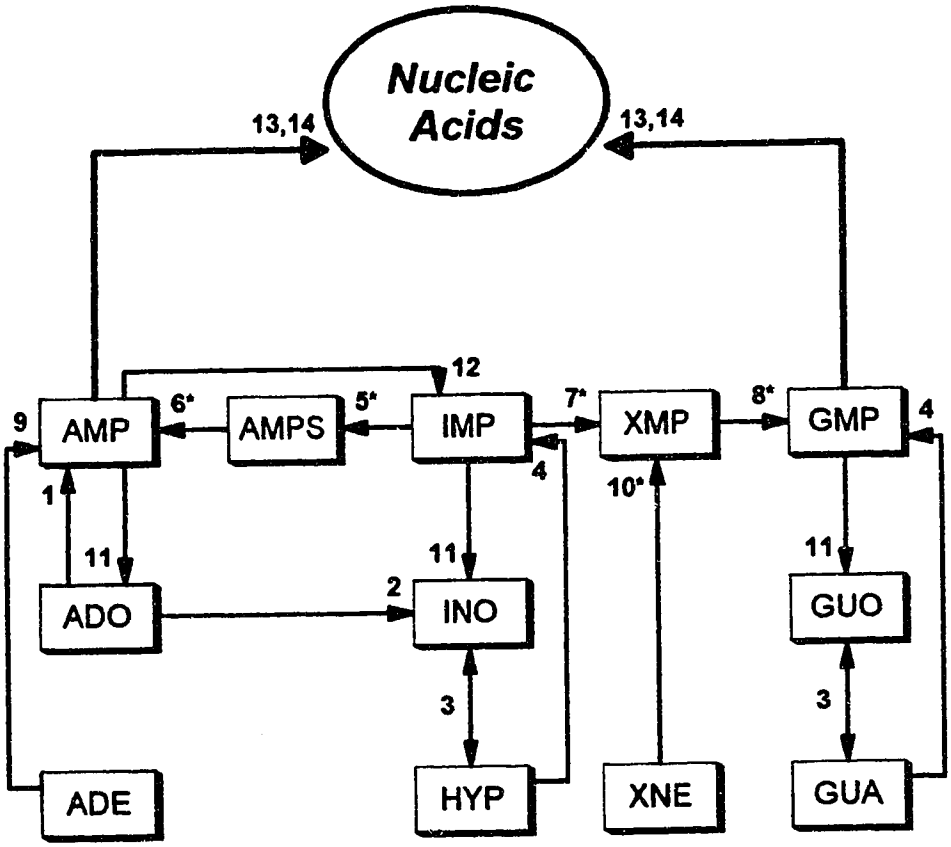

Figure 2. Purine salvage pathways in parasite-infected and normal human erythrocytes.

1. adenosine kinase
2. adenosine deaminase
3. purine nucleoside phosphorylase
4. hypoxanthine/guanine phosphoribosyltransferase
* 5. adenylosuccinate synthetase
* 6. adenylosuccinate lyase
* 7. IMP dehydrogenase
* 8. GMP synthetase
9. adenine phosphoribosyltransferase
* 10. xanthine phosphoribosyltransferase
11. 5'-nucleotidase
12. AMP deaminase
13. purine nucleoside monophosphate kinase
14. purine nucleoside diphosphate kinase

* note: enzyme activities marked with an asterisk are very low or absent in mature human erythrocytes

to Hyp and IMP by purine nucleoside phosphorylase (PNP) and hypoxanthine-guanine phosphoribosyl transferase (HGPRTase), respectively. In mature human erythrocytes, the enzyme activities necessary for further metabolism to AMP or GMP are very low or essentially non-existent (70). GMP can not be obtained from the direct phosphorylation of guanosine (Guo), but rather by the phosphoribosylation of guanine (Gua) by HGPRTase. Guanine can either be salvaged from the circulation or be formed by the intracellular phosphorolysis of Guo by PNP.

Enzymes of Ado metabolism are generally stereoselective for the D-enantiomer. For example, Asai *et al.* (74) and Minoto *et al.* (75) reported that L-Ado was only very slowly deaminated by the ADA from *Aspergillus oryzae*. More recently, Gu *et al.* demonstrated that L-Ado was not phosphorylated or deaminated by the AK or ADA from rat brain (76).

V.3. Nucleoside Metabolism in Malaria-infected Erythrocytes

V.3.A. Pyrimidines

It has been established that *Plasmodia* are capable of *de novo* pyrimidine biosynthesis (20,21,22). Krootch *et al.* (77) were the first to report DHO-DHase activity in rodent *Plasmodia*. The appearance of the parasite equivalents of the other enzyme activities was reported by Reyes *et al.* (71) and Gero *et al.* (72). A comparison of the parasite and erythrocytic enzymes in *Plasmodium*-infected erythrocytes indicated substantially higher specific activities for many of the parasite enzymes relative to those of the host (71,72).

Though pRBCs can take up pyrimidine nucleosides (28), they are unable to incorporate exogenously provided pyrimidine nucleosides into nucleic acids due to a lack of pyrimidine nucleoside kinase activity in these cells (70).

V.3.B. Purine Nucleosides

Although *Plasmodia* are capable of *de novo* pyrimidine synthesis, they are unable to synthesize purines and are dependent on an exogenous source of purines for survival (20,21). Although the host erythrocyte is capable of purine salvage, infection with *P. falciparum* results in an increased ability to salvage purines due to the activity of new gene products of parasitic origin (70) (see Fig. 2). The parasite enzymes appear to differ from the RBC enzymes. Reyes *et al.* found increased specific activities for many parasite enzymes when compared with the host enzymes, including HGPRTase, xanthine phosphoribosyl-transferase (XPRTase), PNP and ADA (71). The increase in ADA activity may explain the utilization of Hyp as the primary purine source (78, 79, 80, 81,82) although the parasite is capable of growth in the absence of the ADA pathway (83). It is also becoming apparent that the enzymes differ in terms of substrate specificity and inhibition. For example, the parasitic, but not host, HGPRTase can use xanthine as a substrate (84). There also appear to be immunological differences between the parasite and human enzymes. The *P. lophurae* PNP was not cross-reactive with the human enzyme (85) nor was ADA isolated from *P. falciparum* (86). The ADA activity of *P. falciparum* was of much lower sensitivity to inhibition by *erythro*-9-(2-hydroxy-3-nonyl) adenine (EHNA) (IC_{50} parasite ~ 120,000 nM, IC_{50} human ~ 14nM), although both enzymes were potently inhibited by 2'-deoxycoformycin (deCof) (IC_{50} parasite ~0.32 nM, IC_{50} human ~ 0.42 nM) (86).

VI. PURINE AND PYRIMIDINE METABOLISM IN MALARIAL PARASITES: POTENTIAL THERAPEUTIC APPROACHES

VI.1. Modulation of Metabolism

The altered metabolism and membrane permeability of *Plasmodium*-infected erythrocytes have been suggested as potential targets for anti-malarial intervention (e.g. 46,87). It may be possible to interfere with parasite growth and development by manipulation of either pyrimidine biosynthesis or purine salvage.

VI.1.A. Pyrimidine biosynthesis

The expression of all six pyrimidine *de novo* synthesis enzymes by the parasite suggests the possibility of utilizing these enzymes as targets for anti-malarial drugs (87). As most cells in host organisms are capable of pyrimidine salvage, and therefore would not be affected by inhibition of pyrimidine synthesis (70), this suggests the ability to selectively kill parasite-infected cells. Three of the parasite-specified pyrimidine synthesizing enzymes may be relevant therapeutic targets. Aspartate transcarbamoylase (ATCase) is inhibited by N-phosphonoacetyl-L-aspartate (PALA), however, there is no anti-malarial effect *in vitro*, possibly due to a lack of PALA permeation of the host erythrocyte (70). A second possible target is the orotate-phosphoribosyltransferase/ orotidylate decarboxylase (OPRTase-ODCase) complex, as the ODCase inhibitor pyrazofurin (3-β-ribofuranosyl-4-hydroxypyrazol-5-carboxamide) has been shown to be malaria-toxic *in vitro* though with a significant level of host toxicity in mice (88). As mentioned above, the host erythrocyte is unable to synthesize pyrimidines due to the absence of DHO-DHase activity. Therefore the parasite DHO-DHase provides a third potential target for intervention. In this case the absence of the host enzyme would also prevent the erythrocyte from

providing the enzyme activity necessary to circumvent toxicity. DHO-DHase can be inhibited *in vitro* by pyrimidine analogs (72) and compounds that effect linkage of the enzyme to electron transfer. For example, the ubiquinone analog, BW566C, has potent anti-malarial activity through interfering with parasite electron transfer (70). The orotate analog, 5-fluoro-orotic acid, inhibited *P. falciparum* growth in culture with an IC_{50} of ~6nM possibly by inhibiting the activity of DHO-DHase and therefore the synthesis of UMP (89).

VI.1.B. Purine salvage

It may be possible to affect purine salvage by inhibition of nucleoside or nucleobase entry into pRBCs or by inhibition of purine metabolism. Inhibition of nucleoside permeation in parasite-infected cells may prevent the entry of purine nucleosides into pRBCs and decrease purine metabolism by the parasite.

There are a number of parasite-specified purine salvage enzymes which are absent in the host cell (marked with an asterisk in Fig. 2) and may provide appropriate targets for antimalarial intervention. Webster *et al.* (23) showed that hadacidin (N-formyl hydroxyaminoacetic acid) inhibited adenylsuccinate synthetase. Webster and Whaun also showed (90) that bredinin inhibited the conversion of IMP to GMP. However, the existence of these purine-metabolizing enzymes in other cell types in the host, may preclude the use of these drugs as anti-malarial agents.

VI.2. Nucleosides as Potential Anti-malarial agents

VI.2.A. General considerations

Alterations in the structure of the physiological nucleosides may result in a cytotoxic nucleoside. The key to using such nucleoside drugs therapeutically is to develop a strategy that increases the therapeutic index of the drug. This

may be achieved by selectively delivering the drug to the targeted cells, or by utilizing some property of the targeted cells to allow a selective action of the drug.

Nucleoside analogs are currently used clinically as anti-cancer and anti-viral agents. Cytosine arabinoside (ara-C), deCof, fludarabine (Fara-A), and 2-chloro-2'-deoxyadenosine (2-CdA) can all be used as anti-tumour agents. Many cytotoxic nucleosides act by competing with physiological nucleosides for anabolic enzymes (e.g., kinases) and/or by the incorporation of nucleoside phosphate esters into nucleic acids. The uncontrolled proliferation of tumour cells may provide some therapeutic selectivity based on the increased incorporation of cytotoxic drugs into tumour cells relative to host cells. Some cytotoxic nucleosides (e.g. 2-CdA) can act through the induction of apoptosis (91).

Nucleoside analogs are currently being used as anti-viral agents as well. For example, adenine arabinoside (araA), azidothymidine (AZT), 2',3'-dideoxyinosine (ddI), 2'3'-dideoxycytidine (ddC), acyclovir and ganciclovir all achieve selectivity by virtue of the properties of viral enzymes. For example, araA is phosphorylated to AraATP which is a much more effective inhibitor of the *Herpes* viral DNA polymerase than the host enzyme (DNA polymerase α) (92).

VI.2.B. *P. falciparum*

The fact that pyrimidines are not salvaged by the parasite probably precludes their use as anti-malarials, although 5-fluoro-orotate does have some activity *in vitro* (see above). An obvious anti-malarial target is the purine salvage pathway. A number of potentially malaria-toxic nucleosides have been screened in an *in vitro P. lophurae* system by McCormick *et al.* (93). Some of these agents, including 3'-deoxyadenosine (3'-dAdo), tubercidin (7-deaza-adenosine),

and 6-mercaptopurine riboside (6-MP riboside) inhibited [^{14}C]Ado incorporation into parasite DNA by >90% at test nucleoside concentrations of 20-40μM (93).

A potentially significant problem is that of host toxicity because none of the aforementioned drugs are selective for the parasite. A possible solution to this problem may be the use of "host-protection" tactics as proposed by Paterson *et al.* (94) in which targeted cells are exposed to lethal doses of a cytotoxic nucleoside, while the host is protected by, for example, NBMPR. In pRBCs, this treatment regimen would involve the administration of a malaria-toxic nucleoside together with an inhibitor of the host nucleoside transporters, for example, NBMPR. This tactic has been used with success in the treatment of parasite infections in mice. El Kouni *et al.* (95) treated *Schistosoma mansoni* or *S. japonicum*-infected mice with a combination of tubercidin and NBMPR. They found that NBMPR protected the host from the toxicity of tubercidin while allowing the parasite to be eradicated. Gati *et al.* (30) also demonstrated the effectiveness of this technique by prolonging the survival of *P. yoelii*-infected mice when they were treated with a combination of tubercidin and NBMPR.

Another approach to using nucleosides as anti-malarial agents, is to identify malaria-toxic nucleosides that are substrates for the parasite-induced route(s) of nucleoside entry, but will not enter uninfected host cells. In addition, it may be possible to find nucleosides that are selectively metabolized to cytotoxic agents by the parasite enzymes.

VII. THESIS OBJECTIVES

As discussed above, *Plasmodia* have been shown to be dependent on an exogenous source of purines for their growth. A possible approach to the treatment of malaria would employ cytotoxic nucleosides as sources of purines for the parasite. In order to rationally use nucleosides as anti-malarials, it is

necessary to understand nucleoside permeation processes and nucleoside metabolism in *Plasmodia*-infected cells. The potential for the use of nucleosides in the treatment of malaria would be greatly increased by the development of a parasite-toxic nucleoside that could be targeted to parasite-infected cells because of selective uptake into pRBCs or the selective metabolism by parasite enzymes. This study attempted to determine some of the characteristics of nucleoside permeation and metabolism in *Plasmodium falciparum*-infected human erythrocytes.

We compared Ado influx in malaria-infected human erythrocytes and uninfected erythrocytes with the assumption that a parasite-toxic purine nucleoside analog would have permeation properties similar to those of Ado. The observation by Gati *et al.* (31) that L-Ado entered *P. yoelii*-infected, but not uninfected, mouse erythrocytes suggested the possibility of utilizing parasite-toxic L-nucleosides (to be developed, concept only) as anti-malarial agents if these compounds were permeants for a similar, parasite-induced route, in *P. falciparum*-infected human erythrocytes. The permeability of L-nucleosides in pRBCs was examined by measuring the inward fluxes of radiolabelled L-Ado ([^{3}H]L-Ado) in pRBCs containing schizont and trophozoite growth-stages of the parasite, as previous experiments with *P. yoelii* had indicated that these stages allowed the greatest level of L-Ado entry.

A second aim of this project was to examine some of the other characteristics of Ado entry into pRBCs in an attempt to determine if Ado shared the entry route previously described for the parasite-induced entry of L-glucose (L-Gluc) and D-sorbitol (D-Sorb) (35). This would involve comparing the kinetic characteristics of inward fluxes of these permeants. As well, similar effects of inhibitors of nucleoside transport or other membrane permeation processes, on the entry of Ado, L-Gluc, and D-Sorb into pRBCs, would suggest the possibility of

a shared route of entry for these permeants. Mutual inhibition of influx by these permeants would also provide evidence for a shared pathway.

The entry of L-Ado into pRBCs, but not into RBCs, would suggest the potential for selectively delivering L-nucleosides to parasite-infected cells. However, in order to be useful clinically, a L-nucleoside would have to be converted to a parasite-toxic metabolite. This study asked if L-Ado was phosphorylated or deaminated in pRBCs, but not RBCs.

MATERIALS and METHODS

I. MATERIALS

I.1. Cell Culture Media

RPMI 1640 powdered medium (with glutamine, without sodium bicarbonate) and Gentamicin sulfate (50 mg/ml) were obtained from Gibco Life Technologies, Burlington, ON. N-[2-Hydroxyethyl]piperazine-N'-[2-ethane sulfonic acid] (HEPES) was purchased from Sigma Chemical Co., St. Louis, MO.

I.2. Radiolabelled Permeants and Substrates

[2,8-^{3}H]D-Ado (39 Ci/mmol), [2,8-^{3}H]L-Ado (15 Ci/mmol), [1-^{3}H]L-Gluc, and [U-^{14}C]sucrose (360 mCi/mmol) were from Moravek Biochemicals Inc., Brea, CA. [1-^{14}C]L-Gluc (55 mCi/mmol) and [U-^{14}C]D-Sorb (325 mCi/mmol) were from Amersham Canada Ltd., Oakville, ON. [^{3}H]H_2O (1.8 mCi/mmol) was from ICN Radiochemicals, Irvine, CA.

I.3. Non-radioactive Permeants, Substrates and Inhibitors

D-Ado, D-Sorb, L-Gluc, Hyp, Ino, AMP, IMP, DPM, CB, phloridzin, and furosemide were purchased from Sigma Chemical Co., St. Louis, MO. Dilazep was a gift from Hoffman-LaRoche, Basel, Switzerland. L-Ado was synthesized by Ms. Danuta Madej, Dept. of Medical Microbiology and Infectious Diseases, University of Alberta. NBMPR (96) was a gift from Dr. A.R.P. Paterson, Department of Pharmacology, University of Alberta.

I.4. Other Materials

LiCl, H_3BO_3, $MgCl_2$, Tris (hydroxymethyl) aminomethane (Tris base), and paraffin oil (Saybolt viscosity 125/135) were purchased from Fisher Scientific Co., Fair Lawn, NJ. Dow Corning® 550 silicone oil was from Dow Corning

Canada Inc., Mississauga, ON. Triton X-100 was purchased from Sigma Chemical Co. St. Louis MO. EcoLite™ scintillation cocktail was from ICN Biomedicals, Irvine, CA. Percoll was purchased from Pharmacia Canada Ltd., Dorval, Que. or Pharmacia Biotech Inc., Baie D'Ufré, Que. All other chemicals used were reagent grade.

II. HUMAN ERYTHROCYTES AND SERUM

Type A Rh positive packed human erythrocytes as well as A positive or AB positive human serum were obtained from the Blood Transfusion Service, Canadian Red Cross, Edmonton, AB. We gratefully acknowledge the assistance of Dr. A.R. Turner in this respect. Human erythrocytes were stored up to 5 wks at 4°C. Serum was stored at -20°C until required.

III. HUMAN MALARIAL PARASITES

Plasmodium falciparum, strain FCR-3/FMG, ATCC 30932 batch #SF2032 was obtained from the American Type Culture Collection.

Cryopreserved stocks of *P. falciparum*-infected human erythrocytes (0.5ml, 50% hematocrit in 3% sorbitol / 0.65% NaCl / 28% glycerol) were prepared from ring-stage-infected cultures and stored in the liquid phase of a liquid nitrogen refrigerator in sterile, sealed glass ampoules or plastic, screw-capped vials.

IV. SOLUTION COMPOSITION

IV.1. Culture Medium (RHBGS)

RHGBS culture medium consisted of RPMI 1640 medium containing 2.5mM HEPES, 0.04mg/ml Gentamicin, and 0.2% (w/v) sodium bicarbonate at pH 7.4 with 7.5 or 10% (v/v) human serum.[1]

IV.2. Dulbecco's Phosphate Buffered Saline (97) + 5mM Glucose (D-PBS)

D-PBS contained 0.9mM $CaCl_2$, 2.7mM KCl, 1.5mM KH_2PO_4, 0.5mM $MgCl_2$-$6H_2O$, 9.1mM Na_2HPO_4-$7H_2O$, 137mM NaCl, and 5mM glucose at pH 7.4.

IV.3. 10X-Phosphate Buffered Saline, pH 7.4

10X-phosphate buffered saline contained 2.7mM KCl, 14.7mM KH_2PO_4, 91.1mM Na_2HPO_4-$7H_2O$ and 1.37 M NaCl at pH 7.4.

IV.4. 30 mM Sodium Phosphate Buffer (98)

Thirty mM sodium phosphate buffer was an isotonic (~295 mOsm) solution containing 30 mM sodium phosphate, 2.8 mM potassium chloride and 117 mM sodium chloride at pH 7.4. If necessary, pH was adjusted with 1M HCl or 1M NaOH.

IV.5. 9 mM Sodium Phosphate Buffer (98)

Nine mM sodium phosphate buffer was a hypotonic solution (~20 mOsm) containing 9 mM sodium phosphate and 0.8 mM potassium chloride at pH 7.4. If necessary, pH was adjusted with 1M HCl or 1M NaOH.

IV.6. Transport Oil

Transport oil was prepared at a density of 1.03 g/ml by mixing silicone and paraffin oil in the ratio 85:15 (v/v).

---

[1]Serum concentration was adjusted according to growth conditions. Freshly thawed parasites were grown in 10% (v/v) human serum, however once the cultures were established and growing quickly, it was possible to lower the serum level to 7.5% (v/v) with no effect on the rate of growth.

IV.7. Thin Layer Chromatography (TLC)

The solvent used in the separation of nucleobases, nucleosides and nucleotides on Polygram® Silica G UV_{254} thin layer plastic sheets (Brinkmann Instruments (Canada) Ltd, Rexdale, ON) was chloroform / methanol / 15% NH_4OH, 3:2:1 (v/v) (99).

The solvent used in the separation of nucleobases, nucleosides and nucleotides on Polygram® CEL 300 PEI/UV_{254} cellulose thin layer plastic sheets (Brinkmann Instruments (Canada) Ltd, Rexdale, ON) consisted of 1M LiCl, 1.15M H_3BO_3 at pH 7.0.

Buffer for extraction of nucleobases, nucleosides and nucleotides from thin layer sheets contained 0.7M $MgCl_2$ and 0.02M Tris-Cl at pH 7.4 (100).

V. INCUBATION OF UNINFECTED HUMAN ERYTHROCYTES

Human erythrocytes were stored up to 5 weeks at 4°C before use. Prior to experiments utilizing uninfected erythrocytes, these cells were suspended at a 5% hematocrit in RHGBS medium and incubated for 4-5 days at 37°C in a humidified atmosphere of 5% CO_2, 5% O_2, and 90% N_2. Erythrocytes were maintained in Nunc 28cm^2 plastic culture dishes (Gibco Life Technologies, Burlington, ON.) with daily medium change which involved the aspiration of spent medium and its replacement with fresh medium.

VI. MAINTENANCE OF PARASITE CULTURES

Parasites were maintained by a modification of the original methodology of Trager and Jensen (32). Uninfected human erythrocytes were inoculated with samples of pRBC-containing cultures to achieve an initial parasitemia of about 1% and a hematocrit of 3-5% in RHGBS medium. Seven ml of the cell suspension were transferred to a Nunc 80cm^2 culture flask (Gibco Life

Technologies, Burlington, ON.) and incubated at 37°C in a humidified atmosphere of 5% CO_2, 5% O_2, and 90% N_2. Each day, spent medium was replaced with fresh medium by allowing the cells to settle in the flasks and removing most of the spent medium by aspiration. Fresh medium was added according to the growth requirements of the cultures so that 5ml of fresh medium was added to ~4ml of partially spent medium after 24 hours. At 48 and 72 hours of growth, 7ml of fresh medium was added to cultures from which almost all of the spent medium was removed. Cultures were subcultured every ~96 hours. Cultures, synchronized by an adaptation of the method of Lambros and Vanderberg (33), were given an additional 24 hours of parasite growing time (total growing time ~120 hours) (and 9ml of medium) to produce mature stages for experiments. Synchronization was achieved by pelleting the cells from cultures containing ring-stage-infected erythrocytes (800xg, 5 min) and re-suspending the cells in RHGB medium containing 300mM sorbitol at ~20% hematocrit. Following a 10-min, room temperature, incubation to allow sorbitol uptake by trophozoite- and schizont-containing pRBCs, the cells were centrifuged and re-suspended in isotonic RHGB. The return to isotonic conditions resulted in osmotic lysis of erythrocytes containing mature (trophozoite and schizont) forms of the parasite. The cell debris was removed by a single wash step with RHGB before proceeding with subculturing. Parasitemia (percent infected cells) was determined throughout the growth period by examination of Giemsa stained thin films.

VII. ISOLATION OF PARASITE-INFECTED ERYTHROCYTES

When growth-stage-synchronized cultures containing schizonts reached a parasitemia of 10-15%, parasite-infected cells were recovered for experiments. Isolation was based on modifications of the methodologies of Dluzoski *et al.*

(101) and Aley *et al.* (102,103) and employed low speed centrifugation of cells on sorbitol-containing Percoll step gradients.

VII.1. Preparation of Gradients

Percoll gradients for the enrichment of *P. falciparum*-infected erythrocytes were prepared as follows: 1 volume of 10X phosphate-buffered saline was slowly added to 9 volumes of stock Percoll suspension with constant stirring to provide a 90% Percoll stock suspension. Next, 5.5% (w/v) sorbitol was added, with stirring, to the 90% Percoll suspension to make it hypertonic. After being adjusted to pH 7.4 with 1M HCl, the 90% suspension was diluted with RPMI^t or D-PBS containing 5.5 % (w/v) sorbitol (S-RPMI^t or S-D-PBS, pH 7.4) to make suspensions containing 37% and 75% Percoll. Three ml of the 75% suspension was added to the bottom of a 15-ml screw-cap polypropylene centrifuge tube then 2ml of the 37% solution was carefully layered over the 75% solution using a syringe tipped with a short length of tubing (this allowed controlled addition of the 37% solution both in speed and positioning). This gradient was easily scaled up for use in 50-ml tubes if a large volume of cells was required.

VII.2. Separation and Recovery of Cells

Parasite-infected erythrocytes were obtained from growth-stage-synchronized cultures and centrifuged (800xg, 5 min, at room temp in an IEC HN-S table-top centrifuge) to form a pellet of cells. The supernatant was removed and the cells were re-suspended to ~ 30% hematocrit in S-RPMI^t or S-D-PBS and left to equilibrate 10 min. A 2.5-ml aliquot of the cell suspension was then layered onto the gradient with a tubing-equipped syringe.

Separation of parasite-infected cells from uninfected cells was accomplished by centrifugation (1500xg, 10 min, 25°C). After centrifugation, three distinct bands were seen on the gradient:

a) above 37% Percoll - cell debris

b) 37% / 75% interface - schizont and late trophozoite pRBCs

c) pellet - RBCs

Band b) was removed and washed three times by centrifugation (800xg, 5 min) with increasing (10-20) volumes of isotonic RPMI[1] or D-PBS. The wash medium was added slowly to provide for a gradual change in osmolarity to prevent the osmotic lysis of the relatively fragile pRBCs. Populations of pRBCs containing schizonts and late trophozoites were obtained at parasitemias of >95% using this method.

Control cells (uninfected erythrocytes) were prepared and separated in the same manner; however, only a single band (band c) was observed and recovered from the gradients.

VIII. MEASUREMENT OF INWARD PERMEANT FLUXES

The permeabilities of RBCs and pRBCs were examined by plotting progress curves for the uptake of various radiolabelled solutes into these cells. Uptake measurements were carried out using established methodologies (e.g., see ref. 31). Inward fluxes were determined as the slopes of the initial, linear segments of progress curves. The rate between 3 and 5 sec was used for the the measurement of the inward flux of Ado entry and the rate between 5 and 15 sec was used for the inward fluxes of D-Sorb or L-Gluc entry. All experiments were conducted at room temperature (22-24°C), and in accordance with biosafety practices.

VIII.1. Influx of Radiolabelled Permeants

Human erythrocytes, either normal or infected with *Plasmodium falciparum,* were recovered from cultures and suspended in RPMI[t] or sodium phosphate buffer at the appropriate concentration (2 or $4x10^8$ cells/ml), which was determined by counting in a Coulter counter.

Permeant influx was measured by performing single tube assays in duplicate or triplicate for each time point. Immediately before transport measurements, the cell suspension (100µl containing $2x10^6$cells/ml or 50µl containing $4x10^8$cells/ml) was layered over 100µl of "transport oil" (silicone oil / paraffin oil, density 1.03 g/ml) in a 1.5-ml plastic microfuge tube placed in the rotor of an Eppendorf microcentrifuge (model 5414).

The influx of solute was initiated at time (T)=zero by the rapid addition of 100µl (at 2X permeant concentration) or 150µl (at 1.33X permeant concentration) of radiolabelled permeant solution (± inhibitor) to the cell suspension for a final reaction volume of 200µl. The tube was quickly closed.

At T=X sec (metronone signals at 120 beats/min, X=1-121sec) influx was ended by starting the centrifuge, which pelleted the cells under the oil layer (15000xg, 30 sec). This procedure yielded uptake intervals of X+2 sec due to the time required for the cells to pass through the oil layer (56).

Cell pellet water space measurements were determined in parallel assay mixtures with [^{3}H]H_2O to measure the total water space and [^{14}C]sucrose to measure the extracellular water space (30). Time intervals of cell exposure to radioactive agents were approximately three sec.

Experiments utilizing inhibitors required the following modifications: NBMPR, DZP and DPM were added only to permeant solutions, whereas CB (or

dimethylsulfoxide (DMSO) in controls), phloridzin and furosemide were present in both cell suspensions and permeant solutions. Cells were incubated at room temperature with CB for 30 min and with phloridzin or furosemide for 15 min before inward fluxes of the appropriate permeants were measured.

VIII.2. Recovery of Cell-associated Radioactivity

Supernatants were aspirated from the tube above the oil layer and the inside surface of the tube above the oil layer was washed once with water. The water and oil were removed by aspiration and the cell pellet was re-suspended in 0.4 ml of 1% (v/v) Triton X-100 and left at room temperature overnight.

The following day, the suspension was extracted with 0.75ml of ice-cold 5% trichloroacetic acid (TCA). After 15 min in a cold room (6-8°C), mixtures were centrifuged (15,000xg, 3 min, 4°C) to pellet acid-insoluble material. One ml of the supernatant was transferred to a scintillation vial and 5 ml of EcoLite™ was added. Radioactivity was measured in a liquid scintillation counter. Background radioactivity was determined by measuring the radioactivity of vials containing only Ecolite™.

VIII.3. Calculation of Cell-associated Radioactivity

Total water space

$$\mu l = \frac{(H_2O \text{ sample cpm} - \text{bkg cpm})}{(H_2O \text{ standard cpm} - \text{bkg cpm})} \cdot (20\mu l \cdot \text{diln factor})$$

Extracellular water space (EWS)

$$\mu l = \frac{(\text{Sucrose sample cpm} - \text{bkg cpm})}{(\text{Sucrose standard cpm} - \text{bkg cpm})} \cdot (20\mu l \cdot \text{diln factor})$$

Intracellular water space (IWS)

$$\mu l = (\text{Total water space} - \text{Extracellular water space})$$

Specific Activity (SA)

$$\text{cpm/pmol} = \frac{\text{Permeant standard cpm - bkg cpm}}{\text{20µl standard} \cdot \text{stock permeant concentration (µM)}}$$

Radioactivity in the extracellular space (TP)

$$\text{cpm} = \frac{\text{(Permeant std cpm - bkg cpm)}}{\text{(20µl std} \cdot \text{diln factor)}} \cdot \text{EWS (µl)}$$

Calculation of cell content of permeant as pmol/µl cell water

$$\text{pmol/µl cell water} = \frac{\text{sample cpm - bkg cpm - TP cpm}}{\text{(SA [cpm/pmol])} \cdot \text{(IWS [µl])}}$$

Calculation of cell content of permeant as pmol/10^7cells

$$\text{pmol/}10^7\text{cells} = \frac{\text{(sample cpm - bkg cpm - TP cpm)} \cdot 1.15\text{ml} \cdot 1\text{x}10^7}{\text{(SA [cpm/pmol])} \cdot \text{(1ml)} \cdot \text{(cells per assay tube)}}$$

IX. METABOLISM

IX.1. The Conversion of Ado to Metabolites

The purpose of these experiments was to examine the formation of metabolites from [^{3}H]D-Ado or [^{3}H]L-Ado in RBCs or pRBCs.

One hundred µl of radiolabelled substrate solution (2X concentration in D-PBS) was added to 1.5ml microfuge tubes and incubated for 10 min in a 37°C water bath, then the tubes were removed from the water bath, 100µl of RBC or pRBC cell suspension (2x10^8cells/ml in D-PBS at 37°C) was added, and the tube contents mixed before being returned to the water bath to start the metabolism reactions.

After specified time intervals (5-30 min), the tubes were removed from the water bath and quickly transferred to an ice bath. After 5 min, the tubes were centrifuged (15,000xg, 20 sec) to pellet the cells. The supernatant was quickly

removed by aspiration and 0.5ml of cold (-20°C) 70% methanol solution was added to the pellet.[2] The cells were quickly re-suspended and the tube placed in a -20°C freezer and left overnight.

IX.2. Separation of metabolites by TLC

For the separation of metabolites on Silica Gel G thin layer sheets, a glass chromatography tank was lined with chromatography paper, and chromatography solvent added to a depth of approximately 0.5 cm. The tank was sealed with vacuum grease and left to equilibrate at room temperature overnight. This tank preparation was not necessary for the separation of metabolites on PEI-cellulose thin layer sheets.

---

[2] In some experiments the cell pellet was washed once by re-suspension in ice-cold D-PBS followed by immediate centrifugation for 20 sec.

Tubes for substrate and cell controls were set up to contain either 1) ^{3}H-substrate solution with the later addition of D-PBS at T=10 min, or 2) D-PBS with the later addition of cells at T=10 min. These tubes were processed as above with the exception that the tubes without cells were not centrifuged, but were supplemented with 0.5ml 70% methanol after chilling.

After overnight storage at -20°C, the cell-containing tubes were centrifuged for 30 sec at 4°C to pellet methanol-insoluble material. The supernatants were dried under a stream of nitrogen, and the residues re-dissolved in small volumes (~12µl) of 50% methanol. Residues from the cell pellets of tubes that contained cells, but not radioactivity (tube 2 above), during the incubation were redissolved in an equivalent volume (~12µl) of the non-cell-containing radioactive extract (tube 1 above).

Silica Gel G thin layer sheets were used directly out of the package, but PEI-cellulose thin layer sheets were washed once in 50% methanol. Using a pencil, origin locations were marked ~1.5 cm apart and 1.5 cm from the bottom of Silica Gel G or PEI-cellulose thin layer sheets. A line was drawn 2.5 cm from the top of the sheet to indicate the limit of solvent migration.

Five µl of a solution containing a mixture of UV-absorbing nonradioactive standards (at ~1.2mg/ml each in 50% methanol) was spotted at each origin spot to allow the location of metabolites to be determined after development of the thin layer sheets. Five µl of each radioactive metabolite-containing extract was spotted on top of the standard spots after they had been allowed to dry. To serve as a measure of the amount of radioactivity spotted at the origin, an equal volume of the extract was spotted in 1 cm diameter circles drawn at the top of the sheet opposite the origin spots. All solutions were applied to the thin layer sheet in small portions and allowed to dry.

TLC sheets were allowed to develop until the solvent approached the line at the top of the plate (~60 min Silica Gel G, ~120 min PEI-cellulose). After drying, the plates were examined under UV light, the positions of standards marked, and the locations recorded (see Results - Fig. 23). The spots marked on the plate were transferred to scintillation vials, 1 ml of extraction buffer was added, and the vials left overnight at room temperature. The next day, 4 ml of EcoLite™ was added to the vials and the radioactivity counted in a liquid scintillation counter.

The amount of radiolabelled metabolites formed in each sample was determined by expressing the radioactivity (cpm) in each spot as a percent of the total radioactivity recovered from the lane in which the sample was chromatographed.

X. DATA ANALYSIS

All of the graphs in this thesis were produced using the GraphPad™ InPlot 4.04 computer program (GraphPad Software, San Diego, CA.). Curves were fitted to the data by least squares linear regression or by non-linear regression in which parabolas or hyperbolas were fitted to the data. Curves for which an insufficient number of data points were available to determine linear or non-linear relationships, were drawn point-to-point.

Statistical analysis was performed by using the two-tailed Student's t-test or a two-tailed Dunnett's multiple range test (104). The t-tests determined the statistical significance of differences between results found in uninfected and malaria-infected erythrocytes. Potential differences between the effects of various conditions and a control (in the same cell type) were determined by analysis of variance (F-tests) (104). The statistical analysis of these differences employed Dunnett's multiple range test after ranking the data (means) from lowest to highest (104).

RESULTS

I. THE ENRICHMENT OF *PLASMODIUM FALCIPARUM* - INFECTED HUMAN ERYTHROCYTES

The entry of nucleosides into human erythrocytes has been extensively studied by others. We were interested in comparing the entry of Ado into pRBCs and RBCs. Although a number of authors have performed experiments with cell preparations containing relatively low (50-70%) parasitemias, in order to make more valid comparisons between the characteristics of nucleoside influx into pRBCs with those of RBCs, it was desirable to use the most highly enriched preparation of pRBCs attainable. The use of Percoll step gradients containing sorbitol allowed the enrichment of *P. falciparum*-infected human erythrocytes to >95% parasitemia from a growth-stage-synchronized culture of *P. falciparum*-infected human erythrocytes at a parasitemia of ~15%. This is a level of enrichment as good as or better than any previously reported in the literature.

II. THE INFLUX OF D-ADENOSINE INTO UNINFECTED AND MALARIA-INFECTED HUMAN ERYTHROCYTES

II.1. The uptake of 1μM D-Ado by human erythrocytes

Fig. 3 illustrates the time course of 1μM [^{3}H]D-Ado uptake into human erythrocytes that had been maintained in parallel with pRBCs (see Materials and Methods, Section V.). The progress curve of D-Ado uptake in RBCs expressed in terms of either cell number (Fig. 3-A) or cell water space (Fig. 3-B) indicated that the rate of uptake into these cells was linear up to at least five sec despite the fact that the cell content of radiolabel exceeded the extracellular concentration. Measurement of uptake over the range of three to five sec

Figure 3. The uptake of 1μM D-Ado by human erythrocytes.

The cellular content of [^{3}H]D-Ado[3] was determined at the indicated intervals after the addition of 1μM [^{3}H]D-Ado to 2x10^7 human erythrocytes as described in Materials and Methods (Section VIII.)

Each point is the mean ± S.D. from nine determinations obtained in three experiments. Data are expressed in terms of cell number (Fig. 3-A) or cell water space (Fig. 3-B).

---

[3] In this, and subsequent experiments, the cell content of [^{3}H]D-Ado refers to radiolabelled adenosine equivalents, which includes those metabolites formed during the intervals of cell exposure to [^{3}H]D-Ado.

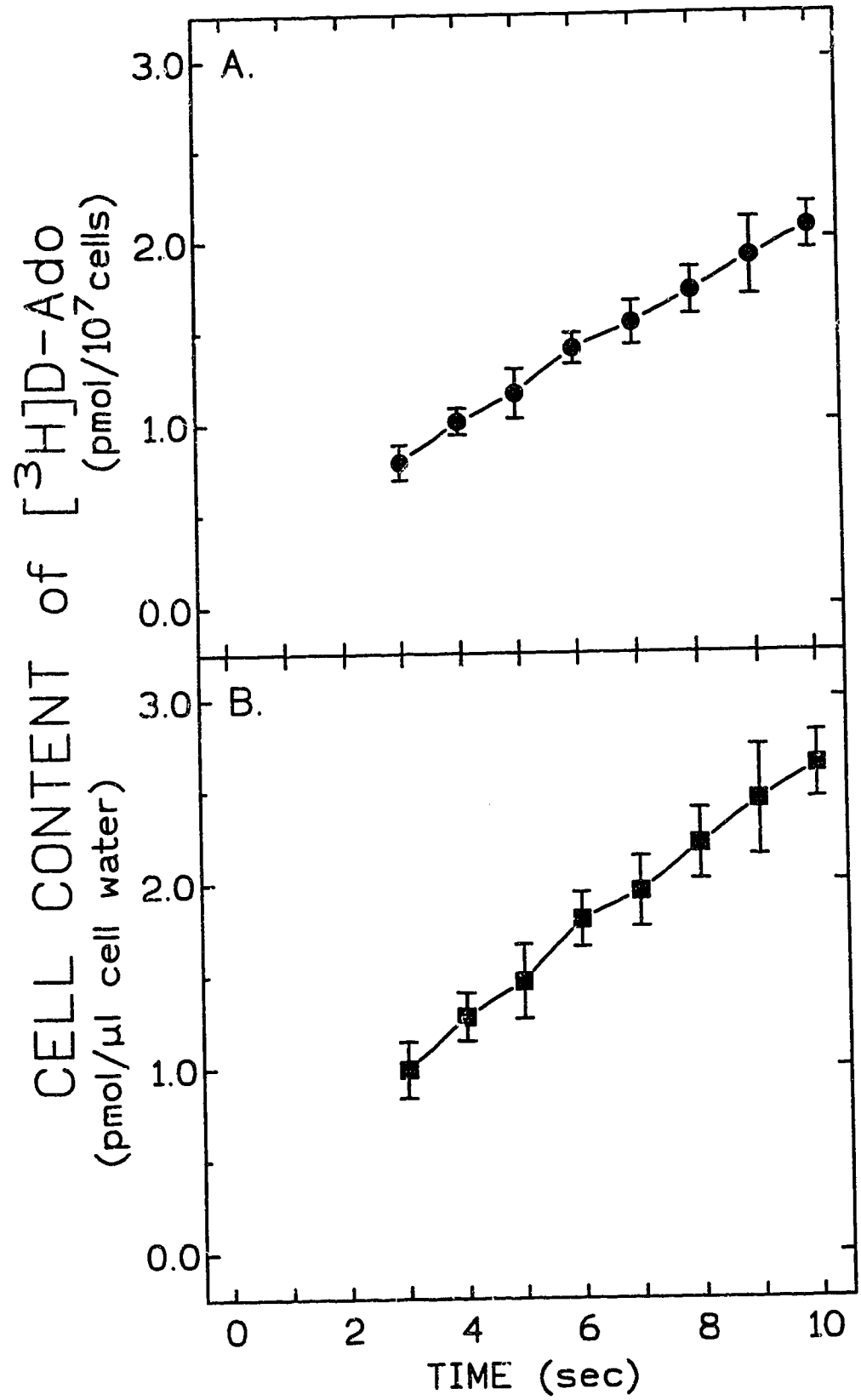
A.
B.
3.0
2.0
1.0
0.0
0
2
4
6
8
10
TIME (sec)
CELL CONTENT of [3H]D-Ado
(pmol/10^7 cells)
(pmol/µl cell water)

therefore provided a measure of the inward flux, and was, therefore, used in subsequent experiments.

II.2. The inward flux of 1μM D-Ado in RBCs and pRBCs

An examination of the slope obtained from the time course of [^{3}H]D-Ado uptake in RBCs (Fig. 4) measured at 3-5 sec allowed the calculation of the rate of D-Ado influx into these cells of 0.18 ± 0.03 pmol/10^7cells/sec (0.33 ± 0.01 pmol/μl H_2O/sec). By comparison, the inward flux of D-Ado in pRBCs was 0.22 ± 0.04 pmol/10^7cells/sec (0.50 ± 0.02 pmol/μl H_2O/sec), an increase of approximately 20% above that determined in RBCs. This difference, though relatively small, was consistent from experiment to experiment, suggesting an increased ability of pRBCs to take up D-Ado compared to RBCs.

II.3. The effect of nucleoside transport inhibitors on the inward flux of 1μM D-Ado in RBCs and pRBCs

Nucleoside entry into human erythrocytes is potently inhibited by a number of compounds including NBMPR, DPM and DZP. Inhibition by these agents of D-Ado entry into pRBCs was examined in the experiments of Fig. 5. D-Ado entry into RBCs was virtually abolished by the addition of 1μM concentrations of any of these inhibitors (inward fluxes <0.005 pmol/10^7cells/sec). In contrast, these agents only partially inhibited D-Ado influx in pRBCs. Approximately 25% of the D-Ado influx into pRBCs was not inhibited by 1μM NBMPR (0.05 ± 0.01 pmol/10^7cells/sec), DPM (0.06 ± 0.01 pmol/10^7cells/sec) or DZP (0.06 ± 0.01 pmol/10^7cells/sec). Statistical analysis (Student's t-test) indicated that there was a significant difference ($p<0.001$) between the effects of the nucleoside transport inhibitors in RBCs and pRBCs. The inhibitor-insensitive flux was not through a non-selective leak pathway as

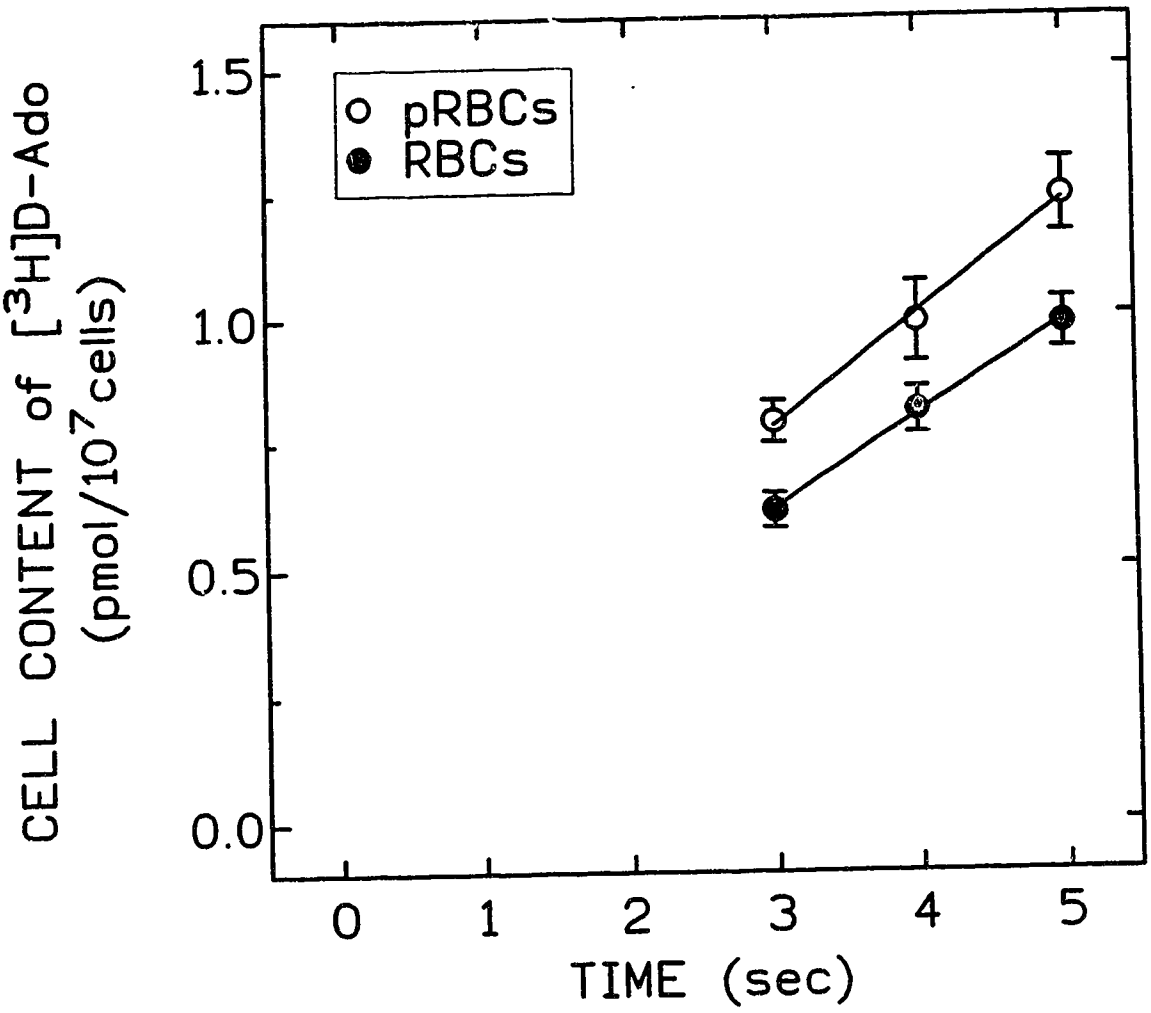

Figure 4. The inward flux of 1μM D-Ado in pRBCs or RBCs.

The cellular content of [^{3}H]D-Ado was measured in pRBCs (O) and RBCs (●) after the indicated intervals of exposure to 1μM [^{3}H]D-Ado.

For pRBCs, each point is the mean ± S.E.M. for 12 expts (3 sec), 7 expts (4 sec), and 12 expts (5 sec) with duplicate or triplicate determinations in each experiment. Analysis of the data by least squares linear regression yielded an inward flux of 0.22 ± 0.04 pmol/10^7cells/sec.

For RBCs, each point is the mean ± S.E.M. for 19 expts (3,4 and 5 sec) with duplicate or triplicate determinations in each experiment. Analysis of the data by least squares linear regression yielded an inward flux of 0.18 ± 0.03 pmol/10^7cells/sec.

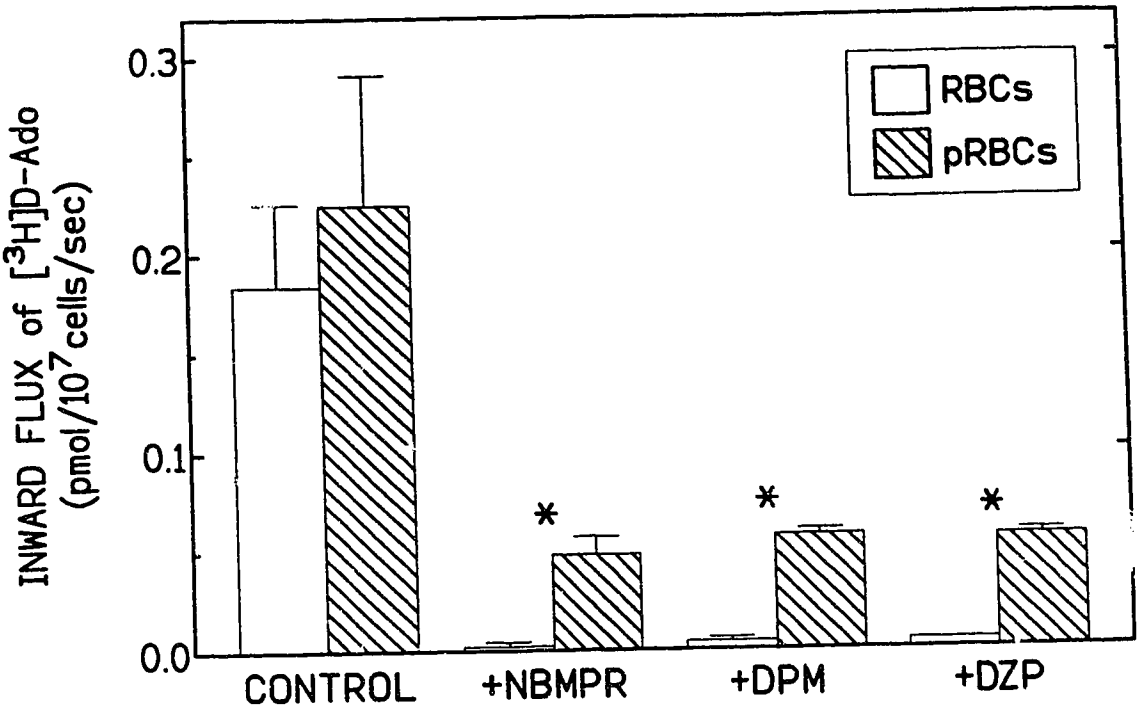

Figure 5. The effect of nucleoside transport inhibitors on the inward fluxes of 1μM D-Ado in RBCs and pRBCs.

The inward flux of 1μM [^{3}H]D-Ado was measured between 3 and 5 sec in RBCs (open bars) and pRBCs (hatched bars) in the absence or presence of 1μM NBMPR, DPM or DZP.

The data are the means ± S.D. or range of the inward flux (pmol/10^7cells/sec) determined in the absence of inhibitors (RBCs: n=19; pRBCs: n=12) or the presence of 1μM NBMPR (RBCs: n=3; pRBCs: n=4), 1μM DPM (RBCs: n=1; pRBCs: n=3) or 1μM DZP (RBCs: n=1; pRBCs: n=2).

Statistical analysis using a two-tailed t-test revealed differences between the inward fluxes in RBCs and pRBCs in the presence of the inhibitors. (*$p<0.001$)

pRBCs remained impermeable to sucrose as has been previously reported (e.g. 45). These results indicated the presence of a parasite-induced pathway of D-Ado entry into pRBCs of low sensitivity to inhibition by nucleoside transport inhibitors.

III. THE INFLUX OF L-ADENOSINE INTO UNINFECTED AND MALARIA-INFECTED HUMAN ERYTHROCYTES

III.1. The inward flux of L-Ado in RBCs and pRBCs

One of the characteristics of Ado entry into RBCs is the stereoselectivity of the es transporter for D-Ado. As mentioned previously (Introduction, IV.1.C.), L-Ado was determined to be a permeant for a parasite-induced route of nucleoside entry in *P. yoelii*-infected mouse erythrocytes (31). Fig. 6 examined the stereoselectivity of Ado entry into pRBCs by comparing the influx of 1μM [^{3}H] L-Ado in pRBCs with that in RBCs. The data indicated an increase in the inward flux of 1μM L-Ado from 0.02 ± 0.01 pmol/10^7cells/sec (0.04 ± 0.01 pmol/μl H_2O/ sec) in RBCs to 0.06 ± 0.01 pmol/10^7cells/sec (0.15 ± 0.01 pmol/μl H_2O/sec) in pRBCs, suggesting the presence of a route of L-Ado entry into pRBCs that was absent in RBCs. The rate of L-Ado entry into pRBCs was similar to the rates measured for inhibitor-insensitive D-Ado influx into pRBCs (see above, Fig. 5) suggesting the possibility that L-Ado and D-Ado may be permeants for the same parasite-induced route.

Fig. 7 shows the inward flux of 10μM [^{3}H] L-Ado in pRBCs and RBCs. At the L-Ado concentration of 10μM, the inward flux was almost 5-fold greater in pRBCs than in RBCs (0.63 ± 0.08 pmol/10^7cells/sec [1.17 ± 0.26 pmol/μl H_2O/ sec] *vs* 0.13 ± 0.15 pmol/10^7cells/sec [0.24 ± 0.13 pmol/μl H_2O/sec]).

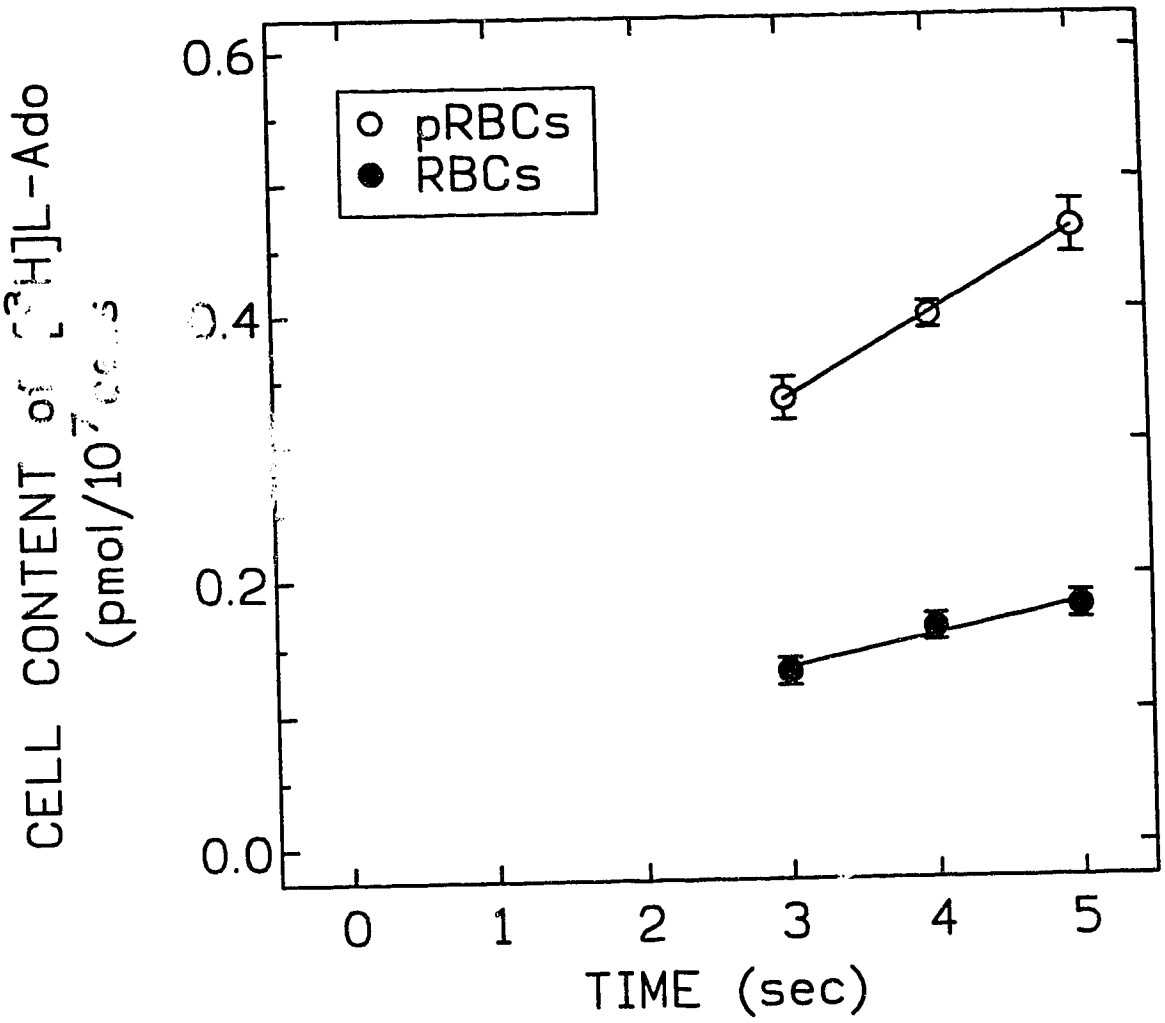

Figure 6. The inward flux of 1μM L-Ado in pRBCs and RBCs.

The cellular content of [^{3}H]L-Ado was measured in pRBCs (O) and RBCs (●) between 3 and 5 sec to determine the inward fluxes in these cells.

For pRBCs, each point is the mean ± S.E.M. for 7 expts (3 and 5 sec) or mean ± range for 2 expts (4 sec) with duplicate or triplicate determinations in each experiment. Analysis of the data by linear regression yielded an inward flux of 0.06 ± 0.01 pmol/10^7cells/sec.

For RBCs, each point is the mean ± S.E.M. for 10 expts with duplicate or triplicate determinations in each experiment. Analysis of the data by linear regression yielded an inward flux of 0.02 ± 0.01 pmol/10^7cells/sec.

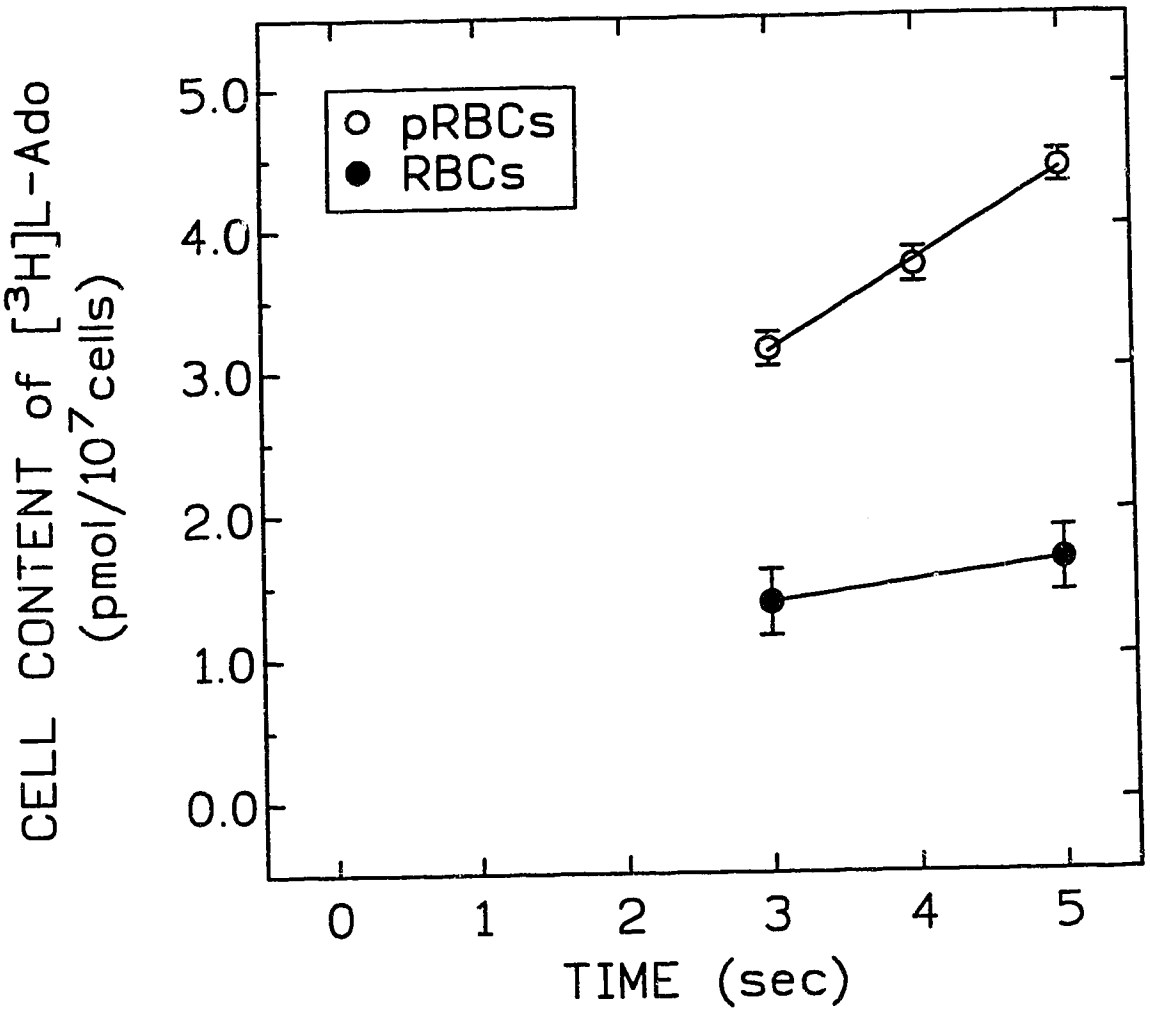

Figure 7. The inward flux of 10μM L-Ado in pRBCs and RBCs.

The cellular content of [^{3}H]L-Ado was measured in pRBCs (O) and RBCs (●) between 3 and 5 sec to determine the inward fluxes in these cells.

For pRBCs, each point is the mean ± S.E.M. for 30 expts (3 and 5 sec) and 14 expts (4 sec) with duplicate or triplicate determinations in each experiment. Analysis of the data by linear regression yielded an inward flux of 0.63 ± 0.08 pmol/10^7cells/sec.

For RBCs, each point is the mean ± S.E.M. for 5 expts with duplicate or triplicate determinations in each experiment. Analysis of the data by linear regression yielded an inward flux of 0.13 ± 0.05 pmol/10^7cells/sec.

Condition	Control	+1μM NBMPR	+1μM DPM	+1μM DZP
RBCs	0.13±0.10	0.07	Not done	Not done
pRBCs	0.66±0.03	0.60±0.06	0.60±0.03	0 09

Table 1. The effect of nucleoside transport inhibitors on the inward flux of 10μM L-Ado in RBCs or pRBCs.

The inward flux of 10μM [^{3}H]L-Ado was measured between 3 and 5 sec in RBCs in the absence or presence of 1μM NBMPR and in pRBCs in the absence or presence of 1μM NBMPR, DPM, or DZP.

For RBCs, the data are the means ± S.E.M. of the inward flux (pmol/10^7cells/sec) determined in the absence of inhibitors (n=5) or the inward flux (pmol/10^7cells/sec) determined in the presence of NBMPR (n=1)

For pRBCs, the data are the means ± S.E.M. of the inward flux (pmol/10^7cells/sec) determined in the absence of inhibitors (n=30) or the mean ± S.D. determined in the presence of NBMPR (n=3), DPM (n=3) or DZP (n=3).

In pRBCs, fluxes in the presence of inhibitors were not statistically different from the control flux.

III.2. The effect of nucleoside transport inhibitors on the inward flux of 10μM L-Ado in RBCs and pRBCs

The results of Table 1 examined the effects of nucleoside transport inhibitors on 10μM L-Ado entry into RBCs and pRBCs. The inward flux of 10μM [^{3}H]L-Ado in RBCs determined in the presence of 1μM NBMPR was ~55% of the control rate in the absence of NBMPR (0.07 *vs* 0.13 pmol/10^7cells/sec). The inward flux of 10μM [^{3}H]L-Ado in pRBCs was determined in the absence or presence of 1μM NBMPR, DPM, or DZP. None of these inhibitors had a significant effect on L-Ado entry into pRBCs. Inward fluxes of L-Ado in the presence of inhibitors were greater than 90% of the control (0.66 ± 0.03 pmol/10^7cells/sec) inward flux (NBMPR: 0.60 ± 0.06, DPM: 0.60 ± 0.03, DZP: 0.62 ± 0.09 pmol/10^7cells/sec). These results indicated that the increase in L-Ado permeability in pRBCs compared to RBCs was not due to the influx of L-Ado via the *es* transporter.

IV. THE EFFECT OF OTHER TRANSPORT INHIBITORS ON ADENOSINE INFLUX INTO UNINFECTED AND MALARIA-INFECTED HUMAN ERYTHROCYTES

IV.1. The effect of CB on 1μM D-Ado entry into RBCs or 10μM L-Ado into pRBCs

Glucose influx in human erythrocytes is potently inhibited by CB. This compound, when present at high concentrations, also inhibits nucleoside entry into a variety of cell types including human erythrocytes and cultured Novikoff rat hepatoma cells (66,105,106). This observation, and the reported functional similarities between the *es* nucleoside transporter and Glut1 (105), led to the examination of the effects of CB on Ado entry into RBCs and pRBCs. In order to examine the effect of CB on Ado entry into RBCs, the inward flux of 1μM D-Ado into these cells was determined in the presence of graded concentrations of CB.

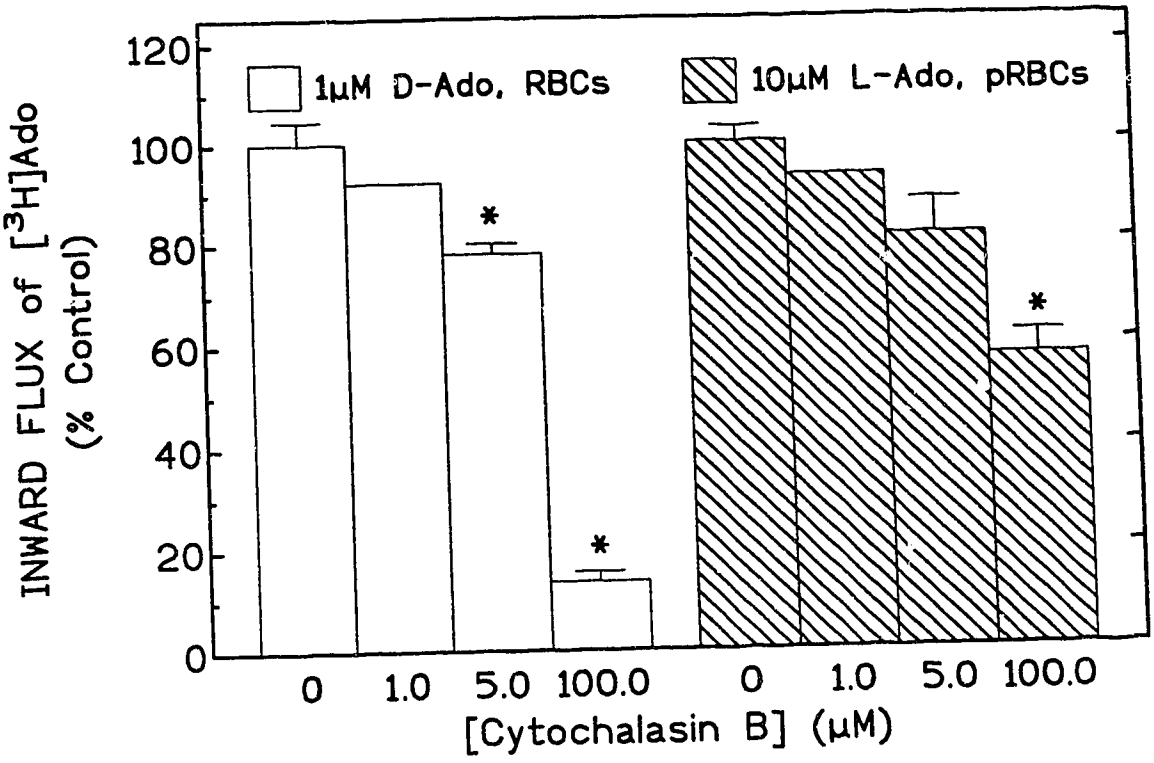

Figure 8. The effect of cytochalasin B on 1μM D-Ado entry in RBCs or 10μM L-Ado entry in pRBCs.

The effect of CB on Ado entry in RBCs and pRBCs was examined by measuring the inward flux of 1μM [^{3}H]D-Ado in RBCs (open bars) or 10μM [^{3}H]L-Ado in pRBCs (hatched bars) in the presence of graded concentrations of CB and compared to controls without CB.

The data are the inward flux (mean ± range) as a percentage of the control rate (1.0μM CB: n=1; 5.0μM CB: n=2; 100.0μM CB: n=2). Control permeant solutions for comparison with CB-containing samples, contained DMSO (see text for details).

The asterisks (*) indicated a significant (Dunnett's multiple range test, α=0.01) inhibition by CB.

The data of Fig. 8 showed that while 1μM and 5μM CB had a fairly limited effect on the entry of D-Ado into RBCs, decreasing the inward flux to 92% and 78 ± 2% of the control inward fluxes, respectively; 100μM CB reduced influx to a level of 14 ± 2% of control influx. Statistical analysis of the data using Dunnett's multiple range test indicated a significant (α=0.01) inhibition of influx by 5μM and 100μM CB. CB, due to its poor water solubility, was dissolved in DMSO, which resulted in low concentrations of DMSO being present in the permeant solutions. However, the inward flux in control preparations was consistent whether in the absence or presence of DMSO as high as 1.6% (v/v) which was the concentration of DMSO in the permeant containing 100μM CB.

The effect of CB on the entry of L-Ado into pRBCs was also examined. The inward flux of 10μM [^{3}H]L-Ado was measured in the absence or presence of 1,5 or 100μM CB in solutions containing DMSO at concentrations of 0.016%, 0.08%, or 1.6% (v/v), respectively. Once again, the DMSO-containing vehicle was without effect on the entry of L-Ado into pRBCs. The effect of CB on L-Ado entry into pRBCs was similar to that found with D-Ado in RBCs. At 1 and 5 μM CB, influx was reduced to 93% and 81 ± 7%, respectively. The inhibitory effect of 100μM CB was less than that seen in RBCs, with L-Ado entry being reduced to 57 ± 4% of control. Only 100μM CB showed a statistically significant (α=0.01) inhibition of L-Ado entry into pRBCs.

The lack of complete inhibition of L-Ado (or D-Ado) influx by low (5μM) concentrations of CB indicated that these permeants were not entering cells via Glut1. The ability of CB to inhibit D-Ado influx in RBCs more effectively than L-Ado influx in pRBCs, also indicated that CB was not a selective inhibitor of the parasite-induced pathway.

IV.2. The effect of phloridzin on Ado entry into RBCs and pRBCs.

Phloridzin, an inhibitor of epithelial sodium-glucose transport in mammalian cells (107), has been previously described as a potent inhibitor of the influx of a wide variety of solutes, such as sorbitol, into pRBCs (e.g. 48,49). Fig. 9 shows the inhibition by phloridzin of Ado entry in RBCs and pRBCs. The inward flux of 1μM D-Ado (in RBCs) or 10μM L-Ado (in pRBCs) was determined in the presence of graded concentrations of phloridzin and expressed as a percentage of the inward flux measured in the absence of phloridzin (control). Phloridzin was able to inhibit the influx of D-Ado into RBCs (control rate: 0.23 ±0.01 pmol/10^7cells/ sec) with an IC_{50} of approximately 100μM. Phloridzin was a slightly more effective inhibitor of L-Ado influx in pRBCs, with an IC_{50} of approximately 50μM (control rate: 0.56 ± 0.09 pmol/10^7cells/sec). However, this IC_{50} was not sufficiently potent to allow the use of phloridzin in the characterization of the parasite-induced Ado permeation pathway.

IV.3. The effect of furosemide on Ado entry into RBCs and pRBCs

Furosemide, an inhibitor of the NaK·2Cl transporter (108) and RBC chloride transport (109), had previously been shown to inhibit the parasite-induced entry of L-Ado into *P. yoelii*-infected mouse erythrocytes (31). Fig. 10 shows the effect of graded concentrations of furosemide on the influx of Ado into RBCs and pRBCs. While the entry of 1μM D-Ado into RBCs was insensitive to inhibition by furosemide up to concentrations of 50μM (the highest concentration examined), parasite-induced entry of Ado into pRBCs was quite potently inhibited. The inward fluxes of both 10μM L-Ado and 10μM D-Ado (in the presence of 1μM NBMPR to inhibit influx via the *es* transporter) were inhibited by furosemide with IC_{50} values of approximately 4μM and 2μM, respectively. These IC_{50} values, and the lack of furosemide inhibition of *es*-mediated flux,

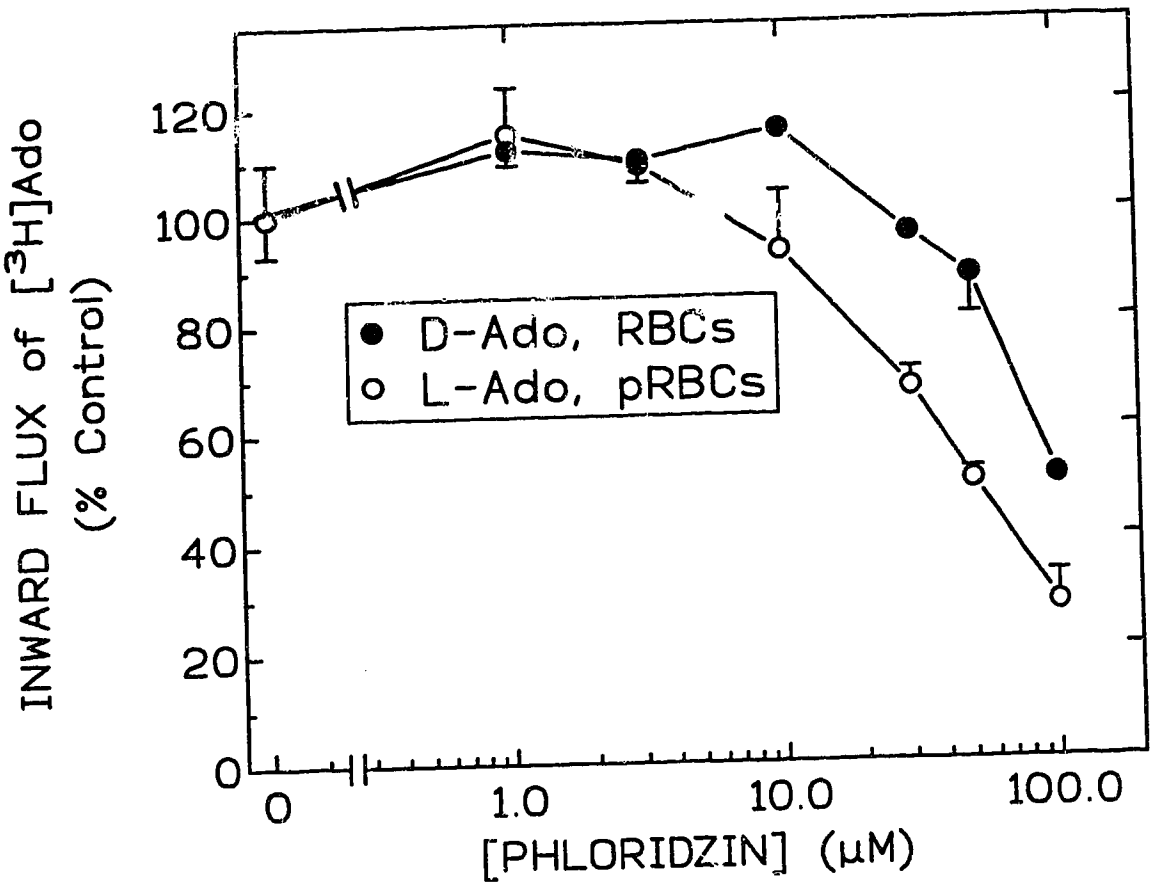

Figure 9. The effect of phloridzin on Ado entry in RBCs and pRBCs.

The effect of phloridzin on Ado entry in RBCs and pRBCs was examined by measuring the inward flux of 1μM [^{3}H]D-Ado in RBCs (●) or 10μM [^{3}H]L-Ado in pRBCs (O) in control cells and in the presence of graded concentrations of phloridzin. Cells were exposed to phloridzin for 15 min at room temperature before measurement of Ado influx; permeant solution also contained phloridzin.

The data are the means ± range or S.D. for 2 expts (●) and 2-3 expts (O) with duplicate or triplicate determinations at 3 and 5 sec of influx in each expt. Control rates in the absence of phloridzin were: 0.24 ± 0.01 pmol/10^7cells/sec, n=2 (●); 0.56 ± 0.09 pmol/10^7cells/sec, n=3 (O). Apparent IC_{50} values were ~100μM (●), and 50μM (O).

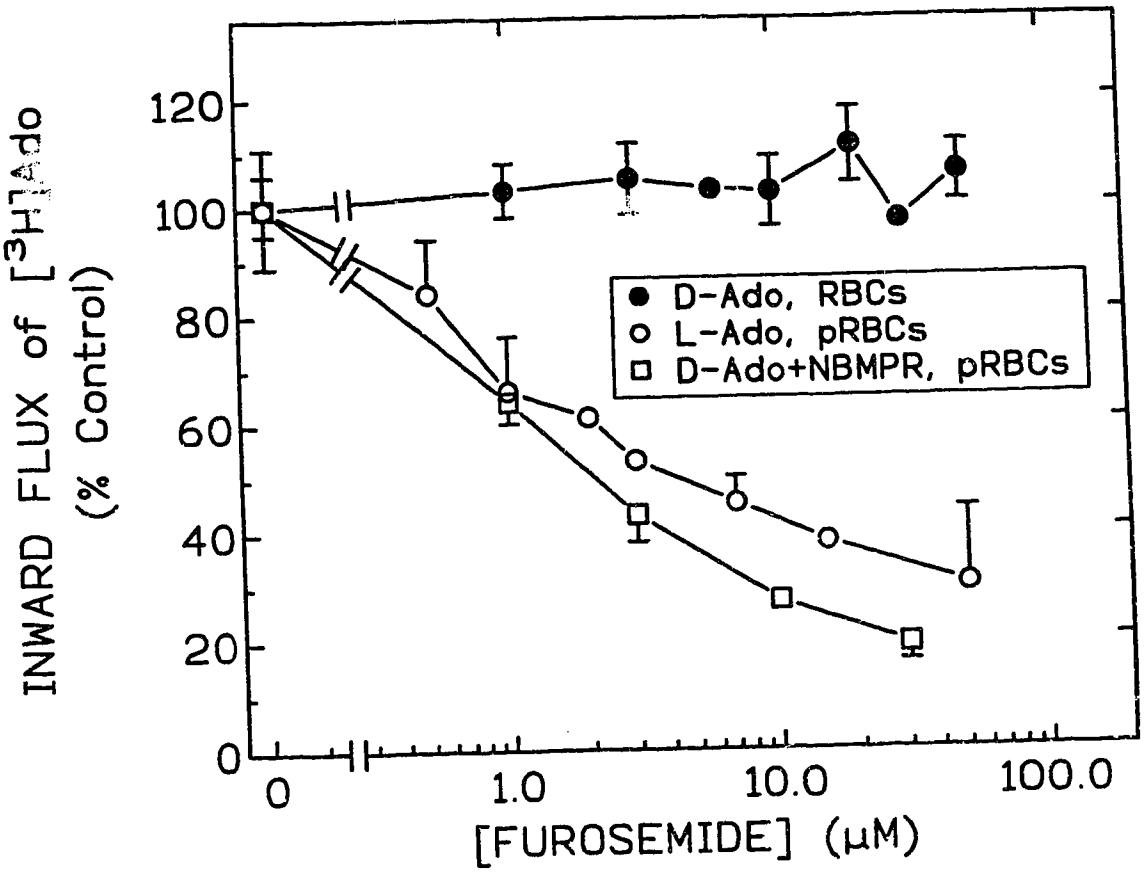

Figure 10. The effect of furosemide on Ado entry in RBCs and pRBCs.

The effect of furosemide on Ado entry in RBCs or pRBCs was examined by measuring the inward flux of 1μM [^{3}H]D-Ado in RBCs (●), 10μM [^{3}H]L-Ado in pRBCs (O) or 10μM [^{3}H]D-Ado + 1μM NBMPR in pRBCs (□) in control cells and in the presence of graded concentrations of furosemide.

The data are the means ± range or S.D. for 2 expts (●), 3-6 expts (O) and 3 expts (□) with each experiment representing the rate (as a percent of the control influx) determined from duplicate or tripiicate determinations at 3 and 5 sec of influx. Control rates in the absence of furosemide were: 0.21 ± 0.02 pmol/10^7cells/sec, n=2 (●); 0.65 ± 0.04 pmol/10^7cells/sec, n=6 (O); 0.57 ± 0.11 pmol/10^7cells/sec, n=3 (□). Apparent IC_{50} values were >50μM (●), ~4μM (O), and ~2μM (□).

indicated that furosemide was a potent, and selective, inhibitor of parasite-induced Ado entry and also suggested that L-Ado and D-Ado may enter pRBCs through the same, parasite-induced, pathway.

V. THE CONCENTRATION-DEPENDENCE OF ADENOSINE ENTRY INTO UNINFECTED AND MALARIA-INFECTED HUMAN ERYTHROCYTES

V.1. The concentration-dependence of D-Ado entry into RBCs

D-Ado enters RBCs through the es nucleoside transporter expressed in those cells (discussed in ref. 57). The concentration-dependence of es-mediated D-Ado influx in RBCs used in this study was examined in the experiments of Fig. 11 by determining the inward flux of [^{3}H]D-Ado at concentrations between 1 and 500μM. D-Ado entered RBCs through a single, saturable route with a Km of 189 ± 16μM and a Vmax of 23.6 ± 0.8 pmol/10^7cells/sec. The efficiency (Vmax/Km) of the es transporter in stored human erythrocytes, which had been incubated for 4-5 days at 37°C under the conditions of parasite growth, was approximately 125 pmol/10^7cells/sec/mM).

V.2. The concentration-dependence of D-Ado entry into pRBCs: The effect of NBMPR

Fig. 12 examines the concentration-dependence of D-Ado entry into pRBCs as well as the effect of NBMPR on this flux. The inward fluxes of [^{3}H]D-Ado were examined at a range of concentrations between 1μM and 20mM in the absence or presence of 1μM NBMPR. The rate of influx of D-Ado was not linearly dependent on the concentration of D-Ado employed, but was saturable. Fitting a rectangular hyperbola to the data indicated a single route of saturable entry for D-Ado with a Km of 13.1 ± 1.8 mM and a Vmax of 949 ± 64 pmol/10^7cells/sec.

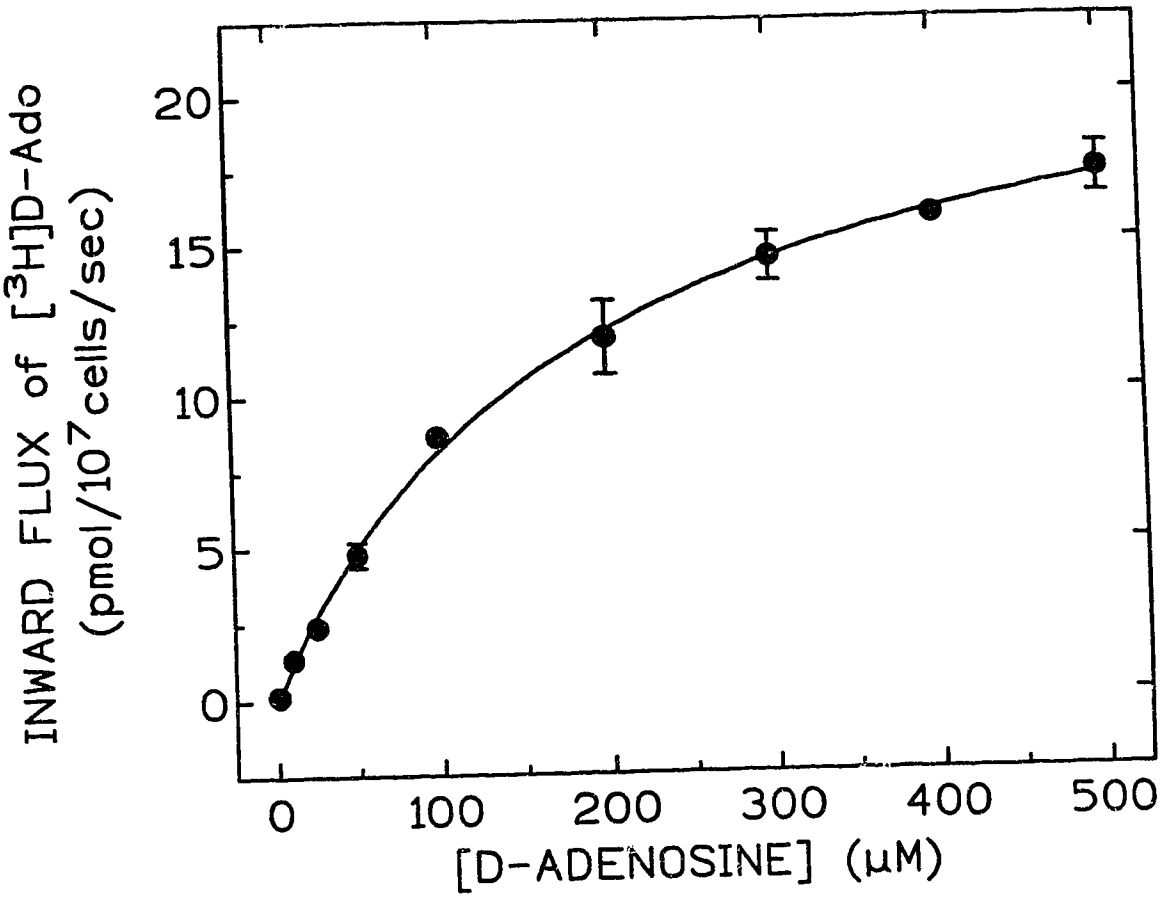

Figure 11. The concentration-dependence of D-Ado entry in RBCs.

The concentration-dependence of D-Ado entry in RBCs was examined by measuring the inward flux (pmol/10^7cells/sec) of graded concentrations of [^{3}H]D-Ado.

Each data point is the mean ± S.D. from 3 experiments with each experiment representing the rate determined from triplicate measurements at 3 and 5 sec of influx. Fitting a hyperbola to the data indicated the presence of a single, saturable route of D-Ado entry with a Km of 189 ± 16μM and a Vmax of 23.6 ± 0.8 pmol/10^7cells/sec.

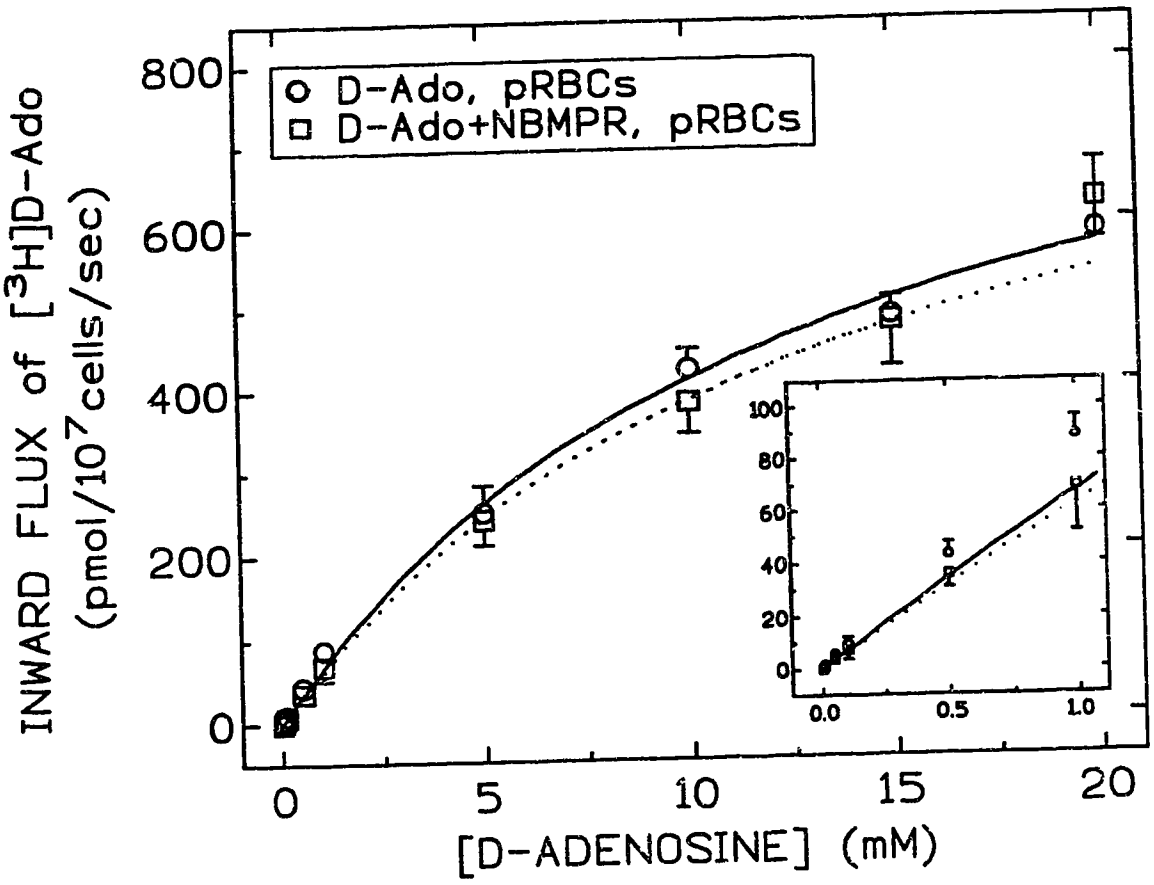

Figure 12. The concentration-dependence of D-Ado entry in pRBCs: The effect of NBMPR.

The concentration-dependence of D-Ado entry in pRBCs was examined by measuring the inward flux (pmol/10^7cells/sec) of graded concentrations of [^{3}H]D-Ado in the absence (O) or presence (□) of 1μM NBMPR.

Each data point is the mean ± S.D. from 3 experiments with each experiment representing the rate deterimined from duplicate or triplicate measurements at 3 and 5 sec of influx. Fitting hyperbolas to the data indicated, in the absence of NBMPR, a single route of saturation with a Km of 13.1 ± 1.8 mM and a Vmax of 949 ± 64 pmol/10^7cells/sec. In the presence of 1μM NBMPR, a similar result was obtained with a Km of 13.8 ± 0.5 mM and a Vmax of 910 ± 17 pmol/10^7cells/sec. (note: the 20mM data point in the presence of NBMPR was omitted forn the curve-fitting procedure - see text).

The inset illustrates the above curves at concentrations up to 1mM.

It was demonstrated previously (Fig. 5), that the entry of 1μM D-Ado into pRBCs and RBCs was inhibited, at least to a large extent, by 1μM NBMPR. However, as seen in Fig. 12, as the concentration of D-Ado was increased the contribution of this NBMPR-sensitive flux was not apparent in the measurement of D-Ado influx into pRBCs. There was no demonstrable effect of 1μM NBMPR on the inward flux of D-Ado into these cells at all but the lowest concentrations of permeant. The concentration-dependence of D-Ado entry into pRBCs in the presence of NBMPR was similar to that in the absence of NBMPR. Non-linear regression analysis suggested the presence of a single, saturable, route of entryof D-Ado in the presence of NBMPR, with a Km of 13.8 ± 0.5 mM and a Vmax of 910 ± 17 pmol/10^7cells/sec.

It must be noted that analysis of the data for D-Ado influx into pRBCs in the presence of NBMPR included concentrations of 1μM to only 15mM. This was done because including the 20mM data point in the calculations resulted in the data being significantly better fit (p=0.0002, F-test) by an equation with a Km of 3.10 ± 1.47 mM and a Vmax of 206 ± 57pmol/10^7cells/sec as well as an unsaturable component with a rate constant of 21.8 ± 2.2 pmol/10^7cells/sec/mM. A number of points argue in favour of the simpler model proposed by analysing the data to 15mM D-Ado. For example, if a saturable component with a Km of ~3mM and a Vmax of ~200mM existed, it should have been distinguishable in the absence of NBMPR as well as in its presence. In addition, the 20mM data point in the presence of NBMPR indicates a greater inward flux than in the absence of NBMPR, which is unlikely. Finally, the 20mM data points in the absence and presence of NBMPR were almost within error of each other.

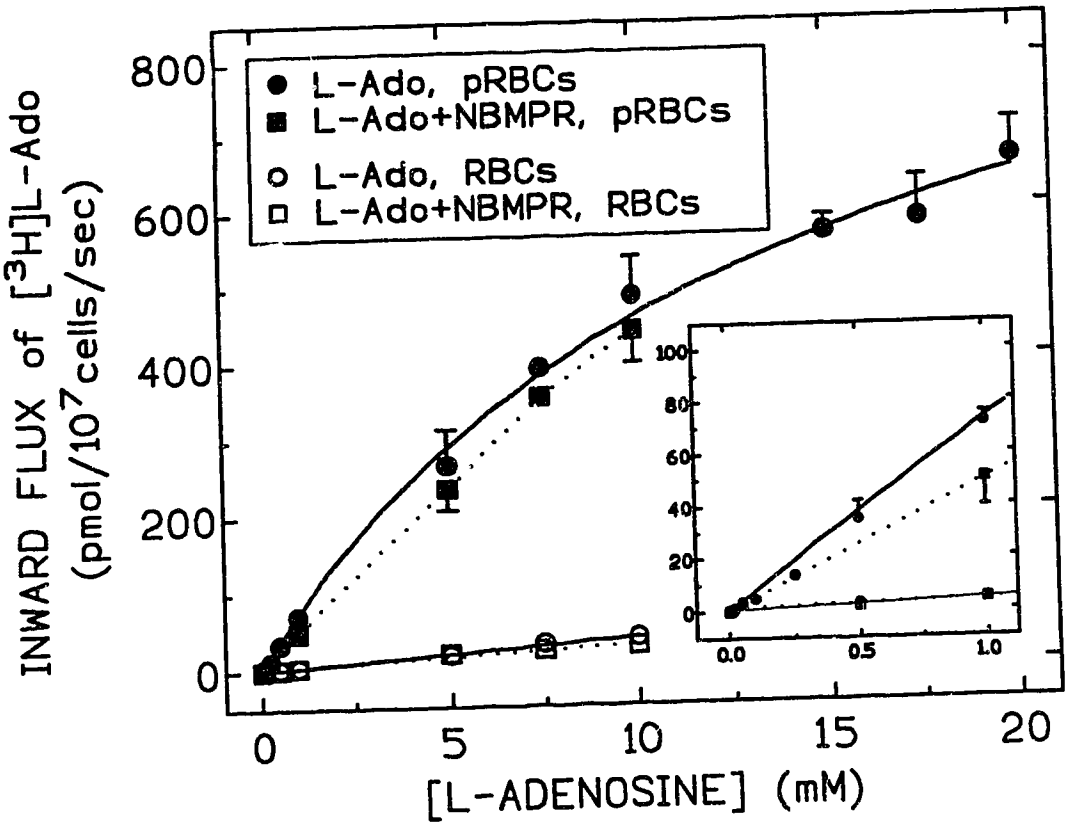

Figure 13. The concentration-dependence of L-Ado entry in RBCs and pRBCs: The effect of NBMPR.

The concentration-dependence of L-Ado entry in pRBCs and RBCs was examined by measuring the inward flux (pmol/10^7cells/sec) of graded concentrations of [^{3}H]L-Ado in RPMI^t or 30mM sodium phosphate buffer (see text). The entry of [^{3}H]L-Ado was examined in pRBCs in the absence (●) or presence (■) of 1μM NBMPR and in RBCs in the absence (O) or presence (□) of 1μM NBMPR.

For pRBCs, each data point is the mean ± range or S.D. from 2-6 experiments (●) or 2-3 expts (■) with each experiment representing the rate deterimined from duplicate or triplicate measurements at 3 and 5 sec of influx. Fitting hyperbolas to the data indicated, in the absence of NBMPR, a single route of saturation with a Km of 14.0 ± 1.6 mM and a Vmax of 1100 ± 62 pmol/10^7cells/sec. In the presence of 1μM NBMPR, a similar result was obtained, however, the data points were joined point-to-point but not analyzed by regression analysis due to the limited number of concentrations examined.

For RBCs, each data point is the mean ± S.D. from 3 experiments (O) or the mean ± range from 2 experiments (□) with each experiment representing the rate deterimined from triplicate measurements at 3 and 5 sec of influx. Analysis of the data by linear regression indicated a rate of 3.85 ± 0.11 pmol/10^7cells/sec/mM in the absence of NBMPR and a rate of 2.84 ± 0.29 pmol/10^7cells/sec/mM in the presence of NBMPR.

The inset illustrates the above curves at concentrations up to 1mM.

V.3. The concentration-dependence of L-Ado entry into pRBCs and RBCs: The effect of NBMPR

The concentration-dependence of L-Ado entry into pRBCs and RBCs was examined, as well as the effect of the nucleoside transport inhibitor NBMPR. Experiments were carried out in either RPMI[t] or 30mM sodium phosphate buffer (used with L-Gluc and D-Sorb, see below) with virtually identical results. In Fig. 13, the inward flux of L-Ado in pRBCs was determined for graded concentrations of [^{3}H]L-Ado in the presence or absence of 1μM NBMPR. As was the case with D-Ado, there was a striking difference in the rate of L-Ado influx in pRBCs compared to RBCs which became very evident as the concentration of L-Ado increased so that at 10mM L-Ado the inward flux in pRBCs was approximately 12 times that measured in RBCs. The influx of L-Ado into pRBCs appeared to occur through a single, saturable route with a Km of 14.0 ± 1.6 mM and a Vmax of 1100 ± 62 pmol/10^7cells/sec. In RBCs, the data were fit by least squares linear regression to yield a linear dependence of rate on concentration with a value of approximately 3.85 ± 0.11 pmol/10^7cells/sec/mM. In comparison to the results in pRBCs, only concentrations of L-Ado up to 10mM were examined due to the limited availability of L-Ado and the questionable value of the additional information to be gained by measuring influx at higher concentrations of this permeant.

Previous experiments had demonstrated only a very slight effect of 1μM NBMPR on the inward flux of L-Ado in pRBCs (see Table 1). In Fig. 13, the effect of NBMPR on the concentration-dependence of L-Ado influx into pRBCs and RBCs was examined. In both RBCs and pRBCs, the concentration-dependence of L-Ado influx in the presence of NBMPR was examined only to 10mM, a concentration high enough to allow a sufficient evaluation of the effect of NBMPR. There appeared to be only a small effect of NBMPR on L-Ado influx

Table 2. Kinetic Constants for Ado influx in RBCs and pRBCs

Condition	Km[a]	Vmax[b]	Vmax/Km[c]
RBCs			
D-Ado (11)	0.189 ± 0.016	23.6 ± 0.8	125
pRBCs			
D-Ado (12)	13.1 ± 1.8	949 ± 64	72.4
D-Ado+NBMPR (12)	13.8 ± 0.5	910 ± 17	65.9
L-Ado (13)	14.0 ± 1.6	1100 ± 62	78.6

[a]Km (mM) [b]Vmax (pmol/10^7cells/sec) [c]Vmax/Km (pmol/10^7cells/sec/mM)

Numbers in parentheses ( ) indicate the figure number from which the data was obtained.

in pRBCs and RBCs at millimolar concentrations of permeant. In pRBCs, the data were not analyzed by regression due to the low number of concentrations examined. However, in RBCs, there were sufficient data to allow the calculation of the apparent relationship between L-Ado concentration and inward flux. Least squares linear regression suggested a linear relationship existed between the concentration of L-Ado and the inward flux into RBCs with a rate constant of approximately 2.8 ± 0.29 pmol/10^7cells/sec/mM. The previously observed effect of NBMPR 10μM L-Ado entry into RBCs (see Table 1), suggested that a portion of L-Ado flux into RBCs was via the *es* nucleoside transporter, however two components of L-Ado entry into RBCs were not identified by non-linear regression of the data of Fig. 13. This may have been due to a lack of sufficient data. The kinetic data obtained for Ado influx in RBCs and pRBCs (summarized in Table 2), indicated a large decrease in the efficiency (Vmax/Km) of D-Ado transport in pRBCs compared to RBCs (~72 and ~125 pmol/10^7cells/sec/mM, respectively). D-Ado influx in pRBCs, in the presence or absence of NBMPR, occured with an efficiency similar to that of L-Ado (~78 pmol/10^7cells/sec/mM).

VI. THE ENTRY OF L-GLUCOSE INTO UNINFECTED AND MALARIA-INFECTED HUMAN ERYTHROCYTES

VI.1. The influx of 2mM L-Gluc into RBCs and pRBCs

Another solute that has been reported to enter rodent (26) and human (35) pRBCs via a non-stereoselective parasite-induced route is L-Gluc. This observation, and the previously discussed similarities between glucose and nucleoside entry routes in RBCs led us to investigate some of the characteristics of the entry of L-Gluc into pRBCs as a comparison with the Ado entry route described above. Fig. 14 demonstrates the lack of stereoselectivity of glucose

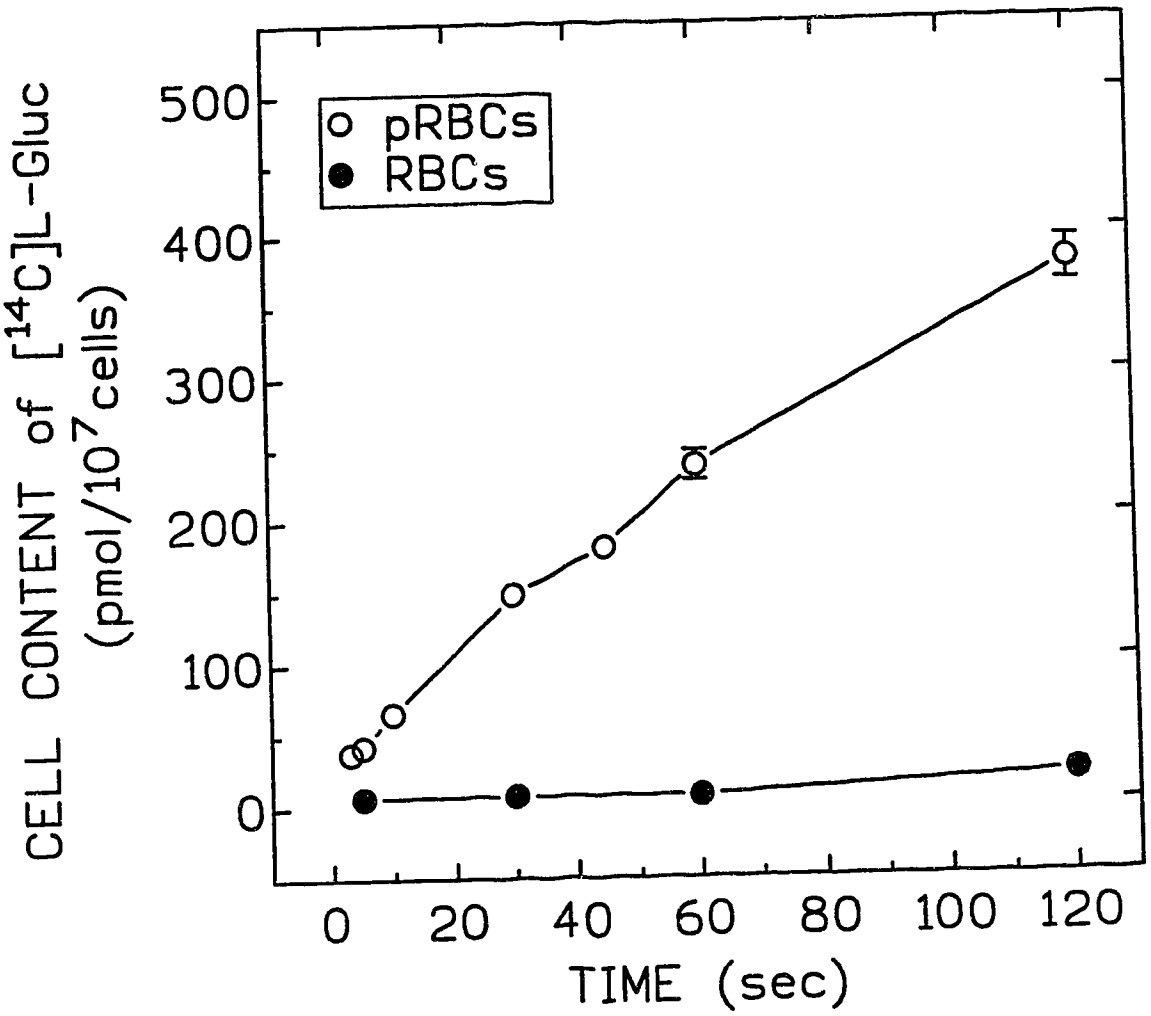

Figure 14. The inward flux of 2mM L-Gluc in pRBCs and RBCs.

The cellular content of [^{14}C]L-Gluc was measured at the indicated intervals after the addition of 2mM [^{14}C]L-Gluc to 2x10^7 pRBCs or RBCs.

The data are those obtained in a single experiment in each of pRBCs (O) or RBCs (●). Each point is the mean ± range from duplicate determinations in pRBCs or the mean ± S.D. from triplicate determinations in RBCs.

transport observed in pRBCs compared to RBCs. This study employed L-Gluc at a concentration (2mM) chosen to be similar to the Km of D-glucose entry into RBCs (110). There was a large increase in the cell content of radiolabelled L-Gluc in pRBCs compared to the uninfected controls at each time point examined. The influx of 2mM L-Gluc into pRBCs was very rapid while the influx into RBCs was almost unmeasurable suggesting the existence of a pathway for the entry of L-Gluc into pRBCs which was absent in RBCs. Although the time course of L-Gluc influx into pRBCs appeared to be linear until approximately one min, subsequent experiments measured only influx between 5 and 15 sec to estimate the inward flux.

VI.2. The effect of NBMPR or CB on the inward flux of 2mM L-Gluc in pRBCs

The ability of the nucleoside transport inhibitor NBMPR, or the glucose transport inhibitor CB, to inhibit the entry of L-Gluc into pRBCs was examined. This allowed a comparison with the data obtained with L-Ado and an evaluation of whether the *es* nucleoside transporter or Glut1 were involved in L-Gluc entry into pRBCs. This was done by measuring the effect of 1μM NBMPR or 5μM CB on the inward flux of 2mM [^{14}C]L-Gluc into these cells. Fig. 15 demonstrates the effect of these agents on 2mM L-Gluc entry into pRBCs. Both NBMPR and CB reduced 2mM L-Gluc influx into pRBCs by less than 20%. The inward fluxes were 4.60 ± 0.37 pmol/10^{7}cells/sec in controls, 3.85 ± 0.25 pmol/10^{7}cells/sec in the presence of 1μM NBMPR and 3.73 ± 0.06 pmol/10^{7}cells/sec in the presence of CB. Statistical analysis (Dunnett's multiple range test) demonstrated that these inhibitory effects were statistically significant (α=0.01), however, the lack of complete inhibition by NBMPR or CB at the concentrations tested suggested that L-Gluc was not entering pRBCs via either the *es* nucleoside transporter or Glut1.

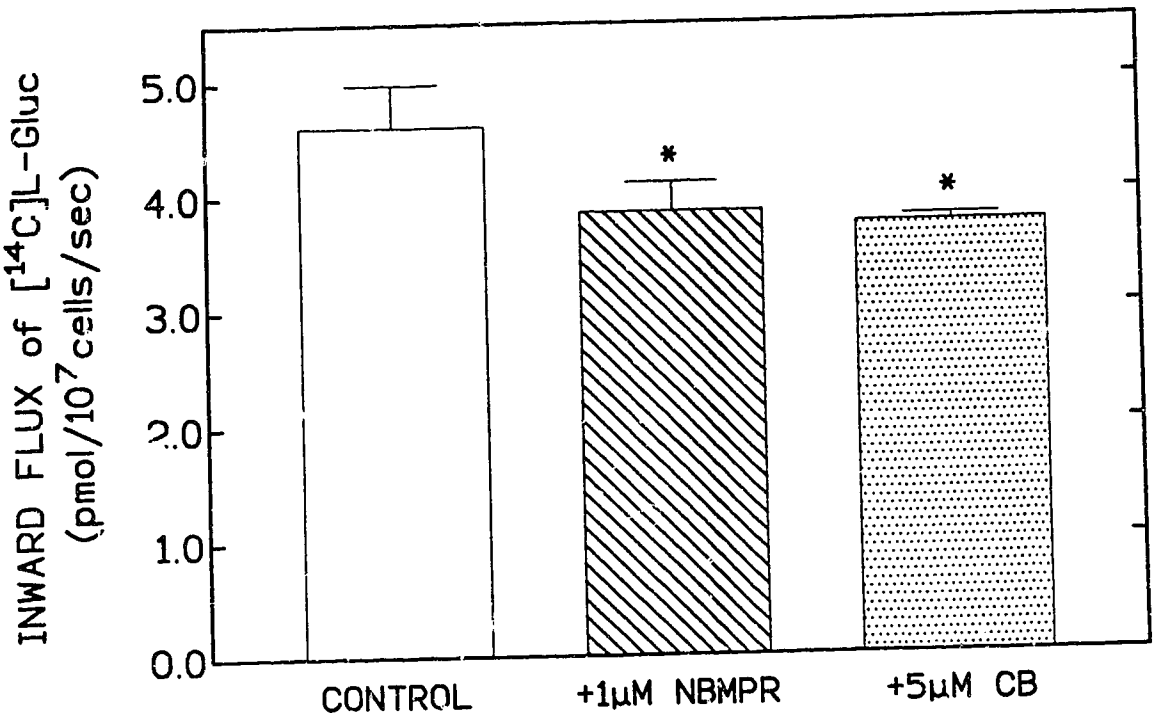

Figure 15. The effect of NBMPR or CB on the inward flux of 2mM L-Gluc in pRBCs.

The ability of NBMPR or CB to inhibit L-Gluc influx into pRBCs was examined by comparing the inward flux of 2mM [^{14}C]L-Gluc in the presence of 1μM NBMPR (hatched bar) or 5μM CB (speckled bar) with the inward flux measured in the absence of inhibitors (open bar). Control permeant solutions for comparison with CB-containing samples, contained 0.08% (v/v) DMSO.

The data are mean ± S.D. for control (n=6), 1μM NBMPR (n=3) or 5μM CB (n=3) experiments with each experiment representing duplicate or triplicate measurements at 5 and 15 sec of influx.

Statistical anaylsis using Dunnett's multiple range test showed significant (α=0.01) inhibition by both NBMPR and CB.

VI.3. The concentration-dependence of L-Gluc entry into RBCs and pRBCs

The concentration-dependence of L-Gluc influx into pRBCs and RBCs was examined. In order to maintain the correct osmolarity of permeant solutions containing high concentrations of L-Gluc, it was necessary to dissolve L-Gluc in a low osmolality buffer (approximately 20 mOsm) containing 9mM sodium phosphate and 0.8mM potassium chloride before being diluted with an iso-osmotic sodium phosphate buffer containing 30mM sodium phosphate, 2.8mM KCl and 117mM NaCl. When fluxes of 2mM to 50mM L-Gluc were measured using this permeant solution and cells suspended in the 30mM sodium phosphate buffer, the entry rates of L-Gluc in pRBCs were virtually identical to those obtained in RPMI[t].

Fig. 16 demonstrates the much higher rates of influx obtained in pRBCs compared to RBCs. By 190mM, the rate of L-Gluc influx into pRBCs was approximately 10-fold higher than that measured in RBCs. In contrast to Ado influx in pRBCs, there was not the obvious saturation of influx of L-Gluc into pRBCs by 20mM. It appeared that the entry of L-Gluc into pRBCs was unsaturable. Regression analysis of the data indicated an unsaturable entry pathway with a rate constant of 1.74 ± 0.08 pmol/10^7cells/sec/mM. In RBCs, the rate of entry of L-Gluc was much lower than that observed in pRBCs at each concentration examined. The concentration-dependence of the inward flux of L-Gluc entry into RBCs appeared to be linear and analysis by least squares linear regression yielded a rate constant of 0.17 ± 0.08 pmol/10^7cells/sec/mM.

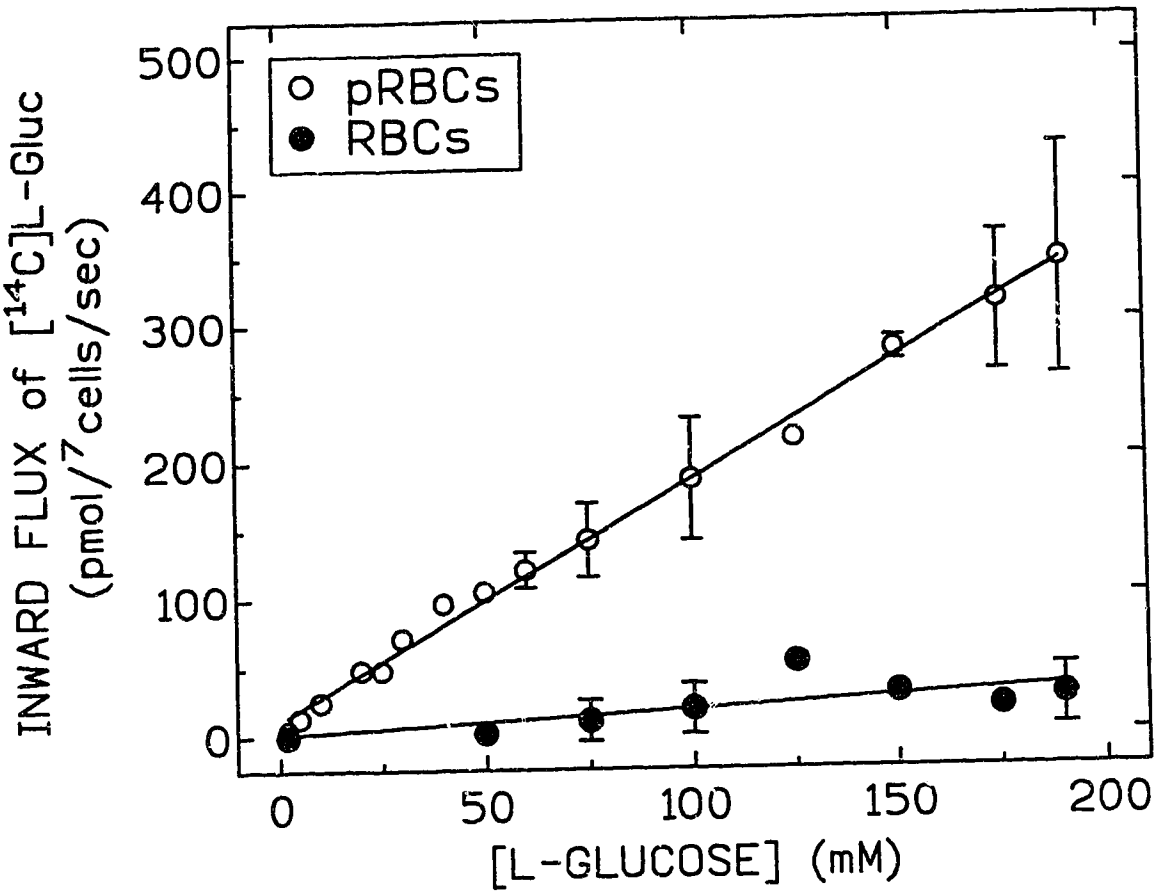

Figure 16. The concentration-dependence of L-Gluc entry in pRBCs and RBCs.

The concentration-dependence of L-Gluc entry in pRBCs (O) and RBCs (●) was examined by measuring the inward flux (pmol/10^7cells/sec) of graded concentrations of [^{14}C]L-Gluc in a sodium phosphate buffer system (see text) at 5 and 15 sec.

For pRBCs, each data point is the mean ± range or S.D. from 2-9 experiments with each experiment representing duplicate or triplicate measurements of influx. The data were best fit by a model for a single route of unsaturable entry with rate of 1.74 ± 0.08 pmol/10^7cells/sec/mM. (note: for this curve only, the inward fluxes were not averaged at each concentration of L-Gluc before analysis by non-linear regression, in order to take into account the differences in "n" values between L-Gluc concentrations.)

For RBCs, each data point is the mean ± range or S.D. from 2 or 3 experiments with each experiment representing triplicate measurements of influx. Analysis of the data by linear regression indicated a rate of 0.17 ± 0.08 pmol/10^7cells/sec/mM.

VII. THE ENTRY OF D-SORBITOL INTO UNINFECTED AND MALARIA-INFECTED HUMAN ERYTHROCYTES

VII.1. The influx of 2mM D-Sorb into RBCs and pRBCs

We also examined some of the characteristics of the entry of D-Sorb into pRBCs, for comparison with Ado and L-Gluc entry. Fig. 17 examined the time course of 2mM D-Sorb entry into pRBCs and RBCs. The cell content of D-Sorb in RBCs was barely measurable, even at 30 sec, while the content of D-Sorb was much higher in pRBCs, suggesting the existence of a parasite-induced route of D-Sorb entry into pRBCs. The time course of D-Sorb entry into pRBCs appeared to be linear for almost 30 sec, and subsequent experiments to measure inward fluxes determined the cell content of [^{14}C]D-Sorb at 5 and 15 sec.

VII.2. The concentration-dependence of D-Sorb entry into pRBCs

The saturability of the route of D-Sorb entry into pRBCs was examined. Fig. 18 demonstrates the concentration-dependence of the inward flux of D-Sorb in pRBCs. The data indicated that D-Sorb influx was linearly dependent on permeant concentration up to at least 190 mM, suggesting that D-Sorb entered pRBCs via an unsaturable pathway. Analysis of the data by least squares linear regression indicated a linear relationship between the inward flux and D-Sorb concentration with a rate constant of 4.56 ± 0.21 pmol/10^{7}cells/sec/mM. As with L-Gluc, it was necessary to use a sodium phosphate buffer system rather than RPMI in order to maintain the correct osmolality. A stock solution of sorbitol dissolved in 9mM sodium phosphate buffer was diluted to the appropriate concentration with 30mM sodium phosphate buffer as described above for L-Gluc.

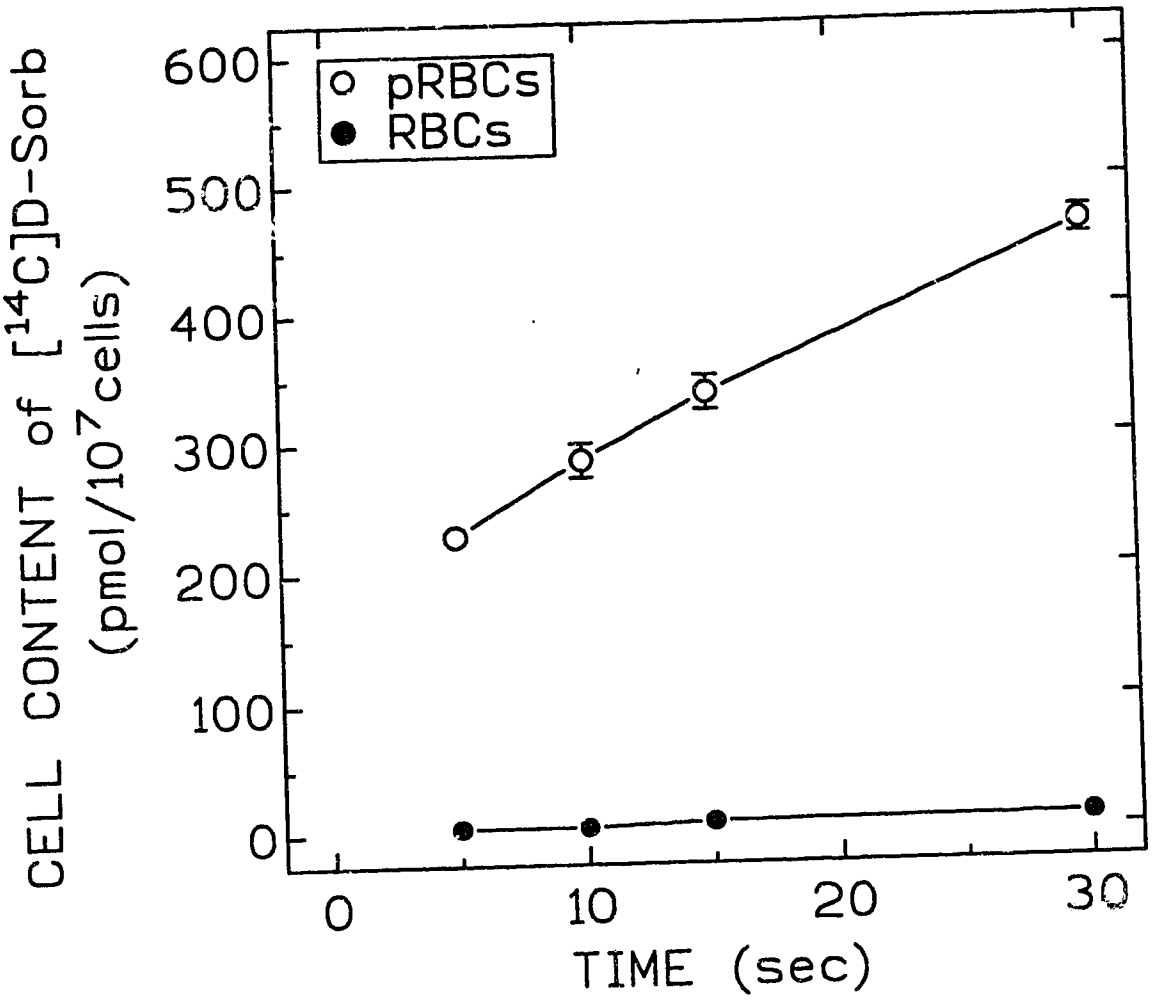

Figure 17. The inward flux of 2mM D-Sorb in pRBCs and RBCs.

The cellular content of [^{14}C]D-Sorb was measured at the indicated intervals after the addition of 2mM [^{14}C]D-Sorb to 2x10^7 pRBCs or RBCs.

The data are those obtained in a single experiment in each of pRBCs (O) or RBCs (●) with each point representing the mean ± range from duplicate determinations in pRBCs or RBCs.

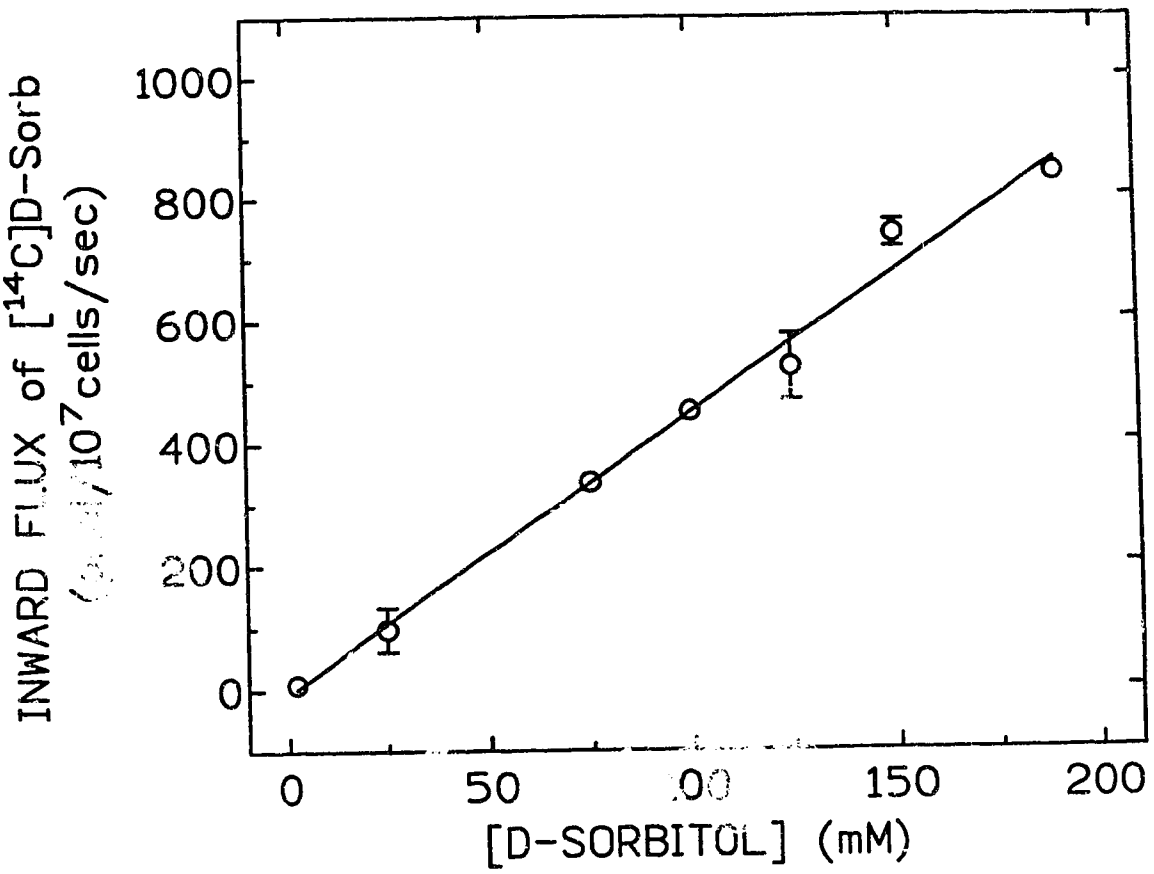

Figure 18. The concentration-dependence of D-Sorb entry in pRBCs.

The concentration-dependence of D-Sorb entry in pRBCs was examined by measuring the inward flux (pmol/10^7cells/sec) of graded concentrations of [^{14}C]D-Sorb in a sodium phosphate buffer system (see text) at 5 and 15 sec.

The data are the mean ± range of the inward flux determined in 2 experiments with duplicate measurements of influx. Analysis of the data by least squares linear regression yielded a single route of unsaturable entry with a rate of 4.56 ± 0.21 pmol/10^7cells/sec/mM.

VIII. DO ADENOSINE, L-GLUCOSE AND D-SORBITOL SHARE A ROUTE OF ENTRY INTO MALARIA-INFECTED HUMAN ERYTHROCYTES?

VIII.1. The effect of furosemide on the entry of L-Gluc or D-Sorb in pRBCs

This study showed that furosemide was a potent inhibitor of D- and L-Ado entry into pRBCs with apparent IC_{50} values in the range of 2-4μM (Fig. 10). Fig. 19 shows the effect of 3 concentrations of furosemide on the entry of L-Gluc or D-Sorb into pRBCs. The inward flux of 2mM [^{14}C]L-Gluc entry into pRBCs (control rate: 4.84 ± 0.32 pmol/10^{7}cells/sec) was reduced to 74 ± 7%, 60 ± 3% and 40 ± 6% of the control rate by the addition of 1μM, 3μM and 10μM furosemide, respectively. This suggested an IC_{50} value for the inhibition of 2mM L-Gluc influx into pRBCs would lie between 3 and 10μM, a value similar to those for the inhibition of L-Ado and D-Ado entry into pRBCs. The inward flux of 2mM [^{14}C]D-Sorb in pRBCs (control rate: 8.30 ± 1.32 pmol/10^{7}cells/sec) was reduced to 44 ± 2%, 29 ± 6% and 15 ± 3% of control rates by the addition of 1μM, 3μM and 10μM furosemide respectively. This suggested an IC_{50} value for the inhibition of 2mM D-Sorb influx into pRBCs of less than 1μM, a value similar to those reported above for D-Ado, L-Ado and L-Gluc, suggesting the possibility that the four permeants shared a parasite-induced route of entry into pRBCs.

VIII.2. Mutual inhibition of the parasite-induced entry of L-Ado, L-Gluc, or D-Sorb in pRBCs

Permeants that enter cells by the same entry process may be able to inhibit each other's entry. The saturability of parasite-induced Ado fluxes in pRBCs suggested an interaction of Ado with this route. Fig. 20 shows the ability of 20mM L-Ado, 190mM L-Gluc or 190mM D-Sorb to inhibit the entry of 10μM [^{3}H]L-Ado, 2mM [^{14}C]L-Gluc or 2mM [^{14}C]D-Sorb in pRBCs.

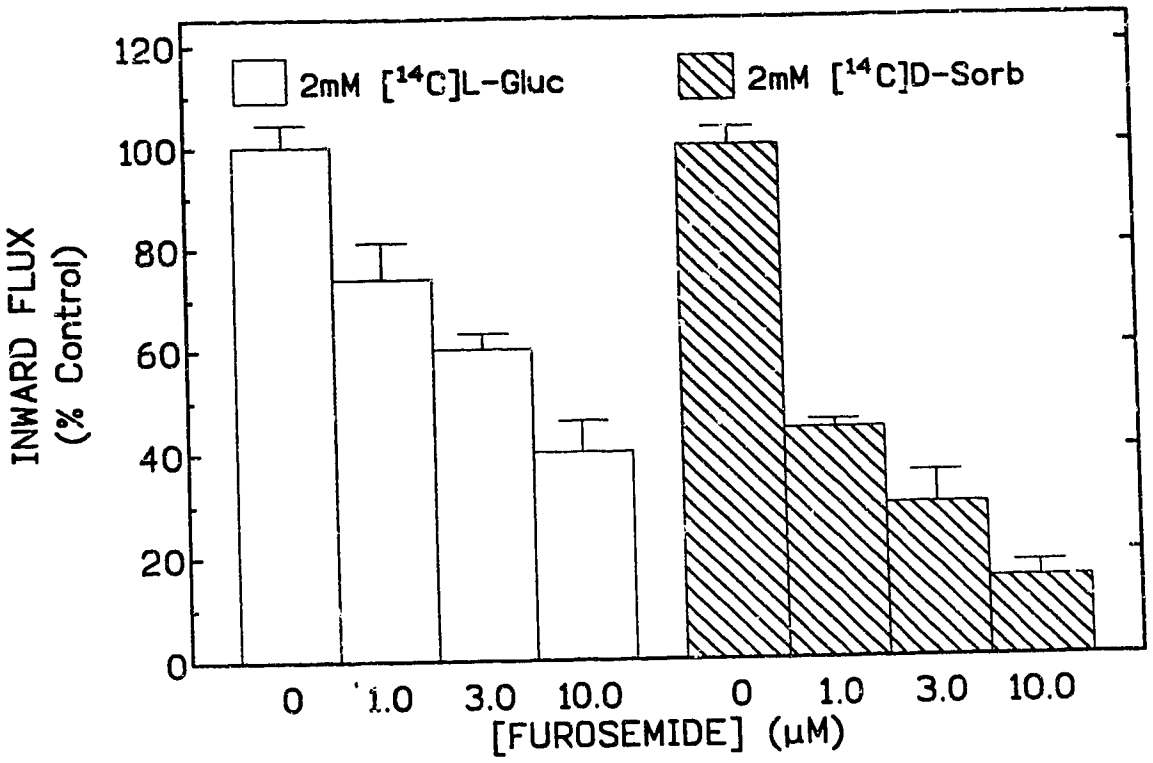

Figure 19. The effect of furosemide on the entry of L-Gluc or D-Sorb into pRBCs.

The inhibition by furosemide of the entry of L-Gluc or D-Sorb into pRBCs was examined by measuring the effect of graded concentrations of furosemide on the inward flux of 2mM [^{14}C]L-Gluc (open bars) or 2mM [^{14}C]D-Sorb (hatched bars) into these cells. The inward flux was determined by measuring the cellular content of radiolabelled permeant (duplicates or triplicates) in pRBCs at 5 and 15 sec of incubation, and expressed as a percentage of the control rate of influx. Cells were exposed to furosemide for 15 min at room temperature before measurement of permeant influx; permeant solution also contained furosemide.

The data are the mean ± range for 2 experiments with each permeant. The inward fluxes in the absence of furosemide were 4.84 ± 0.32 pmol/10^7cells/sec (L-Gluc) and 8.30 ± 1.32 pmol/10^7cells/sec (D-Sorb).

Figure 20. Mutual inhibiton of the parasite-induced entry of L-Ado, L-Gluc, or D-Sorb into pRBCs.

The ability of permeants for a parasite-induced entry process(es) in pRBCs to interact with each other was examined by measuring the effects of non-radioactive permeants on inward fluxes of radiolabelled permeants. The inward fluxes (pmol/10^7cells/sec) were measured in pRBCs with A) 10μM [^{3}H]L-Ado, B) 2mM [^{14}C]L-Gluc and C) 2mM [^{14}C]D-Sorb in the absence or presence of non-radioactive permeants at concentrations of 20mM (L-Ado) or 190mM (L-Gluc and D-Sorb). Inward fluxes were determined by measuring the cell content of radiolabel in duplicate samples at 3 and 5 sec (L-Ado) or in triplicate samples at 5 and 15 sec (L-Gluc and D-Sorb).

The data are expressed as a percentage of the influx in the absence of inhibitors and presented as the mean ± range for two experiments with each condition. Control rates (pmol/10^7cells/sec) were: 10μM L-Ado; 0.66 ± 0.19, 2mM L-Gluc; 4.58 ± 0.08, and 2mM D-Sorb; 9.02 ± 0.36.

Permeants containing L-Gluc or D-Sorb (190 mM) were prepared using the sodium phosphate buffer system described for Fig. 13, 16 and18.

Statistical analysis of the data (Dunnett's multiple range test) demonstrated a significant inhibition of influx where marked with an asterisk (* α=0.01).

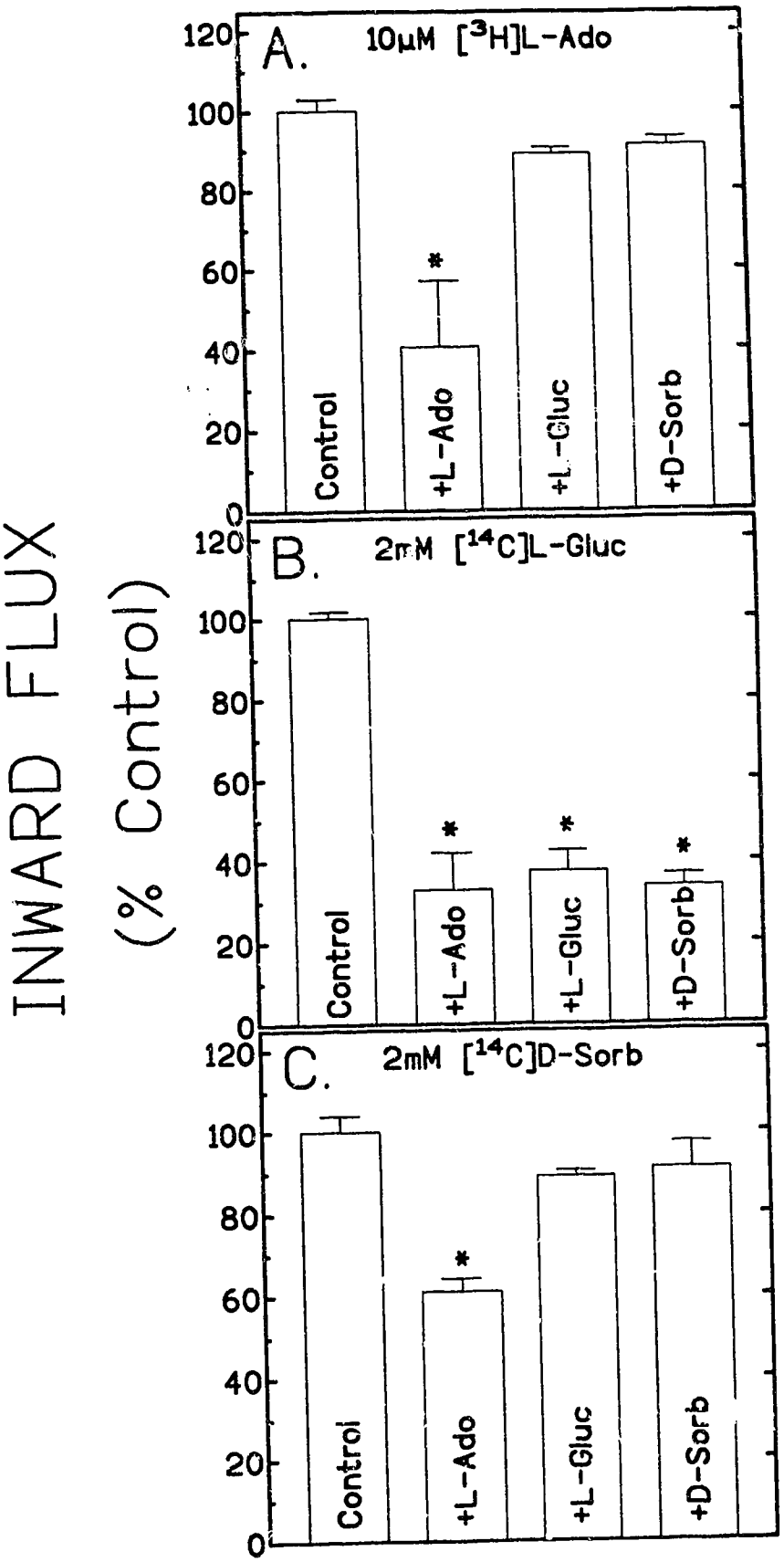
INWARD FLUX
(% Control)
A. 10μM [3H]L-Ado
B. 2mM [14C]L-Gluc
C. 2mM [14C]D-Sorb
Control
+L-Ado
+L-Gluc
+D-Sorb
0
20
40
60
80
100
120
*

In part A of Fig. 20, the addition of 20mM non-radioactive L-Ado to a permeant solution containing 10μM [^{3}H]L-Ado significantly reduced (Dunnett's test, α=0.01) the inward flux to 40.5 ± 16.5% of the flux measured in the absence of excess L-Ado. In contrast, neither 190mM L-Gluc nor 190mM D-Sorb had any statistically significant effect on the entry of 10μM [^{3}H]L-Ado into pRBCs.

In a parallel set of experiments (Fig. 20-B), the effect of non-radioactive L-Ado, L-Gluc or D-Sorb on the inward flux of entry of 2mM [^{14}C]L-Gluc in pRBCs was examined. All three solutes significantly (Dunnett's test, α=0.01) reduced the entry of 2mM L-Gluc into pRBCs. The inward flux was reduced to 33.0 ± 9.0%, 37.5 ± 5.0%, and 33.8 ± 2.9% of the control rate by 20mM L-Ado, 190mM L-Gluc and 190mM D-Sorb, respectively.

In Fig. 20-C, the ability of 20mM L-Ado, 190mM L-Gluc or 190mM D-Sorb to inhibit the entry of 2mM [^{14}C]D-Sorb into pRBCs was examined. Only 20mM L-Ado significantly reduced (61.0 ± 3.0% of control, Dunnett's test α=0.01) the inward flux of 2mM [^{14}C]D-Sorb in pRBCs. There was no significant effect on 2mM [^{14}C]D-Sorb entry by either 190mM L-Gluc or 190mM D-Sorb.

The ability of L-Ado to inhibit the entry of all three pRBC permeants suggests that they may all utilize the same pathway for entry into pRBCs.

VIII.3. Inhibition of the entry of 2mM L-Gluc into pRBCs: The effect of other permeants

Fig. 21 is analogous to part B of Fig. 20 (see above) but involved an examination of the effect of 10mM non-radioactive L-Ado, L-Gluc or D-Sorb on the inward flux of 2mM [^{14}C]L-Gluc into pRBCs. In contrast to the data in Fig 20-B, only 10mM L-Ado and 10mM L-Gluc reduced the entry of 2mM [^{14}C]L-Gluc into pRBCs. Both solutes reduced the inward flux of 2mM [^{14}C]L-Gluc to approximately 60% of the control value. 10mM L-Ado reduced the inward flux of

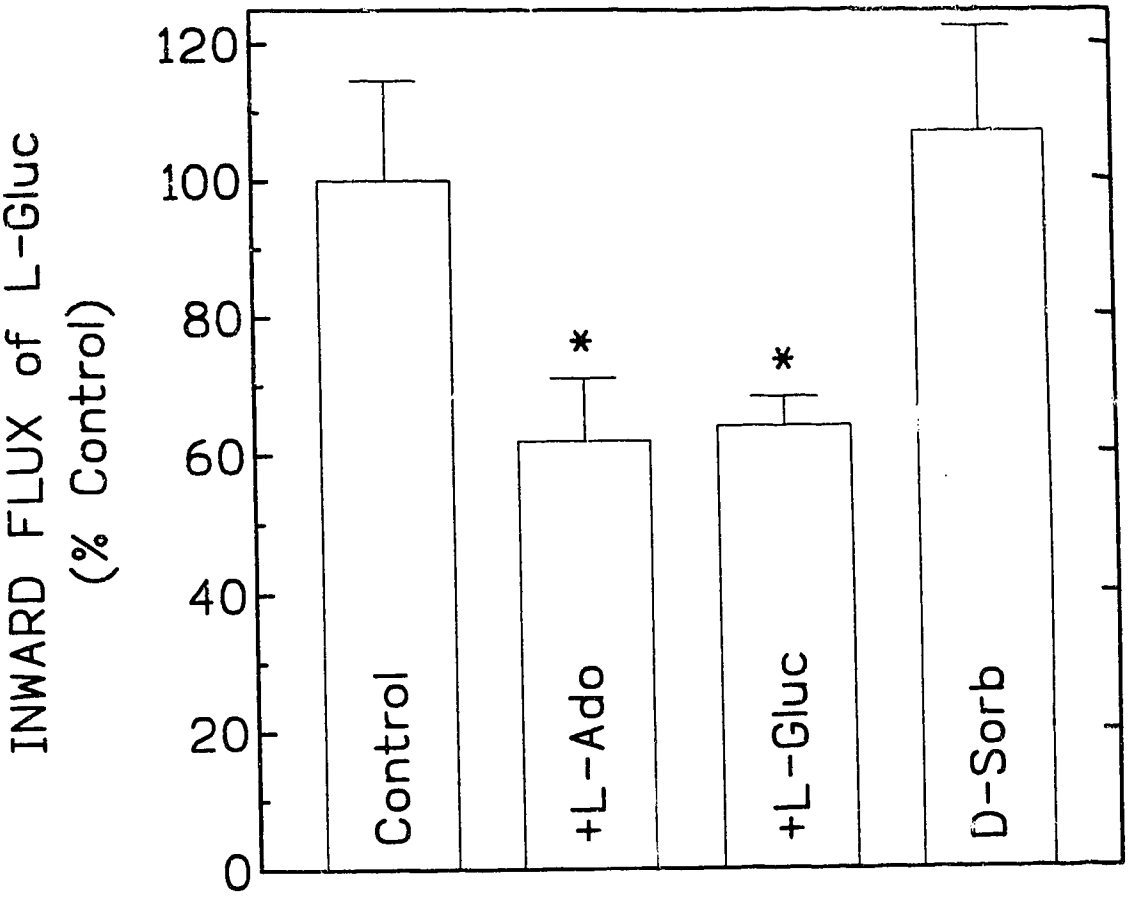

Figure 21. Inhibition of the entry of 2mM L-Gluc into pRBCs: The effects of other permeants.

The effects of non-radiolabelled permeants (10mM L-Ado, L-Gluc or D-Sorb) on the inward flux of 2mM [^{14}C] or [^{3}H]L-Gluc in pRBCs were measured. Inward flux was obtained from duplicate or triplicate measurements of the cell content of radiolabel at 5 and 15 sec of uptake.

The data are the mean ± range or S.D. of the inward flux in the presence of inhibitors as a percentage of the rate measured in the absence of inhibitors for 2 expts (L-Ado and D-Sorb) or 3 expts (L-Gluc). The control rate was 4.41 ± 0.62 pmol/10^7cells/sec, n=7.

Statistical analysis (Dunnett's multiple range test) indicated a significant inhibitory effect for both L-Ado and L-Gluc (* α=0.01).

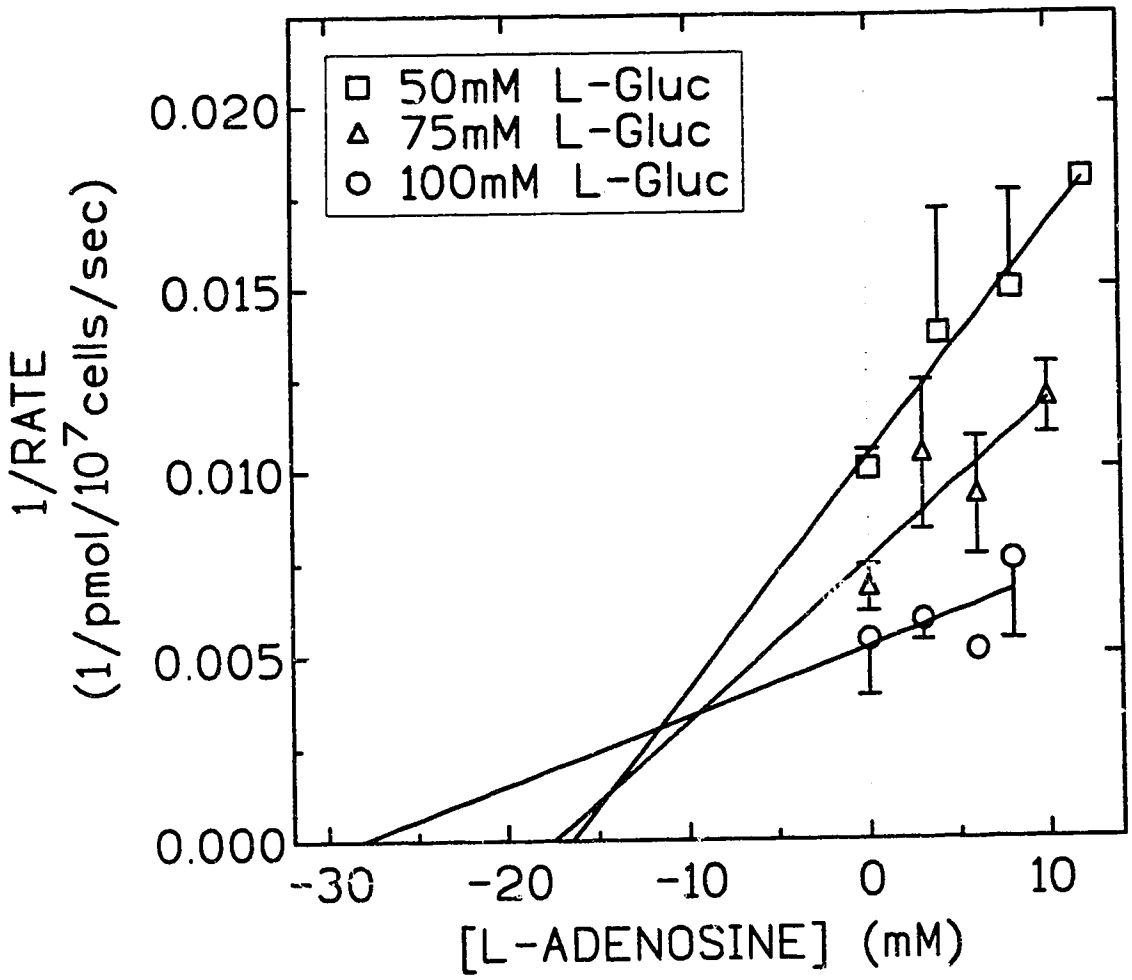

Figure 22. The inhibition of L-Gluc entry in pRBCs by graded concentrations of L-Ado.

The inward fluxes of 50mM, 75mM, or 100mM [^{3}H]L-Gluc were measured in the presence of graded concentrations of non-radiolabelled L-Ado. Inward flux was obtained from duplicate or triplicate measurements of the cell content of radiolabel at 5 and 15 sec of uptake. Experiments were performed with L-Ado and L-Gluc dissolved in sodium phosphate buffer as in Fig. 13 and Fig. 16.

The data are the mean ± S.D. of the inward flux in the presence or absence of L-Ado for 3 expts and are expressed in a Dixon plot.

2mM [^{14}C]L-Gluc to 61.8 ± 9.1% of the control value and 10mM L-Gluc reduced influx to 63.9 ± 4.2% of the control value. This reduction by L-Ado or L-Gluc was significant (Dunnett's test α=0.01) suggesting that both L-Ado and L-Gluc interacted with the route of L-Gluc entry into pRBCs. The lack of an effect by 10mM D-Sorb suggests that the 190mM concentration used in Fig. 21-B may have had non-specific inhibitory effects on L-Gluc entry into pRBCs.

Fig. 22 shows a Dixon plot describing the inhibition of the inward fluxes of 50mM, 75mM and 10mM [^{14}C]L-Gluc by graded concentrations of L-Ado. L-Ado was able to inhibit L-Gluc flux with an apparent Ki of between 10mM and 30mM. The data did not allow the nature of the inhibition (competitive or non-competitive) to be determined.

IX. THE METABOLISM OF ADENOSINE BY UNINFECTED AND MALARIA-INFECTED HUMAN ERYTHROCYTES

IX.1. The metabolism of 5µM D- and L-Ado in RBCs and pRBCs

Fig. 23-A. shows the separation of AMP, Ino, Hyp and [illegible] obtained using the silica gel thin layer chromatography pr[illegible] in Fig. 24 show the formation of metabolites from 5µM [illegible] and pRBCs during a 5-min incubation at 37°C. In both [illegible] of radiolabelled metabolite recovered after the incubati[illegible] "AMP" (or other nucleotides, see below) >>> Hyp > In[illegible] 24-A also indicated that the amount of "AMP" formed in pRBCs was significantly (Student's t-test, p<0.005) greater than in RBCs (67.2 ± 13.4% and 44.0 ± 13.5% of the total, respectively). The metabolite at the origin of the chromatogram was probably not limited to AMP, but may have included other nucleotides. In pRBCs, AMP, ADP, ATP, GMP, GDP, GTP, IMP, AMPS and XMP can all be formed during the metabolism of D-Ado. By contrast, in RBCs only AMP, ADP,

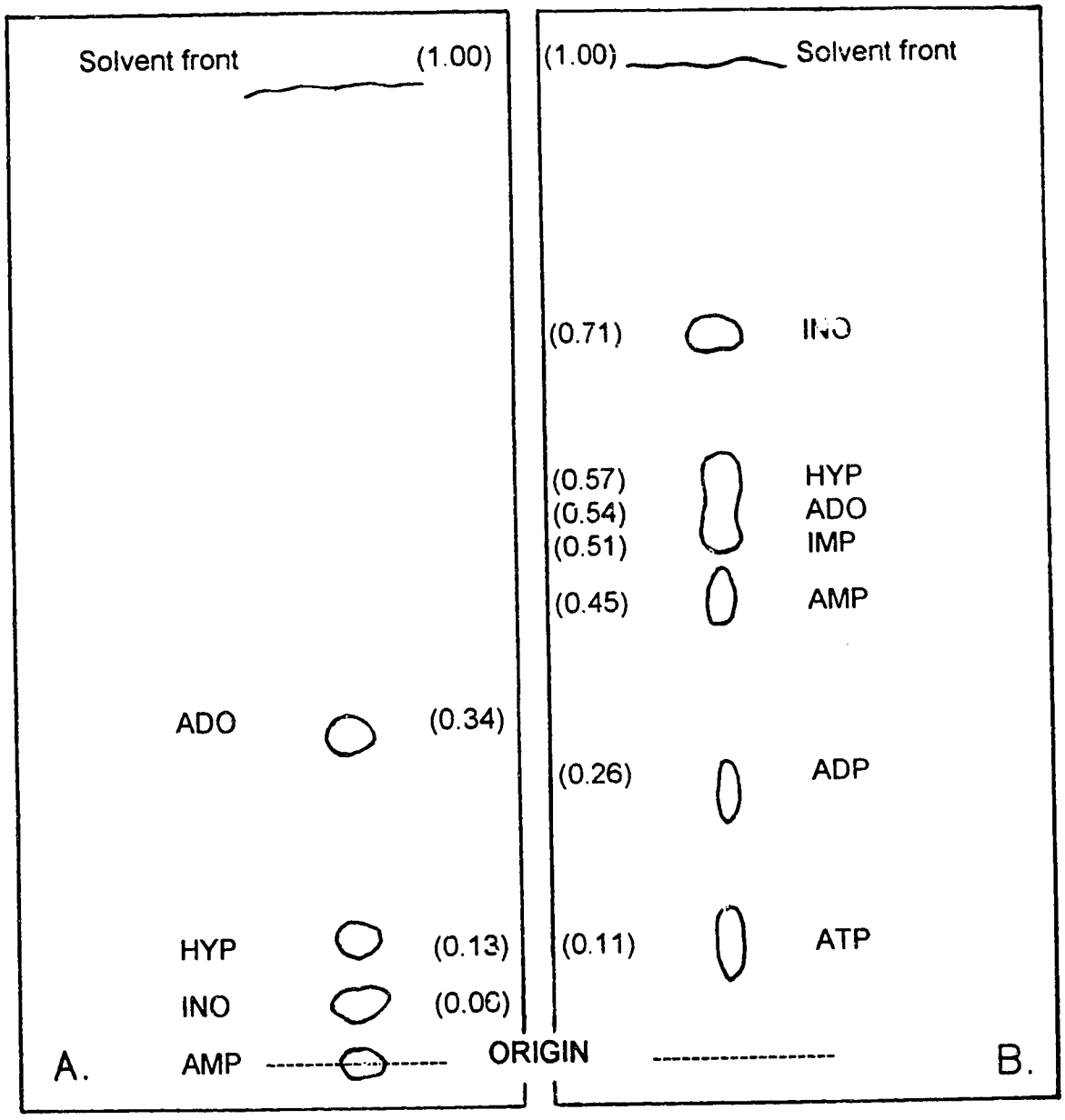

Figure. 23. The separation of Hyp, nucleosides and nucleotides by thin layer chromatography on Silica Gel G and PEI-Cellulose.

Panel A. The separation of AMP, Ino, Hyp and Ado on Silica Gel G thin layer chromatography sheets developed in $CHCl_3$:MeOH:15%NH_4OH (3:2:1, v/v).

Panel B. The separation of AMP, ADP, ATP, IMP, Ino, Hyp and Ado on PEI-Cellulose thin layer chromatography sheets developed in 1M LiCl, 1.15M H_3BO_3, pH 7.0.

Figure 24. The metabolism of 5μM D-Ado and L-Ado in RBCs and pRBCs, during 5-min intervals.

The metabolism of D-Ado and L-Ado was examined in RBCs and pRBCs by following the appearance of radioactive metabolites after the incubation of A) 5μM [^{3}H]D-Ado or B) 5μM [^{3}H]L-Ado at 37°C for 5 min. The metabolites formed were extracted with 70% methanol and separated with the standards of Fig. 23-A on Silica Gel G thin layer chromatography sheets with $CHCl_3$:MeOH: 15%NH_4OH (3:2:1, v/v).

The amount of radioactivity recovered for each metabolite (after subtraction of background radioactivity) is plotted as a percentage of the total amount of radioactivity recovered. The data are the mean ± S.D. from 7 replicates (D-Ado and L-Ado, RBCs), 8 replicates (D-Ado, pRBCs) and 9 replicates (L-Ado, pRBCs).

Statistical analysis (Student's t-test) indicated a significant difference between the metabolites recovered in RBCs compared to pRBCs where indicated (* $p<0.05$, ** $p<0.005$, *** $p<0.001$).

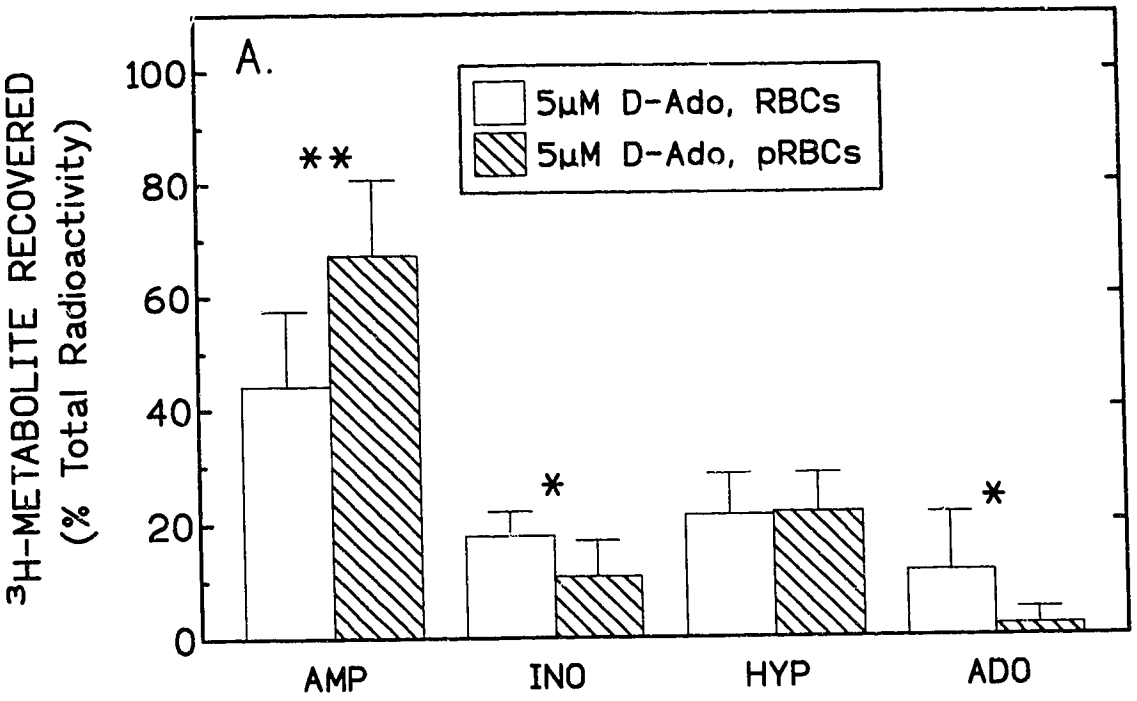
A.
5μM D-Ado, RBCs
5μM D-Ado, pRBCs
^{3}H-METABOLITE RECOVERED
(% Total Radioactivity)
100
80
60
40
20
0
**
*
*
AMP
INO
HYP
ADO

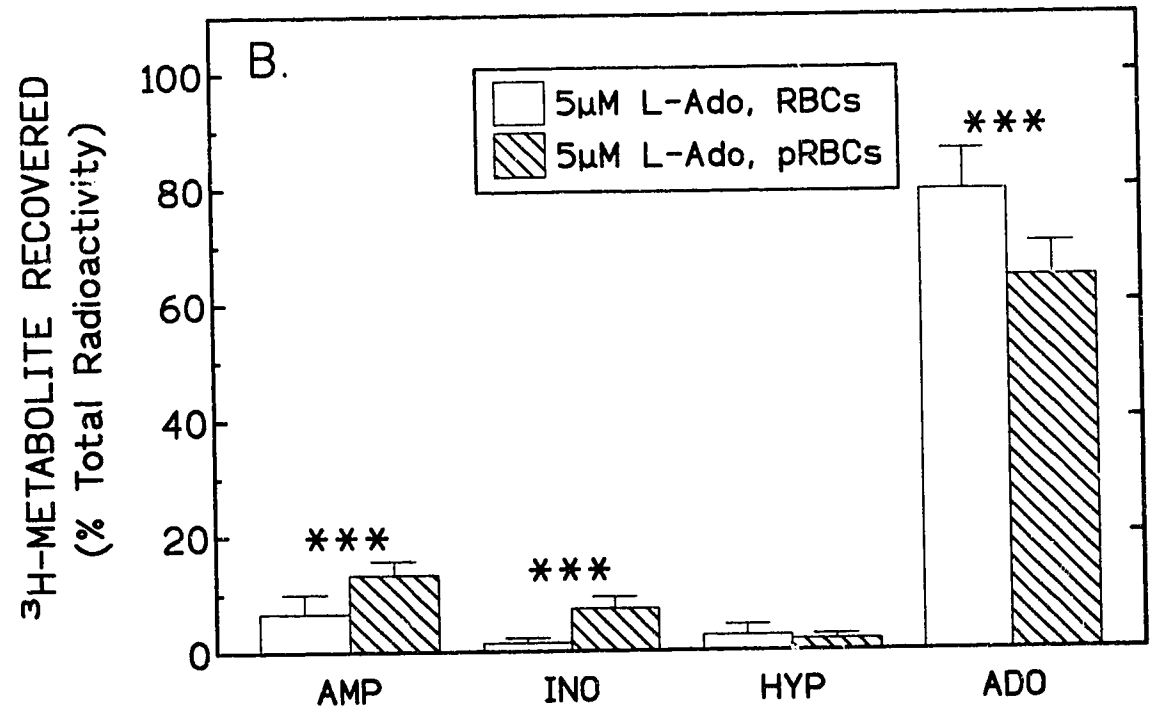
B.
5μM L-Ado, RBCs
5μM L-Ado, pRBCs
^{3}H-METABOLITE RECOVERED
(% Total Radioactivity)
100
80
60
40
20
0
***
***
***
AMP
INO
HYP
ADO

ATP and IMP might be present in the nucleotide spot. There was a statistically significant (Student's t-test, $p<0.05$) difference in the amount of Ino recovered in pRBCs compared to RBCs (10.5 ± 6.5% *vs* 17.8 ± 4.2%), while the amount of Hyp recovered was the same in both cell types. There was also a significant (Student's t-test, $p<0.05$) decrease in the amount of radiolabelled D-Ado in pRBCs compared to RBCs.

The products formed by the metabolism of [^{3}H]L-Ado in RBCs and pRBCs are presented in Fig. 24-B. An obvious difference in the metabolism of L-Ado compared to that observed with D-Ado was the much smaller proportion of "AMP" recovered with the large majority (60-80%) of the radiolabel recovered representing L-Ado. There was also a decrease in the levels of Ino and Hyp recovered in experiments with 5μM [^{3}H]L-Ado as compared to those carried out with 5μM [^{3}H]D-Ado as the substrate. In contrast to the pattern observed with D-Ado, the metabolites formed from 5μM [^{3}H]L-Ado in RBCs were recovered at the levels of L-Ado >> "AMP" > Ino = Hyp. In pRBCs, the same pattern was observed except that Ino was greater than Hyp. As with D-Ado, there was a significant increase in the amount of "AMP" and Ino formed in pRBCs compared to RBCs. "AMP" was 13.3 ± 2.4% of the total in pRBCs compared to 6.6 ± 3.4% of the total in RBCs whereas Ino increased to 7.3 ± 2.0% in pRBCs from 1.4 ± 0.9% in RBCs. As with the metabolism D-Ado, the level of Hyp remained virtually identical in RBCs and pRBCs. There was an approximately 15% decrease in the amount of L-Ado in pRBCs (79.4 ± 6.9%) compared to RBCs (64.4 ± 5.8%). Both the increases in "AMP" and Ino formation, as well as the decrease in L-Ado recovery, were statistically different (Student's t-test, $p<0.001$) in pRBCs and RBCs.

In an attempt to prove that the apparent recovery of "AMP" was not due to the adsorption of metabolites other than nucleotides at the origin, the

METABOLITE	RBCs		pRBCs	
	D-Ado	L-Ado	D-Ado	L-Ado
Origin	3.1±1.0	0.3±0.1	0.2±0.1	0.2±0.1
ATP	38.0±1.8	4.7±0.6	41.6±2.2	9.8±1.1
ADP	17.6±0.6	3.2±0.4	7.3±0.6	2.7±0.2
AMP	6.8±0.3	6.1±1.3	2.1±0.1	6.7±1.8
Ado/Hyp/IMP	24.3±1.3	85.1±1.4	43.2±1.8	79.8±4.5
Ino	11.4±1.0	1.1±0.5	5.8±0.5	3.8±0.2

Table 3. The metabolism of 5μM D-Ado and L-Ado in RBCs and pRBCs: Formation of nucleotides during 5-min intervals.

Table 3 demonstrates the ability of the PEI-cellulose system to separate the nucleotide metabolites formed from 5μM [^{3}H]D-Ado and 5μM [^{3}H]L-Ado during a 5 min incubation in RBCs or pRBCs. The metabolites formed were extracted with 70% methanol and separated with the standards of Fig. 23-B on PEI-cellulose thin layer chromatography sheets with 1M LiCl:1.15M H_3BO_3, pH 7.0.

The data represent the recovery of metabolites as a percentage (mean ± S.D) of the total recovered for a single experiment with triplicate determinations.

metabolites which were formed in some of the above experiments were separated on PEI-cellulose. Fig. 23-B indicates the separation of nucleotides achieved using the PEI-cellulose system. This system is capable of separating metabolites with different charges. There was excellent separation of ATP, ADP and AMP from each other and the origin. There was poor separation of Ado, Hyp and IMP, however, Ado and Hyp were well separated on Silica Gel G, so this was not a concern. The data in Table 3 indicated that radioactivity at the origin on Silica Gel G was not an artifact, but indeed represented AMP, ADP, ATP and possibly IMP. For both D-Ado and L-Ado, ATP accounted for the majority of the nucleotides recovered, followed by ADP and AMP.

IX.2. The effect of increased incubation time on the metabolism of 5μM D- and L-Ado in RBCs and pRBCs

Fig. 25 examines the effect of an increased incubation time on the metabolism of 5μM [^{3}H]D-Ado or 5μM [^{3}H]L-Ado in RBCs and pRBCs. The most obvious difference between the metabolism of [^{3}H]D-Ado with a 5 min (Fig. 24-A) incubation compared to a 30 min (Fig. 25-A) incubation is the increased recovery of "AMP" at 30 min compared to at 5 min in both RBCs and pRBCs. As well, there was decreased Ino, Hyp and D-Ado at the longer incubation time.

The levels of metabolite recovered after the 30 min incubation were "AMP" >>> Hyp > Ino > D-Ado in RBCs and pRBCs with Ado being practically undetectable. Unlike with the 5 min incubation of [^{3}H]D-Ado, only the amount of Ino recovered was significantly different (Student's t-test, $p<0.005$) in RBCs (5.8 ± 3.2% of the total) than in pRBCs (1.3 ± 0.7% of the total).

The major effect of the increased incubation time on the metabolism of 5μM [^{3}H]L-Ado in RBCs and pRBCs was an increase in the formation of nucleotides in both cell types. There was also a time-dependent increase in the

Figure 25. The metabolism of 5μM D-Ado and L-Ado in RBCs and pRBCs during 30-min intervals.

The metabolism of D-Ado and L-Ado was examined in RBCs and pRBCs by following the appearance of radioactive metabolites after the incubation of A) 5μM [^{3}H]D-Ado or B) 5μM [^{3}H]L-Ado at 37°C for 30 min. The metabolites formed were extracted with 70% methanol and separated with the standards of Fig. 23-A on Silica Gel G thin layer chromatography sheets with $CHCl_3$:MeOH: 15%NH_4OH (3:2:1, v/v).

The amount of radioactivity recovered for each metabolite (after subtraction of background radioactivity) is plotted as a percentage of the total amount of radioactivity recovered. The data are the mean ± S.D. from 8 replicates.

Statistical analysis (Student's t-test) indicated a significant difference between the metabolites recovered in RBCs compared to pRBCs where indicated (* $p<0.05$, ** $p<0.005$, *** $p<0.001$).

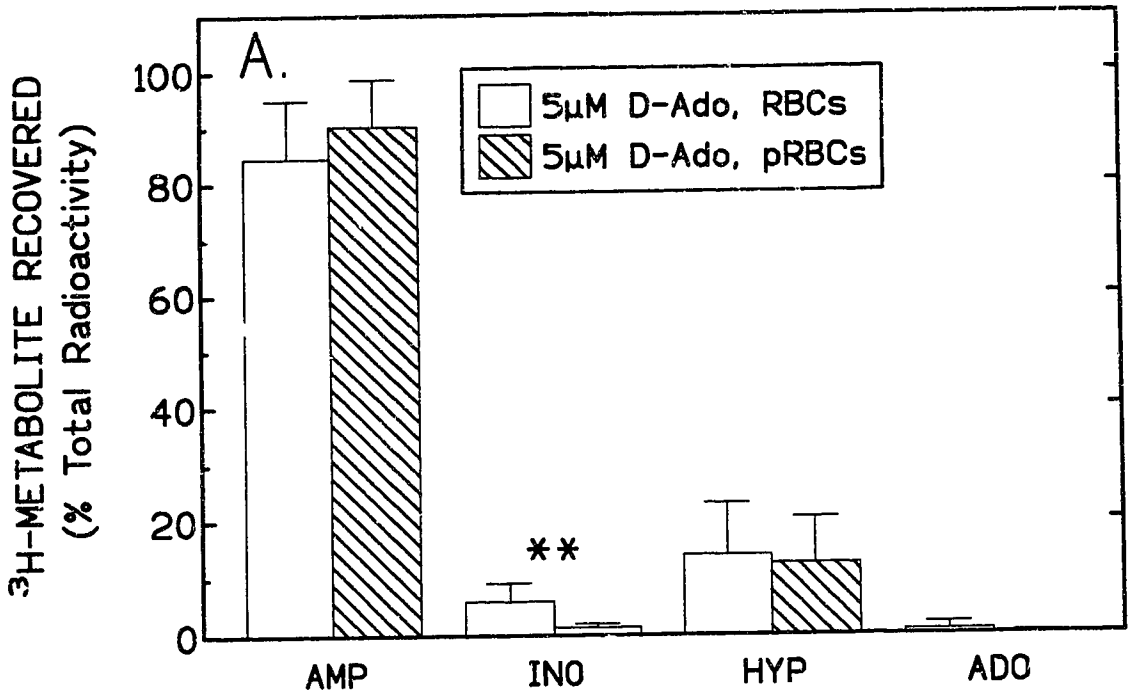
A.
5μM D-Ado, RBCs
5μM D-Ado, pRBCs
^{3}H-METABOLITE RECOVERED
(% Total Radioactivity)
100
80
60
40
20
0
**
AMP
INO
HYP
ADO

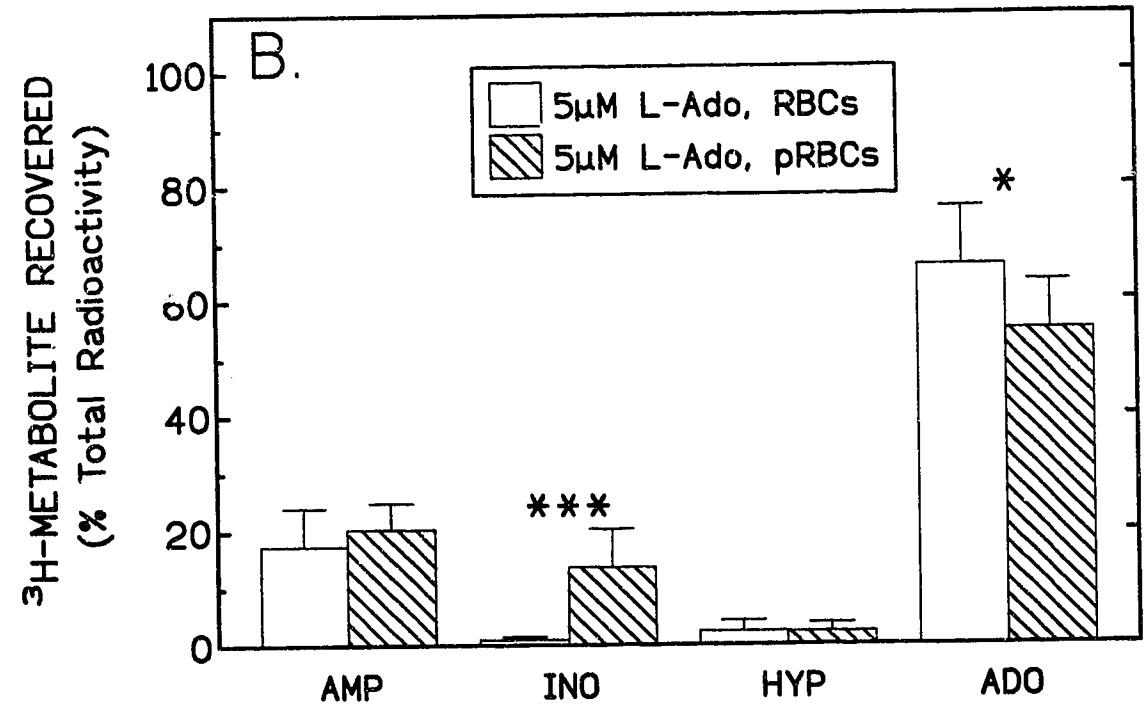
B.
5μM L-Ado, RBCs
5μM L-Ado, pRBCs
^{3}H-METABOLITE RECOVERED
(% Total Radioactivity)
100
80
60
40
20
0
***
*
AMP
INO
HYP
ADO

METABOLITE	RBCs		pRBCs	
	D-Ado	L-Ado	D-Ado	L-Ado
Origin	1.5±1.3	0.2±0.0	3.4±3.3	1.3±1.0
ATP	44.2±19.5	21.3±4.2	39.2±6.4	12.5±1.8
ADP	11.8±1.7	4.5±0.2	13.4±0.6	4.1±0.2
AMP	3.2±1.5	0.4±0.0	1.6±0.1	6.7±0.8
Ado/Hyp/IMP	34.8±17.9	69.2±4.4	40.7±2.2	72.5±3.9
Ino	2.6±1.8	0.6±0.0	0.4±0.2	0.8±0.0

Table 4. The metabolism of 5μM D-Ado and L-Ado in RBCs and pRBCs: Formation of nucleotides during 30-min intervals.

Table 4 demonstrates the ability of the PEI-cellulose system to separate the nucleotide metabolites formed from 5μM [^{3}H]D-Ado and 5μM [^{3}H]L-Ado during a 30 min incubation in RBCs or pRBCs. The metabolites formed were extracted with 70% methanol and separated with the standards of Fig. 23-B on PEI-cellulose thin layer chromatography sheets with 1M LiCl:1.15M H_3BO_3, pH 7.0.

The data represent the recovery of metabolites as a percentage (mean ± S.D) of the total recovered for a single experiment with triplicate determinations.

level of Ino recovered in pRBCs. Fig. 25-B indicated that, once again, the order of metabolite recovery was L-Ado >> "AMP" > Ino ~ Hyp in RBCs and pRBCs. Whereas "AMP" was similar in RBCs and pRBCs, there was a striking 7-fold increase in the amount of Ino in pRBCs compared to RBCs, with Ino accounting for 1.0 ± 0.6% of the total radiolabel in RBCs and 13.6 ± 6.7% of the total in pRBCs. Hyp remained at a very low level in both RBCs and pRBCs but L-Ado decreased from 66.0 ± 10 2% of the total in RBCs to 54.7 ± 8.4% of the total in pRBCs. The decrease in the amount of L-Ado, as well as the increase in the amount of Ino in pRBCs compared to RBCs, were statistically significant at levels of $p<0.05$ and $p<0.001$ (Student's t-test), respectively. As with the 5 mir incubation, separation of metabolites from the 30 min incubation on PEI-cellulose (Table 4) indicated that several Ade nucleotides were present in the "AMP" spot at the origin of silica gel thin layer sheets. Once again, the order of nucleotide formation was ATP > ADP > AMP.

IX.3. <u>The metabolism of 5μM D- and L-Ado in RBCs and pRBCs: The effect of washing the cell pellet.</u>

Fig. 26 shows the data obtained in experiments done in an identical manner to those obtained in Fig. 25, with the exception that the cells were washed by a single re-suspension and centrifugation in ice-cold D-PBS after removal of the incubation medium (see Section IX.2., Materials and Methods). Fig. 26-A shows the recovery of Ino, Hyp and Ado, all of which were less than 5% of the total recovered in both RBCs and pRBCs after a 30 min, 37°C incubation with 5μM [^{3}H]D-Ado. There was no significant difference between RBCs and pRBCs in the levels of any of the metabolites recovered. As was observed previously (Fig. 25-A), "AMP" was the major metabolite recovered (~90% of the total) in both RBCs and pRBCs. The results in Fig. 26-A are

Figure 26. The metabolism of 5μM D-Ado and L-Ado in RBCs and pRBCs during 30-min intervals: The effect of washing.

The metabolism of D-Ado and L-Ado was examined in RBCs and pRBCs by following the appearance of radioactive metabolites after the incubation of A) 5μM [^{3}H]D-Ado or B) 5μM [^{3}H]L-Ado at 37°C for 30 min. In this set of experiments, a step was included to wash the cells of excess radiolabel (see Materials and Methods - Section IX.3). The metabolites formed were extracted with 70% methanol and separated with the standards of Fig. 23-A on Silica Gel G thin layer chromatography sheets with $CHCl_3$:MeOH: 15%NH_4OH (3:2:1, v/v).

The amount of radioactivity recovered for each metabolite (after subtraction of background radioactivity) is plotted as a percentage of the total amount of radioactivity recovered. The data are the mean ± S.D. from 6 replicates (D-Ado, RBCs; L-Ado, pRBCs) or 5 replicates (D-Ado, pRBCs; L-Ado, RBCs).

Statistical analysis (Student's t-test) indicated a significant difference between the metabolites recovered in RBCs compared to pRBCs where indicated (* $p<0.05$, ** $p<0.01$).

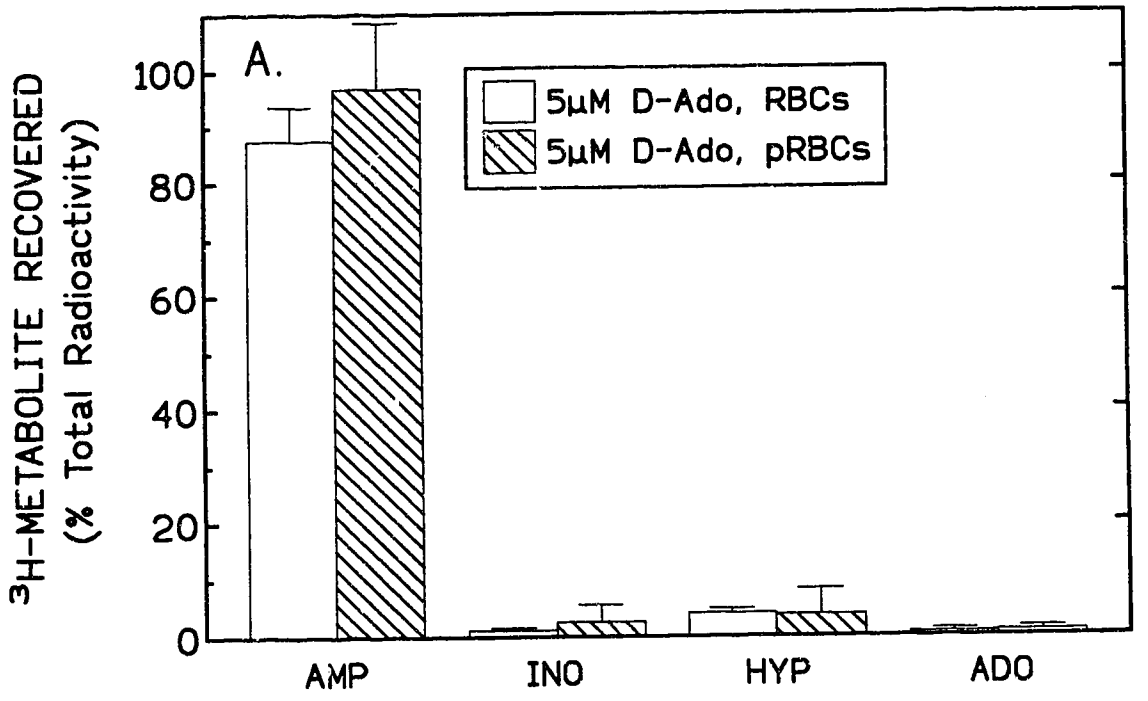
A.
5μM D-Ado, RBCs
5μM D-Ado, pRBCs
^{3}H-METABOLITE RECOVERED
(% Total Radioactivity)
100
80
60
40
20
0
AMP
INO
HYP
ADO

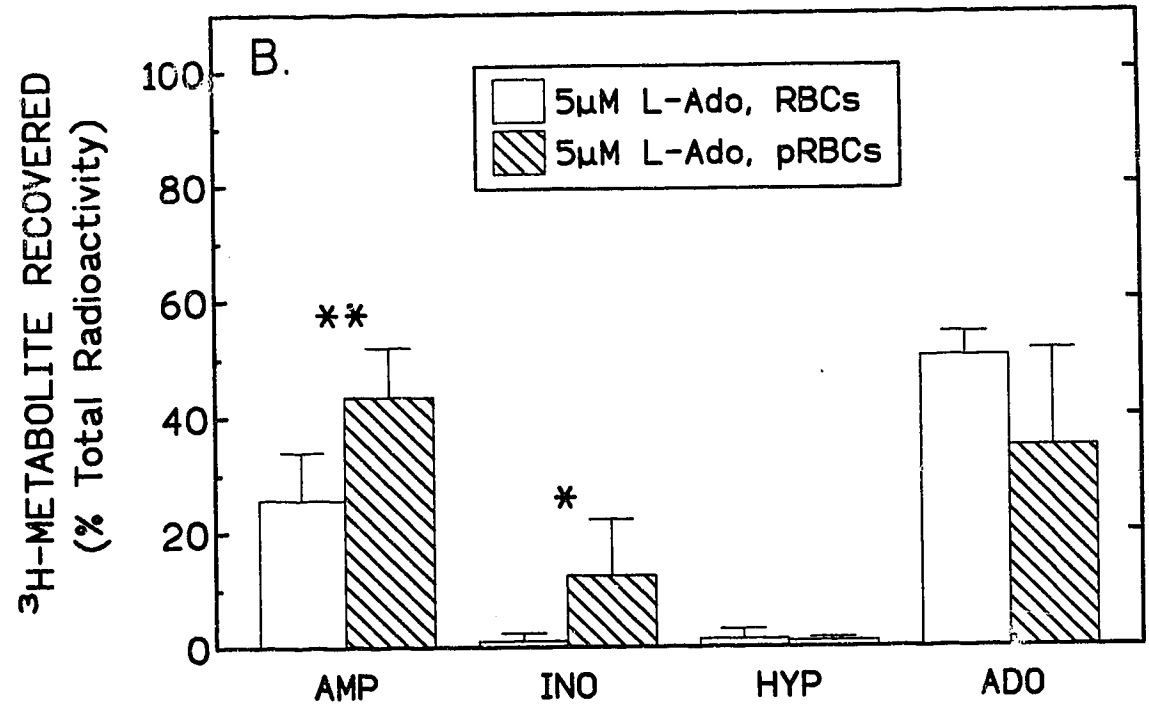
B.
5μM L-Ado, RBCs
5μM L-Ado, pRBCs
^{3}H-METABOLITE RECOVERED
(% Total Radioactivity)
100
80
60
40
20
0
**
*
AMP
INO
HYP
ADO

qualitatively similar to those of Fig. 25-A, however, there are a number of quantitative differences. The addition of a washing step in Fig. 26-A reduced the levels of Ino, Hyp and Ado recovered from the metabolism of 5μM [^{3}H]D-Ado in both RBCs and pRBCs. For example, Hyp in RBCs decreased from 13.9 ± 9.0% of the total recovered in the absence of a washing step to 4.0 ± 0.8% of the total recovered with a washing step. A similar effect was observed in pRBCs, with Hyp recovery decreasing from 12.3 ± 8.1% to a level of 3.6 ± 4.6% of the total radiolabel recovered. The decrease in metabolite recovery was likely due to solute efflux through the host and/or parasite-induced permeability pathways during the re-suspension in D-PBS. Fig. 26-B. shows the recovery of "AMP", Ino, Hyp and Ado after a 30 min, 37°C incubation of RBCs or pRBCs with 5μM [^{3}H]L-Ado. Statistical analysis of the data (Student's t-test) indicated a number of significant differences in the levels of metabolite recovered in RBCs *vs* pRBCs. The levels of "AMP" and Ino increased significantly ($p<0.01$ and $p<0.05$, respectively) in pRBCs compared to in RBCs. As well, there was a decrease in the percentage of radiolabel recovered as L-Ado in pRBCs (~55%) compared to RBCs (~66%).

The washing step affected the results of experiments that measured [^{3}H]L-Ado metabolism. The loss of Ino and Hyp during the washing step was less apparent with the metabolism of 5μM [^{3}H]L-Ado (Fig. 26-B) than with D-Ado (Fig. 26-A). However, there was an almost 20% lower recovery of L-Ado in both RBCs and pRBCs, possibly due to the efflux of this solute from the cells, when the washing step was included. It may have been this lower recovery of L-Ado which allowed "AMP" to be present as a higher percentage of the amount of radiolabel recovered in washed samples compared to those which had not been washed.

It appears that the data obtained without the washing step are more likely to give information about the complete spectrum of metabolites formed by the metabolism of D- or L-Ado. This may be due to the apparent loss of non-nucleotide metabolites during the washing step.

IX.4. The effect of deoxycoformycin on the metabolism of 5μM D- and L-Ado in RBCs and pRBCs

The data in Table 5 indicated that the addition of 2.5μM deCof to the incubation mixture containing RBCs or pRBCs with 5μM D-Ado or L-Ado resulted in inhibition of metabolism via the ADA pathways. Table 5-A shows that deCof abolished the metabolism of D-Ado to Ino, and therefore Hyp, in RBCs. The apparent increase in Ino formed in pRBCs in the presence of deCof is likely due to experimental error in the single experiment performed, as the lowered amount of Hyp recovered in the presence of deCof suggested an inhibition of Ino formation. The inhibition of ADA was also indicated by the increased recovery of D-Ado in the presence of deCof in both RBCs and pRBCs. The reduced deamination of Ado in pRBCs in the presence of deCof indicated that deCof was able to inhibit the parasite ADA and the host enzyme.

The data of Table 5-B indicated that L-Ado metabolism in pRBCs was also inhibited by deCof, as Ino formation was reduced from 13.6 ± 6.7% of the total in the absence of deCof to 2.8% of the total recovered in the presence of deCof. This suggested that L-Ado was deaminated to Ino in pRBCs, an effect not seen in RBCs, indicating a lack of stereoselectivity of the parasite enzyme. The fact that the recovery of "AMP" was not decreased in the presence of deCof in either RBCs or pRBCs suggested that the majority of nucleotide formation in these cells may have occurred through the activity of AK rather than via the ADA route.

5-A, D-Ado

	RBCs		pRBCs	
METABOLITE	CONTROL	+deCof	CONTROL	+deCof
AMP	84.4±10.6	88.4	90.2±8.5	70.7
Ino	5.8±3.2	0.3	1.3±0.7	5.9
Hyp	13.9±9.0	0.5	12.3±8.1	0.6
Ado	0.7±1.2	13.5	0.1±0.1	18.5

5-B, L-Ado

	RBCs		pRBCs	
METABOLITE	CONTROL	+deCof	CONTROL	+deCof
AMP	17.4±6.6	26.8	20.3±4.7	20.7
Ino	1.0±0.6	2.0	13.6±6.7	2.8
Hyp	2.4±1.9	4.0	2.3±1.4	4.3
Ado	66.0±10.2	76.7	54.7±8.4	74.0

Table 5. The effect of 2.5μM deoxycoformycin on the metabolism of 5μM D-Ado and L-Ado in RBCs and pRBCs.

The effect of 2.5μM deoxycoformycin (deCof) on the metabolism of 5μM D-Ado (Table 5-A) and 5μM L-Ado (Table 5-B) in RBCs and pRBCs was examined in a single experiment by following the appearance of radioactive metabolites after the incubation of A) 5μM [^{3}H]D-Ado or B) 5μM [^{3}H]L-Ado at 37°C for 30 min. The metabolites formed were extracted with 70% methanol and separated with the standards of Fig. 23-A on Silica Gel G thin layer chromatography sheets with $CHCl_3$:MeOH:15%NH_4OH (3:2:1, v/v).

The amount of radioactivity recovered for each metabolite (after subtraction of background radioactivity) is plotted as a percentage of the total amount of radioactivity recovered. The data are single determination in the presence of deCof and the mean ± S.D. from 8 replicates for control samples (from Fig. 25).

DISCUSSION

I. ADENOSINE PERMEATION IN UNINFECTED AND MALARIA-INFECTED HUMAN ERYTHROCYTES

This thesis focuses largely on an examination of the characteristics of Ado entry into *Plasmodium falciparum*-infected human erythrocytes. The ability to obtain highly enriched preparations of schizont-containing pRBCs was critical to our experiments. Previous work in *P. yoelii*-infected mouse erythrocytes (data not shown) had indicated that nucleoside (D- and L-Ado) influx was growth-stage-dependent, with the greatest rate of influx being observed in preparations of schizont or late-trophozoite containing pRBCs. It was further demonstrated by Gero *et al.* that Ado influx into *P. falciparum*-infected human erythrocytes was also growth-stage dependent in a similar manner (42). The ability to achieve enrichment of pRBCs to a level of >95 %P allowed a direct comparison of the characteristics of solute entry in pRBCs and RBCs without the extrapolation of influx rates to those expected at 100 %P, as has been used by other authors who have done experiments using cell preparations with lower parasitemias.

In order to make valid comparisons of the transport characteristics of RBCs and pRBCs, it was necessary to measure unidirectional, inward fluxes of permeant that were independent of equilibrative movements and metabolism and were solely indicative of the transport process. Inward fluxes can be determined by measuring the cellular content of radiolabelled permeant within a short period (a few seconds) after the addition of permeant under zero-*trans* conditions. The ability to measure inward fluxes is often limited by the ability to measure influx during the early time period of permeant entry. Very often the cell content of a permeant is affected by permeant efflux which can result in curved uptake curves. Another consideration in measuring inward fluxes is the possible effect

of permeant metabolism. If the metabolism of the radiolabelled solute is the rate limiting step of uptake at the concentration examined, equilibrium of the solute is quickly attained. In those cell types in which metabolism is very rapid, transport itself may be rate-limiting, thus allowing inward fluxes to be measured as long as the extracellular concentration of permeant remains much higher than the intracellular concentration. This can allow the measurement of inward flux at time points after an equilibrium concentration of radiolabel is apparently achieved (111).

As nucleoside fluxes are generally quite rapid, it is necessary to have a methodology that allows the measurement of uptake rates within a few seconds after permeant addition to the cells. This requires an ability to inhibit the entry of the permeant into the cells after a very short time period. In those cell types utilizing only the es transporter, it is possible to quickly terminate influx by the rapid addition of an inhibitor of nucleoside transport (e.g. NBMPR) to the incubation mixture. The presence of a component of Ado uptake in *P. falciparum*-infected erythrocytes which was insensitive to NBMPR (42) precluded the use of this technique in our experiments.

An alternative to the inhibitor-stop methodology is the use of the oil-stop centrifugation method in which permeant influx is stopped by the centrifugal separation of cells from permeant solution. All of the flux measurements in this thesis were obtained using this methodology. A limitation of this methodology is the time required (approximately 2 sec, (56)) for separation of cells and permeant to occur. This imposed a practical lower limit of 3 sec on uptake intervals.

When the cell content of [^{3}H]D-Ado was measured in this manner there was a small, but consistent, increase in the inward flux of D-Ado in pRBCs compared to RBCs. It was important to address the possibility that the increase

in D-Ado entry into pRBCs was due to the presence of a leaky membrane which allowed the non-selective entry of small solutes into these cells. As had been previously reported (e.g. 45), sucrose, a molecule of size similar to that of Ado, did not enter pRBCs. The use of [^{14}C]sucrose as a marker of extracellular water space in these experiments not only demonstrated the lack of sucrose permeability in these cells, but also served to allow the few experiments that contained leaky cells to be discounted. The lack of sucrose permeation also suggested that Ado entry into pRBCs occurred through a pathway with selectivity characteristics beyond that of solute size.

Characterization of the route or routes responsible for Ado entry into pRBCs involved comparing the parasite-induced system(s) with the *es* nucleoside transporter. This involved examining the effects of nucleoside transport inhibitors, as well as compounds that were previously shown to inhibit the entry of other solutes into pRBCs, on Ado influx. The presence of a component of Ado entry into pRBCs that was insensitive to inhibition by nucleoside transport inhibitors was reported by Gero *et al.* (43) using a cell preparation containing 97% trophozoites at a level of 80-90 %P. In our preparations of schizont and mature trophozoite-containing pRBCs (with a greater than 95 %P), we also observed D-Ado entry into pRBCs which was not inhibited by 1μM concentrations of NBMPR, DPM or DZP. This indicated that D-Ado influx in pRBCs was not entirely attributable to influx via the *es* transporter, but rather that a parasite-induced route (or routes) of entry must be present. It had previously been reported that there was a decrease in the abundance of NBMPR binding sites in pRBCs compared to RBCs (~85% of control, 25 %P) (42). However, our uptake measurements did not allow us to observe the expected decrease in the *es* contribution to D-Ado entry in pRBCs as the size of

the NBMPR-sensitive component of D-Ado entry was similar in both pRBCs and RBCs.

A characteristic of Ado influx via the *es* nucleoside transporter is the selectivity for the D-enantiomer of this nucleoside. For example, Gati *et al.* demonstrated that 5μM D-Ado entered mouse erythrocytes ~20 times more rapidly than did 5μM L-Ado (67). In contrast, a separate study that examined the characteristics of Ado entry into *P. yoelii*-infected mouse erythrocytes demonstrated that 1μM L-Ado influx occurred at a rate that was approximately half the rate of 1μM D-Ado entry into these cells (31). The present data indicated a similar relationship between D- and L-Ado entry into human erythrocytes. The data also indicated that there was a substantial (3-5 fold) increase in the influx of L-Ado into pRBCs compared to RBCs at 1μM and 10μM concentrations of permeant. The fact that the influx of 1μM L-Ado occurred at a rate similar to that obtained for the parasite-induced entry of 1μM D-Ado (measured in the presence of NBMPR), suggested that D-Ado and L-Ado may enter pRBCs by the same, non-stereoselective, route.

The expression of L-Ado fluxes in RBCs was not unexpected. Gati *et al.* had demonstrated that the stereoselectivity for D-Ado was not absolute in mouse erythrocytes and L1210 cells, but rather that L-Ado was a poor permeant for the *es* transporter (67). In mouse erythrocytes, 200μM L-Ado entry was reduced to ~15% of control rates by 5μM NBMPR (67). In L1210 cells, the influx of 100μM L-Ado was reduced to ~35% of control rates by 5μM NBMPR (67). In the present study with human erythrocytes, the inward flux of 10μM L-Ado in RBCs was reduced to ~55% of the control rate by 1μM NBMPR. The effect of NBMPR on L-Ado entry into RBCs may explain the apparent difference between the inward flux of 1μM D-Ado + NBMPR and 1μM L-Ado entry into pRBCs, as well as the

small reduction in the inward flux of 10μM L-Ado in pRBCs observed in the presence of the nucleoside transport inhibitors.

In this study, the concentration-dependence of D-Ado influx in RBCs yielded a Km of ~190μM and a Vmax ~23 pmol/10^7cells/sec (~50 pmol/μl H_2O/sec). These values are dramatically higher than those reported in the literature for D-Ado influx in RBCs (e.g. Km ~25μM, Vmax ~15 pmol/μl H_2O/sec) (55). Although the reason for this discrepancy remains unclear, it may relate to the fact that, in contrast to the literature reports that used fresh erythrocytes, our experiments utilized erythrocytes that had been stored at 4°C for three or more weeks, conditions which may result in changes to the kinetic properties. For example, Plagemann and Wohlhueter (112) reported a higher affinity for zero-*trans* Urd influx in outdated compared to fresh RBCs (Km values of 73μM and 120μM, respectively) as well as a decreased maximum velocity (Vmax 9 pmol/μl H_2O/sec *vs* 41 pmol/μl H_2O/sec, respectively). These changes resulted in a decreased efficiency of zero-*trans* Urd flux in outdated RBCs (Vmax/Km =0.12 pmol/μl H_2O/sec/μM) compared to fresh RBCs (Vmax/Km =0.34 pmol/μl H_2O/sec/μM) (112). The present study is consistent with a decreased efficiency of nucleoside transport in stored compared to fresh RBCs. There was a decreased efficiency (Vmax/Km) of D-Ado influx in stored RBCs (0.26 pmol/μl H_2O/sec/μM (this study)) compared to fresh cells (0.6 pmol/μl H_2O/sec/μM (55)).

It had been suggested that solute entry into pRBCs occurred via an unsaturable pathway (e.g., see ref 39,45). However, as mentioned above, the rapid entry into pRBCs of L-Ado and the impermeability of the pRBC membrane to sucrose, suggested that solute entry was not exclusively size-dependant. This study addressed the possibility that parasite-induced Ado entry in pRBCs was mediated. In our experiments, the examination of the concentration-dependence of D-Ado entry in pRBCs indicated saturability of the pathway. As

the concentration-dependence of D-Ado entry into pRBCs was only examined to concentrations that were less than 1.5 times the apparent Km, the kinetic values are approximations, but indicate that, unlike the behavior of other solutes (e.g. D-Sorb), D-Ado entry into pRBCs was saturable. This saturability suggests that D-Ado entry is mediated and provides an explanation for the rapid inward fluxes of D-Ado described above.

As discussed above, NBMPR inhibited the *es* nucleoside transporter-mediated entry of 1μM D-Ado into RBCs and pRBCs. As the concentration of D-Ado increased, the relative contribution of the *es* nucleoside transporter-mediated influx to the total D-Ado influx into pRBCs decreased. This was due to the lower Vmax and Km for D-Ado entry via the *es* nucleoside transporter compared to the parasite-induced route. D-Ado influx occured at much higher rate (Vmax ~949 pmol/10^7cells/sec) in pRBCs than in RBCs (Vmax ~23 pmol/10^7cells/sec). However, the parasite-induced entry of D-Ado in pRBCs occured at a lower efficiency (Vmax/Km =72 pmol/10^7cells/sec/mM) than D-Ado entry via the *es* transporter in RBCs (Vmax/Km =125 pmol/10^7cells/sec/mM) suggesting that at physiological (<1μM) concentrations of Ado, the *es* nucleoside transporter would be the primary entry route of D-Ado entry into pRBCs.

The ability of NBMPR to reduce the inward flux of 10μM L-Ado in RBCs suggested that there should be a saturable component of L-Ado entry into RBCs via the *es* nucleoside transporter. Failure to detect saturability of L-Ado fluxes in RBCs may reflect the low affinity interaction between L-Ado and the *es* nucleoside transporter.

The entry of L-Ado into pRBCs occured via a route with kinetic constants similar to those determined for D-Ado entry. Only a very small portion, if any, of L-Ado flux into pRBCs was inhibited by NBMPR, suggesting that even at high concentrations, there was very little L-Ado entry into pRBCs via the *es*

nucleoside transporter. The saturability of L-Ado fluxes in pRBCs argues against the possibility that increased L-Ado entry into pRBCs occurs due to simple diffusion through the pRBC membrane.

The very similar concentration-dependence of L-Ado and D-Ado influx in the presence (and absence) of NBMPR suggested that L-Ado and D-Ado enter pRBCs by the same, non-stereoselective pathway. The apparent saturability of the parasite-induced route of Ado entry, a characteristic that distinguished Ado from the other pRBC permeants in the literature (39) or this study, supported the idea that Ado entered pRBCs through a mediated pathway that was distinct from other solute entry routes.

As mentioned above, the erythrocytic transporters for nucleosides and sugars have similar structural and functional characteristics (105). As well, there are a number of reports of interactions between permeants for Glut1 and inhibitors of Glut1 with those of the nucleoside transporter (see below). These findings led us to examine the effect of CB, a potent inhibitor of Glut1, on the entry of L-Ado into pRBCs. At low concentrations of CB (1μM) there was no effect on L-Ado entry into pRBCs. However, as the concentration of CB was increased to 100μM, a substantial inhibition of influx (to 60% of control) occurred. The ability of CB to inhibit nucleoside fluxes has previously been reported in a number of cell types. Plagemann and Estensen (106) reported the inhibition by CB of 10μM Urd or 0.25μM Thd entry into cultured Novikoff rat hepatoma cells with Ki values of 2μM and 6μM, respectively. Plagemann and Woffendin (66) reported the inhibition, in RBCs, of 500μM Urd equilibrium exchange fluxes by CB with an IC_{50} of approximately 30μM. Similar effects were reported by Jarvis (105) who demonstrated that 10μM CB reduced the inward flux of 100μM Urd in human erythrocytes to about 70% of the control rate while reducing the influx of 5mM D-glucose into these cells to 6% of the control rate.

In the present study, we found that 100μM CB was more effective at inhibiting 1μM D-Ado influx into RBCs (reduced to14% of the control rate) than it was at inhibiting 10μM L-Ado influx into pRBCs (reduced to 60% of the control rate). Taken together with the literature reports, these results suggested that the inhibitory effects seen with 5 or 100μM CB were not selective for Glut1, the es transporter, or the parasite-induced route of L-Ado entry into pRBCs. However, the ability of CB to inhibit L-Ado influx into pRBCs may suggest structural similarities between the route of L-Ado influx into pRBCs and the erythrocytic glucose and/or nucleoside transporter.

Phloridzin has been used to inhibit the parasite-induced entry of small solutes into pRBCs in a relatively selective and potent manner (e.g. 113). In the present study, the influx of L-Ado into pRBCs was inhibited by phloridzin with an IC_{50} af approximately 50μM. This value was higher than that obtained for inhibition of sorbitol entry into pRBCs (IC_{50}~17μM, (48)), but was within the range reported for a variety of other solutes (49). A possible explanation for the slightly higher concentration needed to inhibit L-Ado influx may be due to the fact that, at low concentrations, phloridzin appeared to increase the influx of L-Ado into pRBCs by about 10%. If this increase were to be taken into account, the IC_{50} would be reduced to a value of 20-30μM, suggesting that L-Ado and D-Sorb use the same, or similar routes of entry into pRBCs. Silfen *et al.* reported that constitutive nucleoside and glucose transport in human erythrocytes was not affected by concentrations of phloridzin up to 20μM (113). Our data also demonstrated that phloridzin was not selective for the parasite-induced route of solute entry. Influx of D-Ado via the es nucleoside transporter was inhibited by phloridzin with an apparent IC_{50} only twice that measured for the inhibition of L-Ado influx in pRBCs. Although significant (>10%) inhibitory effects were only observed at phloridzin concentrations in excess of approximately 30μM, at

concentrations sufficient to inhibit all L-Ado entry in pRBCs (>100μM) the effect of phloridzin on the *es* nucleoside transporter would likely be considerable, thus precluding the use of phloridzin as a selective inhibitor of parasite-induced fluxes.

The search for a more selective inhibitor of parasite-induced Ado entry in pRBCs led to the examination of furosemide. Furosemide was previously used by Gati *et al.* to inhibit L-Ado entry into *P. yoelii*-infected mouse erythrocytes, a flux that was relatively insensitive to inhibition by phloridzin (31). In the present study, furosemide was also a much more potent inhibitor of L-Ado influx in pRBCs than was phloridzin. As well as being at least 10 times more potent than phloridzin, furosemide also appeared to be more selective for the parasite-induced route of L-Ado entry than was phloridzin. Unlike phloridzin, 50μM furosemide was without effect on D-Ado influx into RBCs, indicating a lack of effect on the *es* nucleoside transporter. This resulted in a much higher selectivity for the parasite-induced L-Ado route of entry than was obtainable with phloridzin.

The partial inhibition by NBMPR of D-Ado entry in pRBCs suggested a contribution of the *es* nucleoside transporter to this flux. Inhibition of this route of D-Ado entry by 1μM NBMPR allowed the examination of furosemide as an inhibitor of parasite-induced D-Ado influx in pRBCs. The almost identical responses to furosemide of D-Ado + NBMPR and L-Ado suggested a shared pathway for the entry of D-Ado and L-Ado into pRBCs. The slightly greater inward flux of L-Ado, compared to D-Ado + NBMPR, into furosemide-treated pRBCs, may be due to L-Ado flux via the *es* nucleoside transporter in the absence of NBMPR.

It has been proposed that the action of furosemide in pRBCs may be attributable to inhibition of anion channels (39,45). Kirk *et al.* have suggested

that the parasite-induced route of solute entry in pRBCs has the characteristics of a chloride channel (39,45). The effect of furosemide on the pathway has been postulated to occur through hydrophobic interactions, with the potency of furosemide being affected by the ability of the permeant to compete for the hydrophobic sites (39).

It is interesting to note that NBMPR, which is more hydrophobic than furosemide (octanol/water partition coefficients: NBMPR: 30 (114), furosemide: 0.4 (115)), had no effect on the parasite pathway at 1μM concentrations (this work) or even at 11.25μM concentrations (42). If furosemide could compete with L-Ado for entry in pRBCs, then it may be expected that NBMPR, which is a nucleoside, would also be able to inhibit influx. The lack of an effect by NBMPR may then indicate that hydrophobic interactions are not the principal mechanism by which furosemide inhibits solute flux in pRBCs. Alternatively, it may be that NBMPR, possibly due to its size, is not able to interact with the hydrophobic sites which are available to furosemide. A striking difference between furosemide and NBMPR is the presence of a negatively charged substituent (carboxyl) on furosemide, a factor which may be important in its activity if the parasite-induced entry route has characteristics of an anion channel. Whatever the mechanism of action may be, furosemide is a potent inhibitor of parasite-induced Ado entry and provides evidence that Ado entry into pRBCs is a mediated process.

II. L-GLUCOSE AND D-SORBITOL PERMEATION IN UNINFECTED AND MALARIA-INFECTED HUMAN ERYTHROCYTES

We wished to examine the possibility that L-Ado was entering pRBCs by a pathway that was distinct from the route(s) responsible for the entry of other solutes. Fluxes of L-Gluc were compared with L-Ado fluxes in pRBCs. Although

the rate of L-Gluc entry in pRBCs was much higher than in RBCs, 2mM L-Gluc fluxes in pRBCs were about 30-fold lower than 2mM L-Ado fluxes in those cells. The inward flux of L-Gluc in pRBCs was much higher than in RBCs at any concentration examined. However, unlike the fluxes of D-Ado and L-Ado in pRBCs, L-Gluc flux in pRBCs did not appear to saturate, even at concentrations as high as 190mM. It was also noted that the inward flux of 190mM L-Gluc was only as large as the flux 7mM L-Ado. This suggested either that L-Gluc and L-Ado entered pRBCs by separate routes, or that L-Gluc had a much lower affinity for the same route used by L-Ado. The utilization of a single route would indicate that size was not a major determinant of the rate of solute entry into pRBCs since L-Ado is a larger solute than L-Gluc.

Although both 5μM CB and 1μM NBMPR reduced the inward flux of 2mM L-Gluc in pRBCs to ~80% of control rates, it is unlikely that these effects are attributable solely to inhibition of flux via Glut1 or the *es* nucleoside transporter. The inward flux of 2mM L-Gluc into RBCs, which would include flux via Glut1 or the *es* nucleoside transporter, can account for only ~3% of 2mM L-Gluc influx in pRBCs. In addition, the effect of CB on D-Ado flux in RBCs indicated that inhibitory effects of CB were not limited to Glut1. The data suggest that L-Gluc does not enter pRBCs via either Glut1 or the *es* nucleoside transporter, however, it is possible that the minor effects of these inhibitors were due to the existence of common features between the parasite-induced route of L-Gluc entry in pRBCs and the erythrocytic nucleoside and/or glucose transporters.

The parasite-induced inward flux of 2mM D-Sorb was almost twice that of L-Gluc but still more than 10 times less than that of 2mM L-Ado. D-Sorb entry was unsaturable at the concentrations tested (up to 190mM) suggesting either the existence of different routes for L-Ado and D-Sorb entry into pRBCs or a much lower affinity of D-Sorb for the pathway.

To help characterize the L-Gluc and D-Sorb pathway(s), the effects of furosemide on inward flux of 2mM L-Gluc or 2mM D-Sorb in pRBCs were examined. As L-Gluc and D-Sorb are both smaller solutes than the extracellular water space marker, sucrose, there remained the possibility that these permeants were entering pRBCs through a leaky cell membrane, however, the inhibition by furosemide (IC_{50} values, 1-10μM) suggested that entry of these solutes was mediated. The similar IC_{50} values for inhibition by furosemide of L-Gluc, D-Sorb and Ado inward fluxes in pRBCs, suggested that these permeants may share a common pathway.

III. L-ADENOSINE INHIBITS THE ENTRY OF L-GLUCOSE AND D-SORBITOL INTO pRBCs

In order to determine if two permeants interact with the same transporter, it is possible to test for the inhibition of the entry of one of the permeants by the other. The saturability of L-Ado fluxes in pRBCs suggested that L-Ado may be able to inhibit the (unsaturable) entry of L-Gluc and/or D-Sorb into these cells if these permeants utilized the same pathway. The inhibition of L-Gluc and D-Sorb influx by L-Ado indicated that L-Ado was able to interact with the route(s) responsible for L-Gluc and D-Sorb influx into pRBCs and suggested a common entry pathway for the three solutes. The ability of one permeant to inhibit the influx of another via an apparently unsaturable pathway is not unique to pRBCs. Upston and Gero demonstrated that Ado, which had previously been shown to enter *Babesia bovis*-infected bovine erythrocytes (bRBCs) with a Km of ~2mM (116), was able to inhibit the entry of 60mM D-glucose into bRBCs (117). 15mM Ado inhibited the apparently unsaturable influx of D-glucose through this pathway by over 40%, however the mechanism by which this occurred was unclear (117). In this study, our attempts to determine the nature (competitive or

non-competitive) of the L-Ado inhibition of L-Gluc fluxes in pRBCs by examining the effects of various concentrations of L-Ado on [^{14}C]L-Gluc influx were unsuccessful. Although it appeared that a Ki of 10-30mM would be obtained, it was impossible to determine whether or not the inhibitory effects were competitive, possibly due to the small range of L-Ado concentrations examined (3-12mM) and an inability to utilize L-Ado concentrations significantly greater than the expected Ki value due to the limited water solubility of L-Ado.

The ability of L-Gluc or D-Sorb to inhibit the entry of 10μM [^{3}H]L-Ado into pRBCs was also examined. As the entry of L-Gluc and D-Sorb into pRBCs appeared to be unsaturable, or of very low affinity, the highest possible concentrations of these agents (190mM) were used. Despite the fact that 20mM L-Ado inhibited L-Gluc and D-Sorb influx, neither 190mM L-Gluc nor 190mM D-Sorb had an effect on L-Ado entry into pRBCs. This may mean that the apparently very low affinities of L-Gluc and D-Sorb for the pathway(s) precluded their ability to inhibit L-Ado influx. An alternative explanation may be that the permeants do not compete for the same site(s) in the pathway(s) and that the effect of L-Ado on L-Gluc and D-Sorb entry into pRBCs was allosteric.

We examined the selectivity of the L-Ado effect by determining if other permeants had the same inhibitory effect on L-Gluc or D-Sorb influx into pRBCs. Neither 190mM L-Gluc nor 190mM D-Sorb had any effect on the influx of 2mM D-Sorb into pRBCs. This should be expected, as inward fluxes of these solutes did not saturate. The lack of an effect by other permeants, also suggested that the inhibition of D-Sorb influx by 20mM L-Ado was due to a specific, rather than a general, effect of L-Ado on the entry route.

In a parallel set of experiments, 2mM L-Gluc entry was inhibited to a level identical to that seen with L-Ado by 190mM L-Gluc or 190mM D-Sorb. This result was surprising as it suggested an interaction between not only L-Gluc and the

pathway, but also between D-Sorb and the pathway. In order to address the question of whether or not the effects were due to the high concentrations of L-Gluc and D-Sorb used, the experiments were repeated with 10mM concentrations of L-Ado, L-Gluc and D-Sorb. Under these conditions, only L-Ado and L-Gluc had significant inhibitory effects on 2mM L-Gluc entry into pRBCs. The lack of inhibition by 10mM D-Sorb suggests that the effect seen by 190mM D-Sorb may have been non-selective. The inhibition of inward fluxes of 2mM L-Gluc by 10mM L-Gluc appears to be selective because 10mM is only 5 times the apparent Km for D-glucose flux via Glut1 (110). This result was unexpected due to the apparent unsaturability of L-Gluc entry into pRBCs. However, upon examination of the saturability data, it is apparent that the inward flux of 190mM L-Gluc was less than would have been expected based on a linear extrapolation of the inward flux determined at 2mM. When the inward flux of L-Gluc in pRBCs was averaged at each concentration before analysis of the concentration-dependence of L-Gluc fluxes by non-linear regression, the data was significantly better described (F-Test, $p=0.002$) by an equation for multiple routes of L-Gluc influx rather than an equation for a single, unsaturable route. One route was saturable with a Km of 14.4 ± 20.0 mM and a Vmax of 23.9 ± 14.1 pmol/10^7cells/sec and a second route was unsaturable with a rate constant of 1.67 ± 0.07 pmol/10^7cells/sec/mM. The presence of a saturable component of L-Gluc entry in pRBCs may explain the ability of 10mM L-Gluc to inhibit the influx of 2mM [^{14}C]L-Gluc. However, the large error in the estimates of both the Km and Vmax for the saturable component suggests that caution must be used in proposing the existence of a saturable route of L-Gluc entry into pRBCs.

It must be remembered that the ability of one solute to inhibit the influx of another is not proof that both solutes utilize the same pathway for entry into cells. For example, Thd is able to inhibit glucose entry into human erythrocytes,

yet Thd is not a substrate for Glut1 (105). It is possible that L-Ado, and possibly L-Gluc, are able to inhibit influx by interacting with components of the pathway in a manner which may be analogous to the effect of furosemide. The true nature, or number, of the pathway(s) involved in the entry of these solutes into pRBCs awaits the isolation of the protein(s) responsible, and reconstitution into vesicles of the parasite-induced activity. However, the similar effects of furosemide, phloridzin, and the interactions between permeants suggest that it is likely that a single pathway is responsible for the parasite-induced entry of Ado, L-Gluc and D-Sorb in pRBCs.

IV. POSSIBLE MECHANISMS OF PERMEANT SELECTIVITY IN pRBCs

It appears that Ado may be a preferred permeant for the parasite-induced pathway solute entry in pRBCs because of its rapid entry into pRBCs. This raises questions about the basis for the selectivity of the pathway. It had been proposed that size may be a major determinant of permeant entry into pRBCs (e.g., see ref. 35). Although this may be true for some solutes, including possibly L-Gluc and D-Sorb, it is clearly not the whole story. The saturability of Ado fluxes in pRBCs suggests that the pathway has a degree of selectivity for Ado, and possibly nucleosides in general. It has been proposed by Kirk *et al.* that hydrophobicity may be the major determinant of parasite-induced solute entry into pRBCs (39). They have used the fact that Ado is more hydrophobic than sucrose to explain the observation that Ado enters pRBCs, but sucrose does not. Although this hypothesis may be supported by our data, a number of questions still exist. Although hydrophobicity may account for the greater influx of Thd into pRBCs compared to Urd, it does not explain why Thd can enter pRBCs at the same, or possibly even greater, rate than does Ado (39). Thd is much more soluble in water, and therefore more hydrophilic, than is Ado

(octanol:aqueous partition coefficients; Thd:0.073, Ado:0.105 (118)) which suggests that Ado should enter pRBCs at a greater rate than Thd. The fact that this did not occur in the studies of Kirk *et al.* (39) suggests that there may be characteristics of the permeants beyond hydrophobicity which are important for the entry of relatively large solutes into pRBCs. The saturable nature of Ado fluxes (this study), but not Thd fluxes (39) suggests that Ado may have a higher affinity for the pathway than does Thd. It should also be remembered that whereas the Km for Ado entry into pRBCs was ~14mM, the upper level of the concentrations examined by Kirk *et al.* was 10mM (39).

The identity of the pathway is still unknown, though Kirk *et al.* have suggested it may be a chloride channel (39,45). Alternative explanations may include the modification of an existing transport protein to accommodate the wide variety of solutes which enter pRBCs. The pathway's apparent selectivity for Ado indicated by this study, suggests that a possible candidate for this type of pathway may be the *es* nucleoside transporter. There is also some evidence for the existence of a parasite-induced pathway linking the parasite and the extracellular environment directly (119). The possibility that this "parasitophorous duct" may be responsible for the entry of Ado into pRBCs is worth discussing. Although this route could have the same solute selectivity characteristics as a route through the erythrocytic membrane, a potential concern may be the high rates of solute flux through this route and how the parasite would deal with the almost uncontrolled movement of solutes, including ions. It is also, of course, possible that a combination of routes, with similar characteristics, may be involved in the entry of small solutes into pRBCs.

V. ADENOSINE METABOLISM IN UNINFECTED AND MALARIA-INFECTED HUMAN ERYTHROCYTES

Whatever the nature, and function, of the parasite-induced route of Ado entry may be, its presence in the pRBC membrane suggests a number of possible therapeutic strategies for delivery of parasite-toxic nucleosides. It has been proposed previously (44) that inhibition of the host, *es*, nucleoside transporter could be used to selectively target parasite-toxic nucleosides into pRBCs via the parasite-induced route of Ado entry. An alternative to this approach is to find parasite-toxic nucleosides that are permeants for the parasite-induced route, but unable to enter host cells. The observation in this study that L-Ado entered pRBCs at a much greater rate than RBCs, suggests examining L-nucleosides as possible therapeutic agents. In order to be effective therapeutically, a nucleoside would have to either interfere with parasite nucleoside metabolism or be metabolized to an active product either by the host cell or the parasite enzymes. Once again, Ado provided a model for purine metabolism in RBCs and pRBCs.

The more rapid metabolism of D-Ado by pRBCs compared to RBCs observed in this study was expected because of the reported greater specific activities of several of the parasite enzymes relative to the erythrocytic enzymes (71). The relative levels of metabolites recovered from the metabolism of 5μM [^{3}H]D-Ado in RBCs (Hyp > Ino > Ado) were consistent with order of enzyme activities reported by Reyes *et al.* in which ADA is the rate-limiting enzyme in the deaminase pathway and PNP activity is higher than HGPRTase activity (71). The high level of AMP (or other nucleotides) recovered could be due to the activity of AK as well as the activity of the deaminase pathway with the subsequent formation of IMP from Hyp.

The increased recovery of total radiolabel in pRBCs compared to RBCs was indicative of an increased metabolism of 5μM [^{3}H]D-Ado. Although the activities of the parasite and host AKs have been reported to be almost identical in pRBCs and RBCs, there are definite increases in the activities of the deaminase pathway enzymes (71). In this study, this was reflected in the decrease of radiolabelled D-Ado recovered as well as an increase in the amount of AMP (or other nucleotides) recovered in pRBCs compared to RBCs.

A similar pattern of D-Ado metabolism in RBCs and pRBCs was observed at 5 and 30 min of incubation, however there was a decrease in the levels of Ino and Hyp at 30 min which suggests more AMP was formed via the ADA pathway with the increased incubation period.

L-Ado was regarded as a model to study the metabolism of L-nucleosides by pRBCs. It was obvious, in both RBCs and pRBCs, that L-Ado was much less readily metabolized than was D-Ado. In both cell types, the majority of radiolabel present in cells after exposure to [^{3}H]L-Ado was in the form of free L-Ado. Despite the presence of AMP in RBCs, the low level of AMP (which would include L-AMP) suggested that L-Ado was poorly metabolized by RBCs. The production of AMP likely occurred through the activity of the AK pathway as only extremely small (<5% of the total) levels of Ino and Hyp were recovered in RBCs. As well, it has been reported that L-Ado is poorly metabolized by ADA (e.g. 74-76). The increased recovery of AMP in pRBCs compared to RBCs may have been due either to the phosphorlyation of L-Ado by the parasite AK or the deamination of L-Ado to L-inosine (L-Ino) by the parasite ADA followed by phosphorolysis to Hyp and phosphoribosylation to IMP. Although L-Ado was not a substrate for the host ADA, the increase in L-Ino recovery in pRBCs compared to RBCs suggested that L-Ado was a substrate for the parasite ADA. Only a small level of Hyp was recovered which could indicate either that L-Ino was not a

substrate for the host or parasite PNP or that the Hyp formed was quickly incorporated into IMP by an HGPRTase. The fact that Hyp would no longer contain a sugar with the L-configuration could allow it to be a substrate for both the host and parasite enzymes, resulting in its rapid disappearance from the RBC cytosol. Whether L-Ino is metabolized or not, it appears that the parasite PNP was the rate limiting enzyme for L-Ado metabolism in pRBCs. The presence of ADA activity for L-Ado may suggest that the increase in AMP levels in pRBCs compared to RBCs was due to the metabolism of L-Ado by the ADA pathway, however direct evidence for this is lacking.

The fact that AMP was retained at the origin of the silica gel thin layer sheet raised the possibility that non-specific binding of negatively charged molecules to the plate was occurring. In order to address this question, the products of D-Ado and L-Ado metabolism in RBCs and pRBCs were separated on a PEI-cellulose thin layer sheets to allow the migration of nucleotides away from the origin. These experiments indicated that the phosphates observed with the silica gel system were nucleotides and not contaminants. Another potential problem was the possibility that AMP and Ino were being formed from the metabolism of D-Ado rather than L-Ado. If this were the case, it could be expected that the small amount of radiolabelled D-Ado would have been completely metabolized within 5 min of incubation time. The fact that AMP levels continued to increase between 5 and 30 min suggested that it was L-Ado which was being metabolized to AMP. The ability of 2.5μM deCof to inhibit the formation of Ino in pRBCs, but not in RBCs, was further evidence of the purity of the L-Ado preparation and also indicated that L-Ado was being metabolized by the parasite ADA. The inhibition of L-Ado deamination also resulted in an increase in the amount of [^{3}H]L-Ado recovered in pRBC, but not RBCs, further indicating that L-Ado was metabolized by ADA in pRBCs, but not RBCs.

The addition of a washing step to the extraction procedure resulted in the apparent loss of important nucleoside and nucleobase metabolites, probably due to efflux via erythrocytic (and possibly parasite-induced) transporters. Nucleotides remained trapped in the cells, however, the loss of membrane permeable metabolites may result in the contribution of nucleotides to the metabolite pool being overestimated. It is therefore best to omit the washing step in order to achieve a picture of the entire spectrum of metabolites.

The formation of AMP in the presence of deCof indicated that L-Ado was phosphorylated by an AK to form L-AMP in both RBCs and pRBCs. The recovery of ADP and ATP in these cells indicated that L-AMP and L-ADP must be substrates for the host, and possibly parasite, monophosphate and diphosphate kinases. In RBCs this suggests that the enantiomeric selectivity of the AK is not absolute, however, the amount of AMP recovered from D-Ado metabolism, compared to that from L-Ado metabolism, indicated a strong preference for D-Ado compared to L-Ado. This preference was exemplified by the observation that the amount of radiolabelled AMP recovered (as counts per minute) from L-Ado in RBCs and pRBCs was much less than the levels of AMP formed from D-Ado in the same experiment. This indicates that L-Ado is poorly metabolized compared D-Ado in RBCs and pRBCs.

CONCLUSIONS

1) A component of Ado entry in pRBCs, which was absent from RBCs, was not stereoselective and allowed the entry of L-Ado into pRBCs.

2) L-Ado, and a component of D-Ado entry in pRBCs was not sensitive to inhibition by inhibitors of nucleoside transport in RBCs.

3) Characteristics 1) and 2) suggested the existence of a parasite-induced route of Ado entry in pRBCs.

4) Parasite-induced Ado entry was not potently inhibited by cytochalasin B indicating that Ado flux in pRBCs was not via Glut1.

5) Parasite-induced Ado entry was potently inhibited by furosemide.

6) The fluxes of Ado in pRBCs were saturable, indicating the mediated entry of Ado in pRBCs.

7) L-Gluc and D-Sorb entered pRBCs, but not RBCs, via a parasite-induced route which was inhibited by furosemide with IC_{50} values similar to those obtained for inhibition of Ado entry.

8) L-Ado inhibited the unsaturable fluxes of L-Gluc and D-Sorb in pRBCs.

9) Characteristics 7) and 8) suggested that Ado, L-Gluc and D-Sorb shared a parasite-induced entry pathway in pRBCs.

10) D-Ado was metabolized more readily by pRBCs than RBCs.

11) D-Ado was metabolized more readily than L-Ado by pRBCs and RBCs.

12) L-Ado was a substrate for the parasite, but not host, adenosine deaminase.

FUTURE DIRECTIONS

The influx of L-Ado into pRBCs, as well as its subsequent metabolism, suggests examining L-nucleosides as potential anti-malarial agents. However, there are a number of experiments which could be done to answer more completely some of the questions raised in this study.

1) The ability of L-Ado to inhibit the flux of L-Gluc and D-Sorb has not been completely examined in this study. The nature of the inhibitory effect of L-Ado could help determine if a single pathway of parasite-induced solute entry exists.

2) The possible saturability of a component of L-Gluc flux in pRBCs could also be examined more thoroughly at low permeant concentrations. It may also be useful to examine the concentration-dependence of the inhibition of L-Gluc fluxes in pRBCs in more detail using furosemide or other, more potent, inhibitors to determine if there are multiple components of inhibition of L-Gluc fluxes in pRBCs.

3) The metabolism of L-Ado by pRBCs raises a number of questions. It may be useful to examine L-Ado metabolism with a range of substrate concentrations to determine kinetic values for the enzymes responsible for L-Ado metabolism in pRBCs. This may help identify the optimum concentration for examining L-Ado phosphorylation and deamination by the parasite AK and ADA, respectively. It is also necessary to determine if L-Ino (formed in this study) is a substrate for the parasite (or host) PNP. At present, it is uncertain whether Hyp was formed from L-Ino. Examining the extract for IMP may allow this question to be answered.

BIBLIOGRAPHY

1. Bispham, W.N. (1944). **Malaria**. The William & Wilkin Co. Baltimore.

2. Russel, P.F. (1955). **Man's mastery of malaria**. Oxford University Press. London.

3. World Health Organization. (1990). **Severe and complicated malaria**. Trans. R. Soc. Trop. Med. Hyg. 84(S2):1-65.

4. Markell, E.K., Voge, M., and John, D.T. (1992). **Malaria**. *In*: Medical Parasitology, 7th Edition, (Ozmat, S. ed.) W.B. Saunders Company, Philadelphia. pp.96-125.

5. Slater, A.F.G. (1993). **Chloroquine: Mechanism of drug action and resistance in *Plasmodium falciparum***. Pharmac. Ther. 57:203-235.

6. Ginsburg, H. (1990). **Some reflections concerning host erythrocyte-malarial parasite interrelationships**. Blood Cells. 16:225-235.

7. Fitch, C.D. (1983). *In*: Malaria and the Red Cell Evered, D. and Whelan, J. eds. London: Pitman pp.222-228.

8. Krogstad, D.J. and Schlesinger, P.H. (1987). **Acid-vesicle function, intracellular pathogens, and the action of chloroquine against *Plasmodium falciparum***. New Engl. J. Med. 317:542-549.

9. Slater, A.F.G. and Cerami, A. (1992). **Inhibition by chloroquine of a novel haem polymerase in malaria trophozoites**. Nature 355(9): 167-169.

10. Wellems, T.E. (1992). **How chloroquine works**. Nature 355:108-109.

11. Brasseur, P., Kouamouo, J., Moyou, R.S., and Druilhe, P. (1990). **Emergence of mefloquine-resistant malaria in Africa without drug pressure**. Lancet 336:59.

12. World Health Organization. (1993). **Malaria chemoprophylaxis for travellers.** WHO - Weekly epidemiological record 68(51):377-384.

13. White, N.J. (1994). **Artemisinin: current status**. Trans. R. Soc. Trop. Med. Hyg. 88:Supplement 1, 3-4.

14. Cox, F.E.G. (1993). **That vaccine passes a trial**. Nature 362:410.

15. Bannister, L.H., and Dluzewski, A.R. (1990). **The ultrastructure of red cell invasion in malaria infections: A review**. Blood Cells 16:257-292.

16. Dunn, M.J. (1969). **Alterations of red blood cell sodium transport during malarial infection**. J. Clin. Invest. 48:674-684.

17. Kirk, K., Ashworth, K.J., Elford, B.C., Pinches, R.A., and Ellory, J.C. (1991). **Characteristics of $^{[86]}$Rb+ transport in human erythrocytes infected with *Plasmodium falciparum***. Biochim. Biophys. Acta 1061:305-308.

18. Ginsburg, H. and Krugliak, M. (1983). **Uptake of L-tryptophan by erythrocytes infected with malaria parasites (*Plasmodium falciparum*)**. Biochim. Biophys. Acta 729:97-103.

19. Vander Jagt, D.L., Hunsaker, L.A., Campos, N.M., and Baack, B.R. (1990). **D-Lactate production in erythrocytes infected with *Plasmodium falciparum***. Mol. Biochem. Parasitol. 42:277-284.

20. Polet, H. and Barr, C.F. (1968). **DNA, RNA and protein synthesis in erythrocytic forms of *Plasmodium knowlesi***. Am. J. Trop. Med. Hyg. 17:672-679.

21. Walsh, C.T., and Sherman, I.W. (1968). **Purine and pyrimidine synthesis by avian malaria parasite *Plasmodium lophurae***. Protozool. 15:763-770.

22. Van Dyke, K. (1975). **Comparison of tritiated hypoxanthine, adenine and adenosine, for purine-salvage incorporation into nucleic acids of the malarial parasite *Plasmodium berghei***. Tropenmed Parasitology 26:232-238.

23. Webster, H.K., Whaun, J.M., Walker, M.D., and Bean, T.L. (1984). **Synthesis of adenosine nucleotides from hypoxanthine by human malaria parasites (*Plasmodium falciparum*) in continuous culture-inhibition by hadacidin but not alanosine**. Biochem. Pharmacol. 33:1555-1557.

24. Sherman, I.W., and Tanigoshi, L. (1974a). **Incorporation of [14C]-amino acids by malarial plasmodia (*Plasmodium lophurae*). VI. Changes in the kinetic constants of amino acid transport during infection**. Exp. Parasitol. 35:369-373.

25. Sherman, I.W. and Tanigoshi, L. (1974b). **Glucose transport in the malarial (*Plasmodium lophurae*) infected erythrocyte**. J. Protozool. 21:603-607.

26. Homewood, C.A. and Neame, K.D. (1974). **Malaria and the permeability of the host erythrocyte**. Nature 252:718-719.

27. Izumo, A., Tanabe, K., Kato, M., Doi,S., Maekawa, K. and Takada, S. (1989). **Transport processes of 2-deoxy-D-glucose in erythrocytes infected with *Plasmodium yoelii*, a rodent malaria parasite**. Parasitology 98:371-379.

28. Neame, K.D., Brownbill, P.A. and Homewood, C.A. (1974). **The uptake and incorporation of nucleosides into normal erythrocytes and erythrocytes containing *Plasmodium berghei***. Parasitology 69:329-335.

29. Hansen, B.D., Sleeman, H.K., and Pappas, P.W. (1980). **Purine base and nucleoside uptake in *Plasmodium berghei* and host erythrocytes**. J. Parasitol. 66(2):205-212.

30. Gati, W.P., Stoyke, A. F.-W., Gero, A.M., and Paterson, A.R.P. (1987). **Nucleoside permeation in mouse erythrocytes infected with *Plasmodium yoelii***. Biochem. Biophys. Res. Commun. 145(3):1134-1141.

31. Gati, W.P., Lin, A.N., Wang, T.I., Young, J.D., and Paterson, A.R.P. (1990). **Parasite-induced processes for adenosine permeation in mouse erythrocytes infected with the malarial parasite *Plasmodium yoelii***. Biochem. J. 272:277-280.

32. Trager, W. and Jensen, J.B. (1976). **Human malaria parasites in continuous culture**. Science 193:673-675.

33. Lambros, C. and Vanderberg, J.P. (1979). **Synchronization of *Plasmodium falciparum* erythrocytic stages in culture**. J. Parasitol. 65(3):418-420.

34. Kutner, S., Baruch, D., Ginsburg, H., and Cabantchik, Z.I. (1982). **Alterations in membrane permeability of malaria-infected human erythrocytes are related to the growth stage of the parasite.** Biochim. Biophys. Acta 687:113-117.

35. Ginsburg, H., Kutner, S., Krugliak, M., and Cabantchik, Z.I. (1985). **Characterization of permeation pathways appearing in the host membrane of *Plasmodium falciparum* infected red blood cells.** Mol. Biochem. Parasitol. 14:313-322.

36. Ginsburg, H. and Stein, W.D. (1987). **New permeability pathways induced by the malarial parasite in the membrane of its host erythrocyte: Potential routes for targeting of drugs to infected cells**. Biosci. Rep. 7(6):455-463.

37. Bookchin, R., Lew, V., Nagel, R., and Raventos, C. (1981). **Increase in potassium and calcium transport in human red cells infected with *Plasmodium falciparum*.** J. Physiol. 213:65P.

38. Kutner, S., Ginsburg, H., and Cabantchik, Z.I. (1983). **Permselectivity changes in malaria (*Plasmodium falciparum*) infected human red blood cell membranes.** J. Cell. Physiol. 114:245-251.

39. Kirk, K., Horner, H.A., Elford, B.C., Ellory, J.C., and Newbold, C.I. (1994). **Transport of diverse substrates into malaria-infected erythrocytes via a pathway showing functional characteristics of a chloride channel.** J. Biol. Chem. 269(5):3339-3349.

40. Kanaani, J. and Ginsburg, H. (1991). **Transport of lactate in *Plasmodium falciparum*-infected human erythrocytes.** J. Cell. Physiol. 149:469-476.

41. Elford, B.C., Haynes, V.D., Chulay, J.D., and Wilson, R.J.M. (1985). **Selective stage-specific changes in the permeability to small hydrophilic solutes of human erythrocytes infected with *Plasmodium falciparum*.** Mol. Biochem. Parasitol. 16:43-60.

42. Gero, A.M., Bugledich, E.M.A., Paterson, A.R.P., and Jamieson, G.P. (1988). **Stage-specific alteration of nucleoside membrane permeability and nitrobenzylthioinosine insensitivity in *Plasmodium falciparum* infected erythrocytes.** Mol. Biochem. Parasitol. 27:159-170.

43. Gero, A.M., Scott, H.V., O'Sullivan, W.J., and Christopherson, R.I. (1989). **Antimalarial action of nitrobenzylthioinosine in combination with purine nucleoside antimetabolites.** Mol. Biochem. Parasitol. 34:87-98.

44. Gero, A.M. and Upston, J.M. (1992). **Altered membrane permeability:a new approach to malaria chemotherapy.** Parasitol. Today 8(8):283-286.

45. Kirk, K., Elford, B.C., Ellory, J.C. and Newbold, C.I. (1992). **A transport pathway responsible for the increased permeability of malaria-infected erythrocytes shows characteristics of a Cl- channel.** J. Physiol. 452:342P.

46. Ginsburg, H., Kutner, S., Zangwil, M., and Cabantchik. Z.I. (1986). **Selectivity properties of pores induced in host erythrocyte membrane by *Plasmodium falciparum*. Effect of parasite maturation.** Biochim. Biophys. Acta 861:194-196.

47. Ginsburg, H., Krugliak, M., Eidelman, O., and Cabantchik, Z.I. (1983). **New permeability pathways induced in membranes *Plasmodium falciparum* infected erythrocytes**. Mol. Biochem. Parasitol. 8:177-190.

48. Kutner, S., Breuer, W.V., Ginsburg, H., and Cabantchik, Z.I. (1987). **On the mode of action of phlorizin as an antimalarial agent in *in vitro* cultures of *Plasmodium falciparum***. Biochem. Pharmacol. 36(1):123-129.

49. Cabantchik, Z.I. (1990). **Properties of permeation pathways induced in the human red cell membrane by malaria parasites**. Blood Cells 16:421-432.

50. Belt, J.A., Marina, N.M., Phelps, D.A., and Crawford, C.R. (1993). **Nucleoside transport in normal and neoplastic cells**. Advan. Enzyme Regul. 33:235-252.

51. Vijayalakshmi, D. and Belt, J.A. (1988). **Sodium-dependent nucleoside transport in mouse intestinal epithelia cells. Two transport systems with differing substrate specificities**. J. Biol. Chem. 263:19419-19423.

52. Crawford, C.R., Ng, C.Y.C., Noel, L.D., and Belt, J.A. (1990). **Nucleoside transport in L1210 murine leukemia cells. Evidence for three transporters**. J. Biol. Chem. 265:9732-9736.

53. Paterson, A.R.P., Gati, W.P., Vijayalakshmi, D., Cass,C.E., Mant, M.J., Young, J.D. and Belch, A.R. (1993). **Inhibitor-sensitive, Na+-linked transport of nucleoside analogs in leukemia cells from patients**. Proceedings of the American Association for Cancer Research 34:14 abst. #83.

54. Kwong, F.P.Y., Davies, A. Tse, C.M., Young, J.D., Henderson, P.J.F., and Baldwin, S.A. (1988). **Purification of the human erythrocyte nucleoside transporter by immunoaffinity chromatography**. Biochem. J. 255:243-249.

55. Paterson, A.R.P. and Cass, C.E. (1986). **Transport of nucleoside drugs in animal cells**. *In:* Membrane Transport of Antineoplastic Agents Goldman, I.D. ed. Pergamon Press. New York. pp.309-329.

56. Paterson, A.R.P., Harley, E.R., and Cass, C.E. (1985). **Measurement and inhibition of membrane transport of adenosine**. *In*: Methods in Pharmacology, Vol 6. Paton, D.M. ed. Plenum Publishing Corporation pp.165-180.

57. Gati, W.P. and Paterson, A.R.P. (1989). **Nucleoside Transport**. *In:* Red Blood Cell Membranes: Structure, function, clinical implications. Agre, P. and Parker,J.C. eds. New York: Marcel Dekker. pp. 635-661.

58. Gati, W.P., Misra, H.K., Knaus, E.E., and Wiebe, L.I. (1984). **Structural modifications at the 2'- and 3'- positions of some pyrimidine nucleosides as determinants of their interaction with the mouse nucleoside transporter**. Biochem. Pharmacol. 33(21);3325-3331.

59. Plagemann, P.G.W., Wohlheuter, R.M., and Erbe, J. (1982). **Nucleoside transport in human erythrocytes. A simple carrier with directional symmetry and differential mobility of loaded and empty carrier**. J. Biol. Chem. 257:12069-12074.

60. Gerlach, E., Becker, B.F., and Nees, S. (1987). **Formation of adenosine by vascular endothelium: a homeostatic and antithrombogenic mechanism**. *In*: Topics and Perspectives in Adenosine Research. Gerlach, E., and Becker, B.F. eds. Berlin and Heidelberg: Springer-Verlag. pp.309-320.

61. Wohlhueter, R.M., Marz, R., Graff, J.C., and Plagemann, P.G.W. (1978). **A rapid mixing technique to measure transport in suspended animal cells: application to nucleoside transport in rat hepatoma cells** Meth. Cell. Biol. 20:211-236.

62. Gati, W.P. and Paterson, A.R.P. (1989). **Interaction of [3H]-dilazep at nucleoside transporter-associated binding sites on S49 mouse lymphoma cells**. Mol. Pharmacol. 36:134-141.

63. Woffendin, D. and Plagemann, P.G.W. (1987). **Interaction of [3H]-dipyridamole with nucleoside transporters of human erythrocytes and cultured animal cells**. J. Memb. Biol. 98:89-100.

64. Ijzerman, A.P., Thedinga, K.H., Custers, A.F., Hoos, B., and Van Belle, H. (1989). **Inhibition of nucleoside transport by a new series of compounds related to lidoflazine and mioflazine**. Eur. Jour. Pharmacol 172:273-281.

65. Carruthers, A. (1990). **Facilitated diffusion of glucose**. Physl. Rev. 70(4):1135-1176.

66. Plagemann, P.G.W. and Woffendin, C. (1987). **Comparison of the equilibrium exchange of nucleosides and 3-O-methylglucose in human erythrocytes and of the effects of cytochalasin B, phloretin and dipyridamole on their transport**. Biochim. Biophys. Acta 899:295-301.

67. Gati, W.P., Dagnino, L., and Paterson, A.R.P. (1989). **Enantiomeric selectivity of adenosine transport systems in mouse erythrocytes and L1210 cells**. Biochem. J. 263:957-960.

68. Gutteridge, W.E. and Trigg, P.I. (1970). **Incorporation of radioactive precursors into DNA and RNA of *Plasmodium knowlesi in vitro***. J. Protozool. 17:89-96.

69. Cabantchik, Z.I., Kutner,S., Krugliak, M., and Ginsburg, H. (1983). **Anion transport inhibitors as suppressors of *Plasmodium falciparum* growth in *in vitro* cultures**. Mol. Pharmacol. 23:92-99.

70. Gero, A.M. and O'Sullivan, W.J. (1990). **Purines and Pyrimidines in Malarial Parasites**. Blood Cells 16:467-484.

71. Reyes, P., Rathod, P.K., Sanchez, D.J., Mrema, J.E.K., Rieckmann, K.H., and Heidrich, H.G. (1982). **Enzymes of purine and pyrimidine metabolism from the malaria parasite, *Plasmodium falciparum***. Mol. Biochem. Parasitol. 5:275-290.

72. Gero, A.M., Brown, G.V., and O'Sullivan, W.J. (1984). **Pyrimidine *de novo* synthesis during the life-cycle of the intraerythrocytic stage of *Plasmodium falciparum***. J. Parasitol. 70:536-541.

73. Dawicki, D.D., Agarwal, K.C., and Parks, R.E. Jr. (1988). **Adenosine metabolism in human whole blood - effects of nucleoside transport inhibitors and phosphate concentration**. Biochem. Pharmacol. 37:621-626.

74. Asai, M., Hieda, H., and Shimizu, B. (1967). **Studies on synthetic nucleotides. IV. Preparation of L-β-ribonucleosides and L-β-ribonucleotides**. Chem. Pharm. Bull. 15(12):1863-1870.

75. Minato, S., Tagawa, T., and Nakanishi, K. (1965). **Studies on non-specific adenosine deaminase from Takadiastase**. J. Biochem. 58(6):519-525.

76. Gu, J.G., Delaney, S., Sawka, A.N., and Geiger, J.D. (1991). **L-[^{3}H]Adenosine, a new metabolically stable enantiomeric probe for adenosine transport systems in rat brain synaptoneurosomes**. J. Neurochem. 56(2):548-552.

77. Krooth, R.S., Wuu, K.D., and Ma, R. (1969). **Dihydroorotic acid dehydrogenase: introduction into erythrocyte by the malaria parasite**. Science 164:1073-1075.

78. Manandhar, M.S.P. and Van Dyke,K. (1975). **Detailed purine salvage metabolism in and outside free malarial parasite**. Exp. Parasitol. 37(2):138-146.

79. Van Dyke, K., Trush, M.A., Wilson, M. E., and Stealy, P.K. (1977). **Isolation and analysis of nucleotides from erythrocyte-free malarial parasites (*Plasmodium berghei*) and potential relevance to malaria chemotherapy**. Bull. W.H.O. 55:253-264.

80. Yamada, K. A. and Sherman, I.W. (1980). ***Plasmodium lophurae*-malaria induced nucleotide changes in duckling (*anas-domesticus*) erythrocytes**. Mol. Biochem. Parasitol. 1:187-198.

81. Yamada, K. A. and Sherman, I.W. (1981a). **Purine metabolizing enzymes of *Plasmodium lophurae* and its host-cell, the duckling (*anas-domesticus*) erythrocyte**. Mol. Biochem. Parasitol. 2:349-358.

82. Yamada, K. A. and Sherman, I.W. (1981b). **Purine metabolism by the avian malarial parasite *Plasmodium lophurae***. Mol. Biochem. Parasitol. 3:253-264.

83. Roth, E. Jr., Ogasawara, N., and Schulman, S. (1989). **The deamination of adenosine and adenosine monophosphate in *Plasmodium falciparum*-infected human erythrocytes: *In vitro* use of 2'-deoxycoformycin and AMP deaminase-deficient red cells**. Blood 74(3):1121-1125.

84. Queen, S.A., Vander Jagt, D., and Reyes, P. (1988). **Properties and substrate specificity of a purine phosphoribosyltransferase from the human malaria parasite, *Plasmodium falciparum***. Mol. Biochem. Parasitol. 30:123-134.

85. Daddona, P.E., Wiesmann, W.P., Milhouse, W., Chern, J.W., Townsend, L.B., Hershfield, M.S., and Webster, H.K. (1986). **Expression of human malaria parasite purine nucleoside phosphorylase in host enzyme-deficient erythrocyte culture**. J. Biol. Chem. 261:11667-11673.

86. Daddona, P.E., Wiesmann, W.P., Lambros, C., Kelley, W.N., and Webster, H. K. (1984). **Human malaria parasite adenosine deaminase: characterization in host enzyme-deficient erythrocyte culture**. J. Biol. Chem. 259(3):1472-1475.

87. Sherman, I.W. (1984). **Metabolism**. *In:* Handbook of Experimental Pharmacology. Peters, W., Richards, W.G., eds. New York: Springer-Verlag. 68:31-80.

88. Scott, H.V., Gero, A.M., and O'Sullivan, W.J. (1986). ***In vitro* inhibition of *Plasmodium falciparum* by pyrazofurin, an inhibitor of pyrimidine biosynthesis *de novo***. Mol. Biochem. Parasitol. 18:3-15.

89. Rathod, P.K., Khatri, A., Hubbert,T., and Milhouse, W.K. (1989). **Selective activity of 5-fluoroorotic acid against *Plasmodium falciparum in vitro***. Antimicrob. Ag. Chemother. 33:1090-1094.

90. Webster, H.K. and Whaun, J.M. (1982). **Antimalarial properties of bredinin- prediction based on identification of differences in human host-parasite purine metabolism**. J. Biol. Chem. 70:461-469.

91. Beutler, E. and Carson, D.A. (1993). **2-Chlorodeoxyadenosine: Hairy cell leukemia takes a surprising turn**. Blood Cells 19:559-568.

92. Jawetz, E. (1989). **Antiviral chemotherapy and prophylaxis**. *In*: Basic and Clinical Pharmacology, 4th Edition. Katzung, B.G. ed. Norwalk: Appleton & Lange pp.597-611.

93. McCormick, G.J., Canfield, C.J., and Willet, G.P. (1974). ***In vitro* antimalarial activity of nucleic acid precursor analogues in the simian malaria *Plasmodium knowlesi***. Antimicrob. Ag. Chemother. 6(1):16-21.

94. Paterson, A.R.P., Jakobs, E.S., Harley, E.R., Cass, C.E., and Robins, M.J. (1983). **Inhibitors of nucleoside transport as probes and drugs**. *In*: Development of Target-Oriented Anticancer Drugs. Cheng, Y.-C. *et al.* eds. New York Raven Press pp.41-55.

95. El Kouni, M.H., Messier N.J., and Cha, S. (1987). **Treatment of schistosomiasis by purine nucleoside analogues in combination with nucleoside transport inhibitors**. Biochem. Pharmacol. 36(22):3815-3821.

96. Paul, B., Chen, M.F., and Paterson, A.R.P. (1975). **Inhibitors of nucleoside transport: a structure-activity study using human erythrocytes**. J. Med. Chem. 18:968-973.

97. Dulbecco, R. and Vogt, M. (1954). **Plaque formation and isolation of pure lines with poliomyelitis viruses**. J. Exp. Med. 99:167-182.

98. Batt, E.R. and Schachter, D. (1973) **Transport of monosaccharides: asymmetry in the human erythrocyte mechanism**. J. Clin. Invest. 52:1686-1697.

99. Schwartz, P.M. and Drach, J.C. (1978). **Thin-layer chromatography of purine bases, nucleosides and nucleotides**. *In:* Nucleic Acid Chemistry, Part Two. Townsend, L.B. and Tipson, R.S. eds. John Wiley & Sons. New York pp. 1061-1067.

100. Randerath, K. and Randerath, E. (1967). **Thin-layer separation methods for nucleic acid derivatives**. *In:* Nucleic Acids, Part A. Methods in Enzymology, Vol. XII. Grossman, L. and Moldave, K. eds. Academic Press. New York. pp. 323-347.

101. Dluzewski, A.R., Ling, I.T., Rangachari, K., Bates, P.A., and Wilson, R.J.M. (1984). **A simple method for isolating viable mature parasites of *Plasmodium falciparum* form cultures**. Trans. R. Soc. Trop. Med. Hyg. 78:622-624.

102. Aley, S.B., Sherwood, J.A., and Howard, R.J. (1984). **Knob-positive and knob-negative *Plasmodium falciparum* differ in expression of a strain-specific malarial antigen on the surface of infected erythrocytes**. J. Exp. Med. 160:1585-1590.

103. Aley, S.B., Sherwood, J.A., Marsh, K., Eidelman, O., and Howard, R.J. (1986). **Identification of isolate-specific proteins on sorbitol-enriched *Plasmodium falciparum* infected erythrocytes from Gambian patients**. Parasitology 92:511-525.

104. Glantz, S.A. (1992). **Primer of Biostatistics**, Third Edition. (Jeffers, J.D. and Englis, M.R., eds.) McGraw-Hill Inc. New York.

105. Jarvis, S.M. (1988). **Inhibition by nucleosides of glucose-transport activity in human erythrocytes**. Biochem. J. 249:383-389.

106. Plagemann, P.G. and Estensen, R.D. (1972). **Cytochalasin B: Competitive inhibition of nucleoside transport by cultured Novikoff rat hepatoma cells**. J. Cell Biol. 55:179-185.

107. Koepsell, H. and Madrala, A. (1987). **Interaction of phloridzin with the Na+-D-glucose cotransporter from intestine and kidney**. Top. Mol. Pharmacol. 4:179-202.

108. Velazquez, H. and Wright, A.S. (1986). **Control by drugs of renal potassium handling**. Toxicology 26:293-309.

109. Brazy. P.C. and Gunn, R.B. (1976). **Furosemide inhibition of chloride transport in human red blood cells**. J. Gen. Physiol. 68:583-599.

110. Baldwin, S.A. (1993). **Mammalian passive glucose transporters: members of an ubiquitous family of active and passive transport proteins**. Biochim. Biophys. Acta 1154:17-49.

111. Ogbunude, P.O.J. and Baer, H.P. (1993). **Nucleoside transport in parasites-current status and methodological aspects**. Int. J. Biochem. 25(4):471-477.

112. Plagemann, P.G.W. and Wohlhueter, R.M. (1984). **Kinetics of nucleoside transport in human erythrocytes: alterations during blood preservation**. Biochim. Biophys. Acta 778:176-184.

113. Silfen, J., Yanai, P. and Cabantchik, Z.I. (1988). **Bioflavonoid effects on *in vitro* cultures of *Plasmodium falciparum***. Biochem. Pharmacol. 37(22):4269-4276.

114. Wohlhueter, R.M., Brown, W.E., and Plagemann, P.G.W. (1983). **Kinetic and thermodynamic studies on nitrobenzylthioinosine binding to the nucleoside transporter of Chinese hamster ovary cells**. Biochim. Biophys. Acta 731:168-176.

115. Allen, R.C. (1983). **Sulfonamide diuretics**. *In*: Diuretics. E.J. Cragoe, ed. John Wiley, New York. pp. 49-200.

116. Gero, A.M. (1989). **Induction of nucleoside transport sites into the host cell membrane of *Babesia bovis* infected erythrocytes**. Mol. Biochem. Parasitol. 35:269-276.

117. Upston, J.M. and Gero, A.M. (1990). **Increased glucose permeability in *Babesia bovis*-infected erythrocytes**. Int. J. Parasitol. 20(1):69-76.

118. Plagemann, P.G.W. and Wohlhueter, R.M. (1980). **Permeation of nucleosides, nucleic acid bases, and nucleotides in animal cells**. Curr. Top. Membr. Transp. 14:225-330.

119. Pouvelle, B., Spiegel, R., Hsiao, L., Howard, R.J., Morris, R.L., Thomas, A.P., and Tarashi, T.F. (1991). **Direct access to serum macromolecules by intraerythrocytic malaria parasites**. Nature 353:73-75.